

ANALYSIS AND DESIGN OF SPACE VEHICLE  
FLIGHT CONTROL SYSTEMS

VOLUME II - TRAJECTORY EQUATIONS

By Arthur L. Greensite

Distribution of this report is provided in the interest of information exchange. Responsibility for the contents resides in the author or organization that prepared it.

Issued by Originator as GDC-DDE65-058

Prepared under Contract No. NAS 8-11494 by  
GENERAL DYNAMICS CONVAIR  
A DIVISION OF GENERAL DYNAMICS CORPORATION  
San Diego, Calif.

for George C. Marshall Space Flight Center

NATIONAL AERONAUTICS AND SPACE ADMINISTRATION



## FOREWORD

This report was prepared under NASA Contract NAS 8-11494 and is one of a series intended to illustrate methods used for the design and analysis of space vehicle flight control systems. Below is a complete list of the reports in the series:

Volume I	Short Period Dynamics
Volume II	Trajectory Equations
Volume III	Linear Systems
Volume IV	Nonlinear Systems
Volume V	Sensitivity Theory
Volume VI	Stochastic Effects
Volume VII	Attitude Control During Launch
Volume VIII	Rendezvous and Docking
Volume IX	Optimization Methods
Volume X	Man in the Loop
Volume XI	Component Dynamics
Volume XII	Attitude Control in Space
Volume XIII	Adaptive Control
Volume XIV	Load Relief
Volume XV	Elastic Body Equations
Volume XVI	Abort

The work was conducted under the direction of Clyde D. Baker, Billy G. Davis and Fred W. Swift, Aero-Astro Dynamics Laboratory, George C. Marshall Space Flight Center. The General Dynamics Convair program was conducted under the direction of Arthur L. Greensite.



PRECEDING PAGE BLANK NOT FILMED.

## TABLE OF CONTENTS

<u>Section</u>	<u>Page</u>
1. STATEMENT OF THE PROBLEM . . . . .	1
2. STATE OF THE ART . . . . .	3
3. RECOMMENDED PROCEDURES . . . . .	5
3.1 Coordinate Transformations . . . . .	5
3.2 Equations of Motion in Inertial Frame . . . . .	19
3.3 Forces and Moments . . . . .	24
3.3.1 Thrust . . . . .	24
3.3.2 Gravity . . . . .	25
3.3.3 Aerodynamics . . . . .	28
3.4 Complete Equations of Motion . . . . .	32
3.5 Trajectory Equations During Launch . . . . .	41
3.6 Guidance Considerations . . . . .	49

### Appendices

A	TIME RATE OF CHANGE OF LINEAR AND ANGULAR MOMENTUM FOR VARIABLE MASS SYSTEMS . . . . .	77
B	RELATIONS FOR THE INERTIA DYADIC . . . . .	81
C	THRUST OF A ROCKET ENGINE . . . . .	85
D	GEOPHYSICAL CONSTANTS . . . . .	89
	REFERENCES . . . . .	91

# LIST OF ILLUSTRATIONS

<u>Figure</u>		<u>Page</u>
1	Geocentric Inertial Coordinate System . . . . .	6
2	Earth-Fixed Launch Site Coordinate System . . . . .	7
3	Earth-Centered, Launch-Derived Coordinate System . . . . .	8
4	Launch Vehicle Platform-Accelerometer Coordinate System. . . . .	9
5	Launch Vehicle Navigation Coordinate System . . . . .	10
6	Body-Fixed Coordinate System . . . . .	11
7	Geocentric Inertial to Earth-Fixed Launch Site Coordinate Transformation . . . . .	13
8	Local Geocentric Coordinate System . . . . .	17
9	Configuration of Body of Variable Mass Relative to Inertial Reference . . . . .	20
10	Thrust Configuration . . . . .	23
11	Components of Gravity for Oblate Spheroid Earth . . . . .	26
12	Gravity Components in Body Axis System . . . . .	28
13	Definition of Flight Path and Azimuth Angles . . . . .	37
14	Meridian Plane Through an Oblate Spheroid Earth . . . . .	38
15	Orientation of Local Geodetic Coordinate System . . . . .	40
16	Pitch Attitude Control Channel . . . . .	47
16a	Alternate Schematic of Autopilot of Figure 16 . . . . .	47
17	Determination of Range . . . . .	49
18	Elements of a Guidance System . . . . .	50
19	Elements of a Radio Guidance System . . . . .	51
20	Schematic of an Inertial Guidance System . . . . .	51
21	Transition from Vertical Rise to Zero Lift Turn . . . . .	55
22	Step Approximation to Pitch Rate Program . . . . .	55
23	Typical $\alpha$ q Time Histories for Winds Aloft . . . . .	56
24	Typical Pitch Rate vs. Time Program . . . . .	57

# LIST OF ILLUSTRATIONS, Contd

<u>Figure</u>		<u>Page</u>
25	Altitude Time History . . . . .	59
26	Ground Range Time History . . . . .	60
27	Relative Velocity Time History . . . . .	61
28	Inertial Velocity Time History . . . . .	62
29	Relative Flight Path Angle Time History . . . . .	63
30	Mach Number Time History . . . . .	64
31	Axial Acceleration Time History . . . . .	65
32	Dynamic Pressure Time History . . . . .	66
33	Pitch Angle of Attack Time History . . . . .	67
34	Pitch Attitude Time History . . . . .	68
35	Axial Drag Force Time History . . . . .	69
36	Normal Force Time History . . . . .	70
37	Side Force Time History . . . . .	71
38	Total Vehicle Weight Time History . . . . .	72
39	Booster Engine Thrust Time History . . . . .	73
40	Longitude Time History . . . . .	74
41	Geocentric Latitude Time History . . . . .	75
A-1	Momentum Change for Variable Mass Systems . . . . .	78
C-1	Rocket Engine Thrust Configuration . . . . .	88





# NOMENCLATURE

$A_i$	reference area; see Eqs. (35) - (40)
$c_i$	exhaust velocity of $i^{\text{th}}$ mass particle
$C_D$	drag coefficient
$C_N$	normal force coefficient
$\bar{F}$	external force vector
$\bar{F}_A$	aerodynamic force vector
$\bar{F}_g$	gravity force vector
$\bar{F}_T$	thrust vector
$g$	gravity acceleration
$H_G$	altitude
$\bar{I}$	inertia dyadic; defined in Eq. (B-2)
$K_A$	servoamplifier gain
$K_c$	reciprocal of actuator time constant
$K_R$	rate gyro gain
$l$	generic distance along longitudinal axis of vehicle; measured from nose
$l_j$	distance from nose of vehicle to station $j$
$l_c$	distance from origin of body axis system to engine swivel point; see Fig. 10
$l_r$	roll moment arm
$l_\alpha$	distance from origin of body axis system to center of pressure in pitch plane; see Fig. 10

# NOMENCLATURE, Contd

$l_\beta$	distance from origin of body axis system to center of pressure in yaw plane; see Fig. 10
$L_\alpha$	aerodynamic load in pitch plane
$L_\beta$	aerodynamic load in yaw plane
$m$	instantaneous mass of vehicle
$m_i$	mass of $i^{\text{th}}$ particle
$\bar{M}_O$	vector moment about origin of body axis system; see Eq. (13)
$\bar{M}_A$	vector aerodynamic moment
$\bar{M}_g$	vector gravity moment
$\bar{M}_T$	vector thrust moment
$M_j^{(p)}$	bending moment at station $j$ in pitch plane
$M_j^{(y)}$	bending moment at station $j$ in yaw plane
$p, q, r$	angular velocities about roll, pitch, and yaw axes
$R_e$	mean radius of (spherical) earth
$R_{EA}$	equatorial radius of earth
$R_{EB}$	polar radius of earth
$\bar{R}_O$	position vector from center of earth to origin of body axis system
$\bar{R}_i$	position vector from center of earth to $i^{\text{th}}$ mass particle
$t$	time

## NOMENCLATURE, Contd

$T_c$	swivelled thrust
$T_s$	fixed direction thrust
$\bar{U}$	velocity vector of origin of body axis system
$\bar{V}$	airspeed; see Eq. (52)
$W_N$	wind velocity in northerly direction
$W_E$	wind velocity in easterly direction
$u, v, w$	components of $\bar{U}$ in body axis system
$u', v', w'$	components of airspeed in body axis system
$u_I, v_I, w_I$	components of $\bar{U}$ in geocentric inertial system
$u_G, v_G, w_G$	components of velocity with respect to earth surface; expressed in local geocentric system
$x_{cg}, y_{cg}, z_{cg}$	components of $\bar{\rho}_c$ in body axis system
$\alpha$	angle of attack
$\beta$	sideslip angle
$\gamma$	flight path angle
$\gamma_c$	flight path angle relative to local geodetic system
$\Gamma_1$	range angle
$\Gamma_2$	latitude
$\Gamma_G$	local geodetic latitude; see Fig. 14
$\delta_p$	thrust deflection angle in pitch plane
$\delta_y$	thrust deflection angle in yaw plane
$\delta_r$	roll torque signal
$\theta$	pitch attitude angle

## NOMENCLATURE, Contd

$\theta_c$	pitch command
$\Lambda_1, \Lambda_2, \Lambda_3$	Euler angles; see Fig. 7
$\mu$	gravitational constant
$\rho$	atmospheric density
$\bar{\rho}_c$	position vector from origin of body axis system to mass center of vehicle
$\bar{\rho}_i$	position vector from origin of body axis system to $i^{\text{th}}$ mass particle
$\sigma$	azimuth angle
$\sigma_c$	azimuth angle relative to local geodetic system
$\varphi$	roll angle
$\varphi_c$	roll command
$\psi$	yaw attitude angle
$\psi_c$	yaw command
$\bar{\omega}$	angular velocity vector of body
$\Omega_E$	angular velocity of earth
$(\dot{\phantom{x}})$	$\equiv$ time derivative of a scalar
$(\overline{\phantom{x}})$	$\equiv$ a vector
$(\dot{\overline{\phantom{x}}})$	$\equiv$ time derivative of a vector with respect to inertial reference
$(\overline{\dot{\phantom{x}}})$	$\equiv$ time derivative with respect to local coordinate system. If the local coordinate system is at rest with respect to inertial space, then $(\dot{\overline{\phantom{x}}})$ and $(\overline{\dot{\phantom{x}}})$ are equivalent

## 1. STATEMENT OF THE PROBLEM

The control problem in the context of short-period dynamics<sup>(8)</sup> is concerned primarily with ensuring that the vehicle responds satisfactorily to control signals in the form of attitude commands. It is required that response time be reasonably rapid and that induced transients be quickly damped out. Such factors as missile flexibility, fuel sloshing, and instrumentation dynamics have significant influence on the performance and stability quality of the vehicles' short-period response.

The present monograph is concerned with the long-period dynamics of the vehicle; in other words, those factors that determine the capability of a vehicle to accomplish a specific mission. Here, one deals with the trajectory equations and with the relationship between guidance philosophy, control response, and trajectory profile. The main result of this monograph is the development of a set of equations that describe the motion of a space vehicle from launch to either earth impact or orbit injection. The general formulation includes all effects that are known to be significant for purposes of guidance and control; among these are nonspherical rotating earth, variable mass of vehicle, eccentric c.g., and jet damping.

Such higher-order dynamic effects as fuel sloshing, bending, and gyro and actuator dynamics are neglected for purposes of trajectory analysis. The development proceeds from first principles, emphasizing general concepts rather than long, detailed equations. The motivation for this is twofold. First, virtually all aerospace contractors and government agencies have developed trajectory equations that are usually tailored for specific needs or missions. By exhibiting the underlying unity in all these formulations, the assumptions and limitations of each are highlighted. Second, by starting with the most general description, we may proceed with the simplifications of the analysis in a systematic manner, noting where, and under what conditions, various approximations are permissible. Thus, for example, a set of equations derived for purposes of determining an accurate trajectory would differ considerably from those intended to be useful mainly for loads studies. The differences, of course, are due solely to the permissible simplifications.

While certain approximations for specific purposes are immediately evident, it must be recognized that in general, the manipulation of the equations to simplified form is often an art rather than a science, based heavily on experience and engineering judgement. In any event, a firm theoretical foundation is basic, and this is the aim of the present exposition. In this respect, various elements uniquely germane to trajectory simulation studies are considered in detail. These include pertinent coordinate systems and transformation matrices, their relationship to the guidance and control problem, and the assumptions that characterize the final results.

The emphasis in this monograph is on launch trajectories rather than orbital mechanics. Thus the equations developed in Ref. 8 before perturbation techniques are applied are exactly equivalent to the fundamental equations developed here.

## 2. STATE OF THE ART

The modern development of the equations that govern the motion of a space vehicle reflects both the needs of the aerospace industry and the facilities available for processing these equations. On the theoretical side, other than the various perturbation techniques of celestial mechanics, there is little that can be properly described as advances in the state of the art. (We exclude, of course, relativity effects, which are not expected to be of design significance in the foreseeable future.)

The development of trajectory equations has its foundation in the classical theories of celestial mechanics<sup>(11)</sup> and the equations of rigid-body motion. Various texts in recent years have adapted the classical methods to the needs of modern space vehicle guidance and control. (13, 14)

The two fundamental factors that have affected the development of trajectory equations are: the availability of high-speed computing equipment and the refinements in values of geophysical and astrodynamical constants. Consequently, where high precision is required, the means of achieving it has been made available. However, an economical and efficient use of computing equipment requires a harmonious blend of satisfactory accuracy for the specific mission and permissible approximations in the equations of motion. Computer storage and solution time are limited.

The result is that a bewildering variety of specialized computer programs is available in the aerospace industry. Each is generally tailored to specific missions or vehicles and is based on particular forms of the equations of motion. (6, 7, 9, 10)

What may therefore be properly called state of the art in trajectory equations is merely a reflection of refinements in basic data and ingenuity in programming computers efficiently.

Among the factors that demand attention in this respect are:

- a. Rational choice of reference frames.
- b. Determination of those effects that are significant and those that are negligible for the particular problem at hand.
- c. Adaptability for solution in real time when integrated with guidance.
- d. Computer storage and solution time constraints.
- e. Flexibility and ease of modifying computer program as required.

In order to achieve a fuller comprehension of these factors, one must be familiar with the primary elements that are taken into account in these general formulations. The manner in which these are comprehensively integrated is the subject of this monograph. In keeping with the general theme of this series, long, detailed special cases are avoided, although examples are included to enhance comprehension. The overall objective is to provide an engineering foundation suitable for design application in a wide variety of specialized cases.



### 3. RECOMMENDED PROCEDURES

The vehicle equations of motion are most readily derived with respect to an inertial reference frame. Furthermore, for convenience and ease of manipulation, such quantities as velocity, acceleration, and applied forces are expressed in body axis coordinates.

To yield meaningful results, the accelerations and velocities computed in the body coordinate system must be related to a fixed point on the surface of the earth. Furthermore, since various measures of linear and angular motion are usually derived from the instrumentation on an inertial platform, this coordinate system must also be related to the others.

Accordingly, the various coordinate systems to be used are described first, together with the appropriate transformation matrices. This is followed by a detailed discussion of the equations of motion and the manner in which the coordinate transformation matrices are used to obtain results relative to particular reference frames.

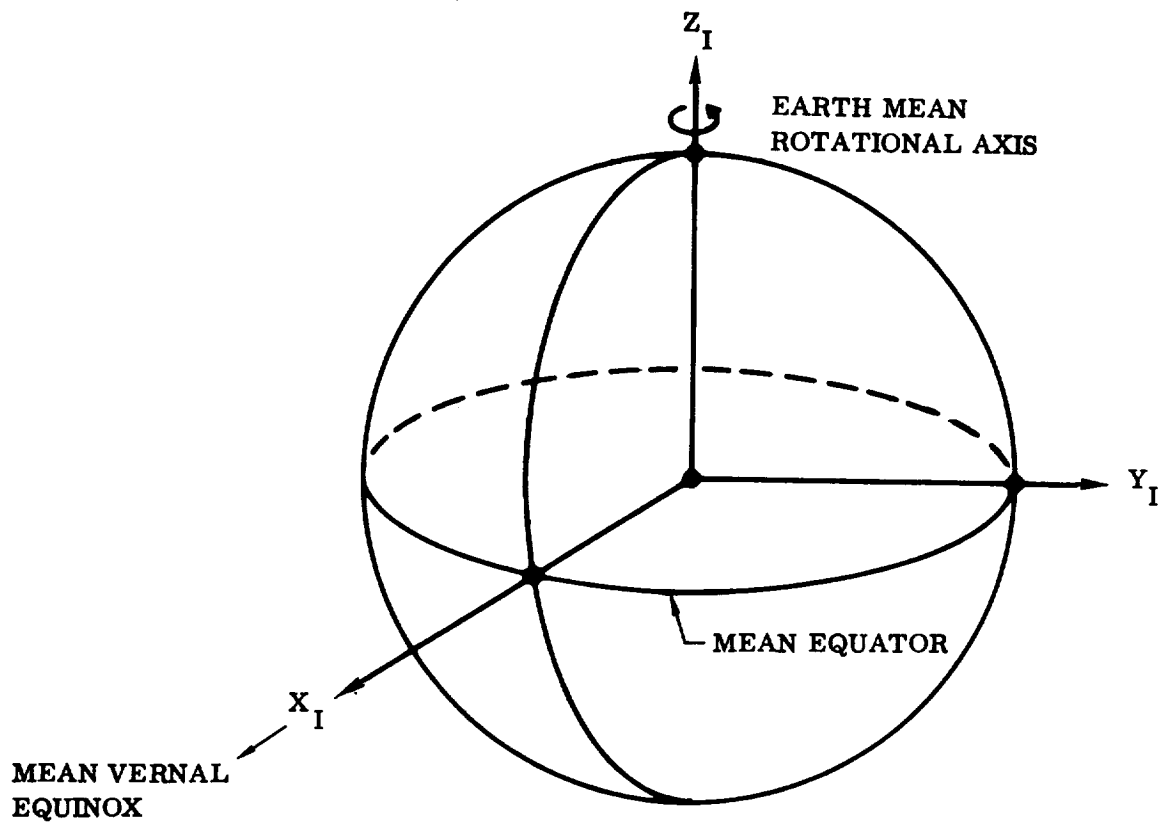
#### 3.1 COORDINATE TRANSFORMATIONS

The coordinate systems needed to fulfill the requirements of guidance, control, and loads analysis are listed below.

- |  |       |
|--|-------|
| a. Geocentric Inertial                   | $S_I$ |
| b. Earth-Fixed Launch Site               | $S_L$ |
| c. Earth-Centered, Launch-Derived        | $S_E$ |
| d. Launch Vehicle Platform-Accelerometer | $S_P$ |
| e. Launch Vehicle Navigation             | $S_N$ |
| f. Body-Fixed                            | $S_B$ |

These are based on standards adopted by the NASA Apollo project office.<sup>(1)</sup> For purposes of brevity, each coordinate system is denoted by the symbol  $S$  with an appropriate subscript. In the ensuing discussion, this will be used to denote either the coordinate system itself or a vector with components in this system; whichever is meant will be clear from the context. A complete description of these coordinate systems is contained in Figs. 1 through 6.

The use of a body axis system permits the usual description of angular rotation about the  $X_B$ ,  $Y_B$ , and  $Z_B$  axes in terms of roll, pitch, and yaw respectively. The launch vehicle platform accelerometer system is used for vehicle attitude



**TYPE:** Nonrotating, earth-referenced.

**ORIGIN:** The center of the earth.

**ORIENTATION AND LABELING:**

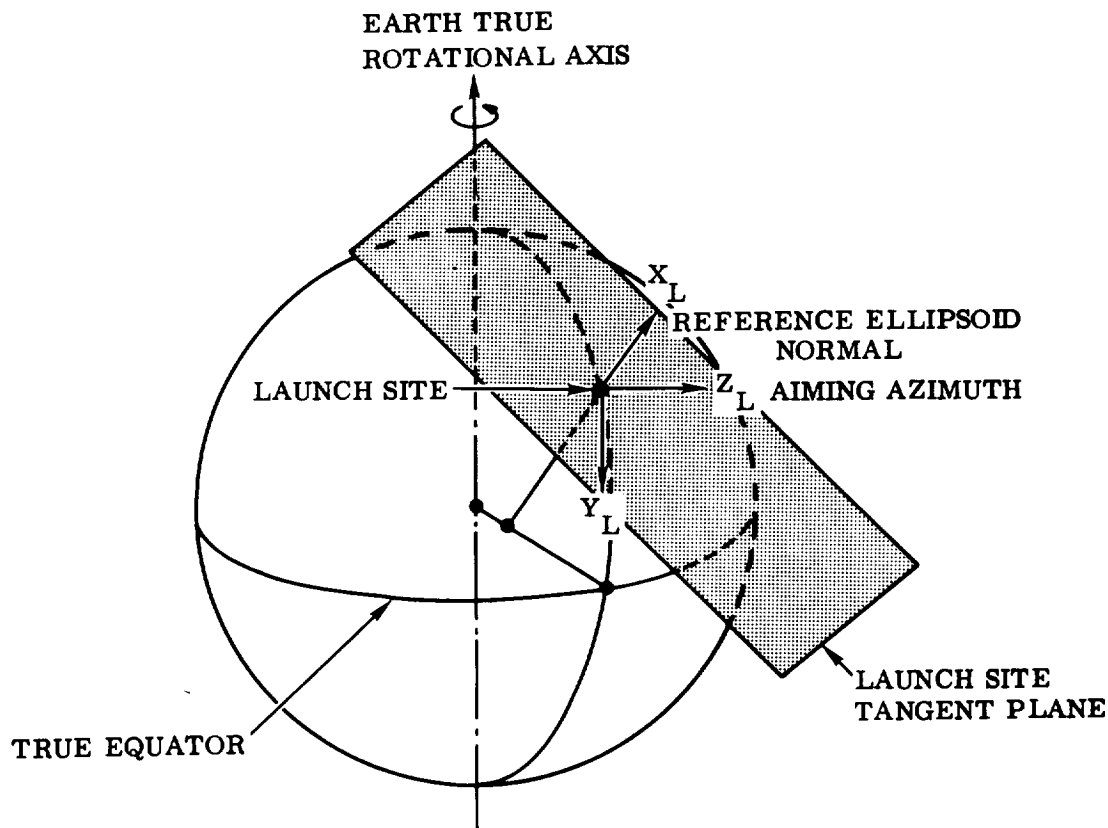
The Z<sub>I</sub> axis is directed along the earth mean rotational axis, positive north.

The X<sub>I</sub> axis is directed toward the mean vernal equinox.

The Y<sub>I</sub> axis completes a standard right-handed system.

The epoch is the nearest beginning of a Besselian year.

**Figure 1. Geocentric Inertial Coordinate System**



TYPE: Rotating, earth-referenced.

ORIGIN: At the intersection of the reference ellipsoid and the normal to it which passes through the launch site.

#### ORIENTATION AND LABELING:

The launch site tangent plane contains the site and is perpendicular to the reference ellipsoid normal which passes through the launch site.

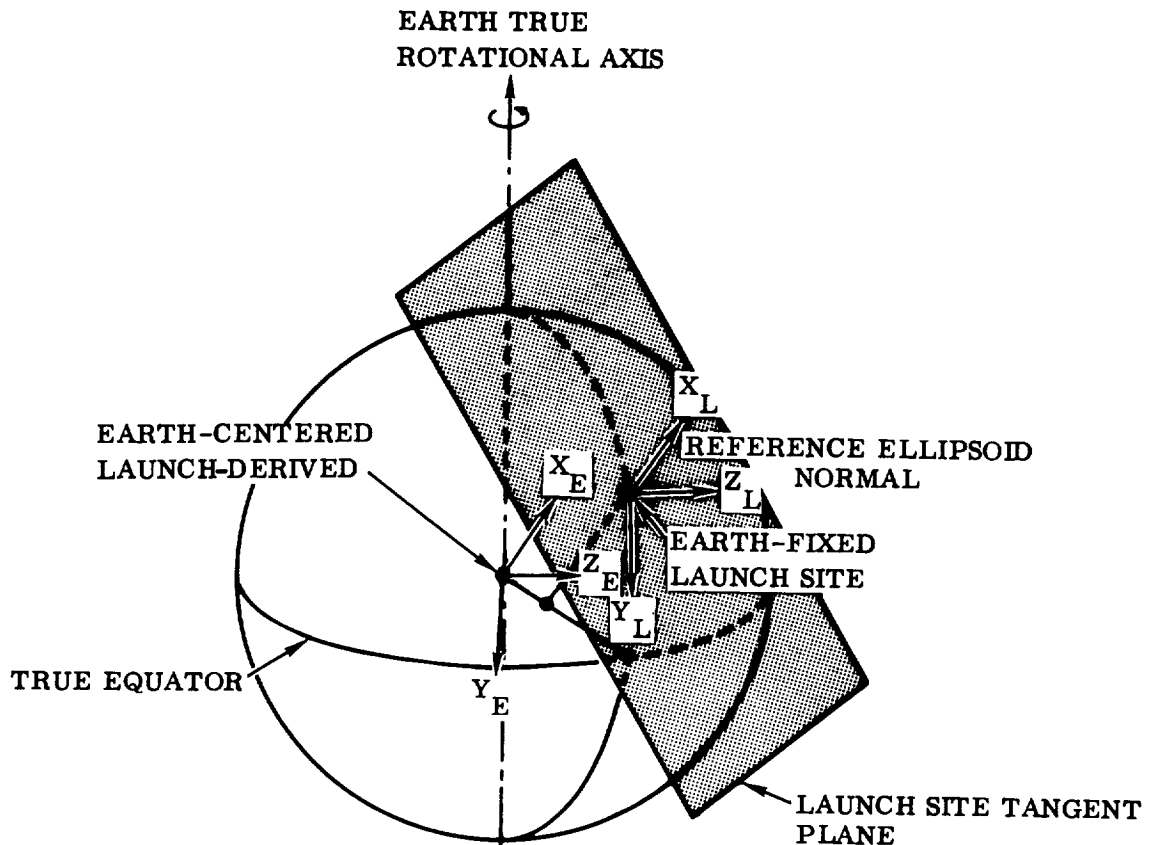
The  $X_L$  axis coincides with the reference ellipsoid normal passing through the site, positive upward.

The  $Z_L$  axis is parallel to the earth-fixed aiming azimuth, defined at guidance reference release time, and is positive downrange.

The  $Y_L$  axis completes a standard right-handed system.

The  $Y_L$ - $Z_L$  plane is the launch site tangent plane.

Figure 2. Earth-Fixed Launch Site Coordinate System



TYPE: Rotating, earth-referenced.

ORIGIN: The center of the earth.

ORIENTATION AND LABELING:

The launch site tangent plane contains the site and is perpendicular to the reference ellipsoid normal which passes through the launch site.

The  $X_E$  axis is parallel to the reference ellipsoid normal passing through the launch site and is positive toward the launch site.

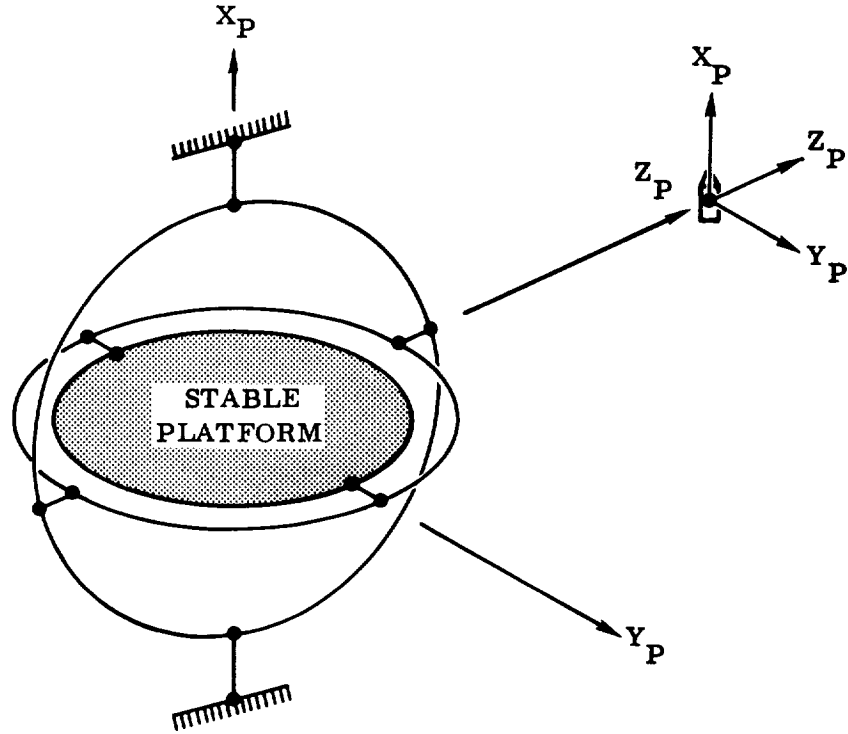
The  $Z_E$  axis is parallel to, and positive in the same direction as, the earth-fixed aiming azimuth.

The  $Y_E$  axis completes a standard right-handed system.

The  $Y_E$ - $Z_E$  plane is parallel to the launch site tangent plane.

This system is translatable with the earth-fixed launch site system.

Figure 3. Earth-Centered, Launch-Derived Coordinate System



**TYPE:** Nonrotating, vehicle-referenced.

**ORIGIN:** The intersection of the primary axes of the accelerometer.

**ORIENTATION AND LABELING:**

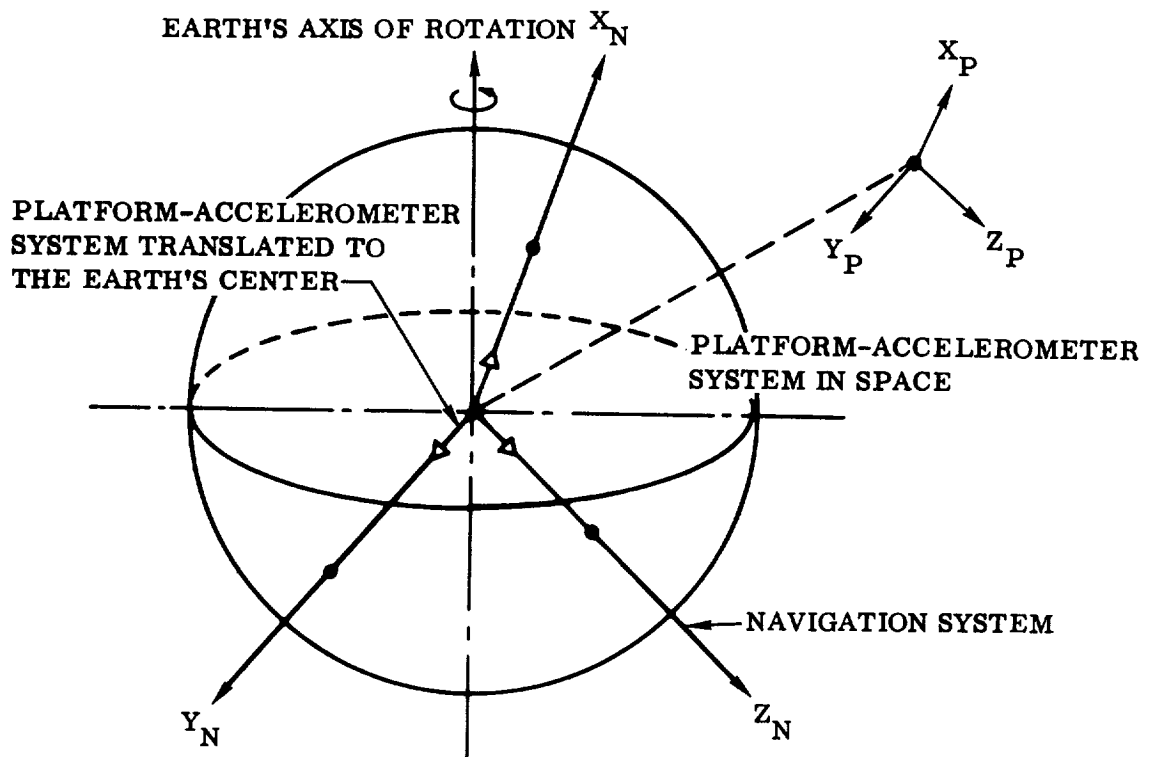
The  $X_P$  axis is parallel to the reference ellipsoid normal through the launch site, positive upward.

The  $Z_P$  axis is parallel to the aiming azimuth, positive downrange.

The  $Y_P$  axis completes a standard right-handed system.

This system is translatable with the earth-fixed launch site system at guidance reference release time.

**Figure 4. Launch Vehicle Platform-Accelerometer Coordinate System**



TYPE: Nonrotating, earth-referenced.

ORIGIN: The center of the earth.

#### ORIENTATION AND LABELING:

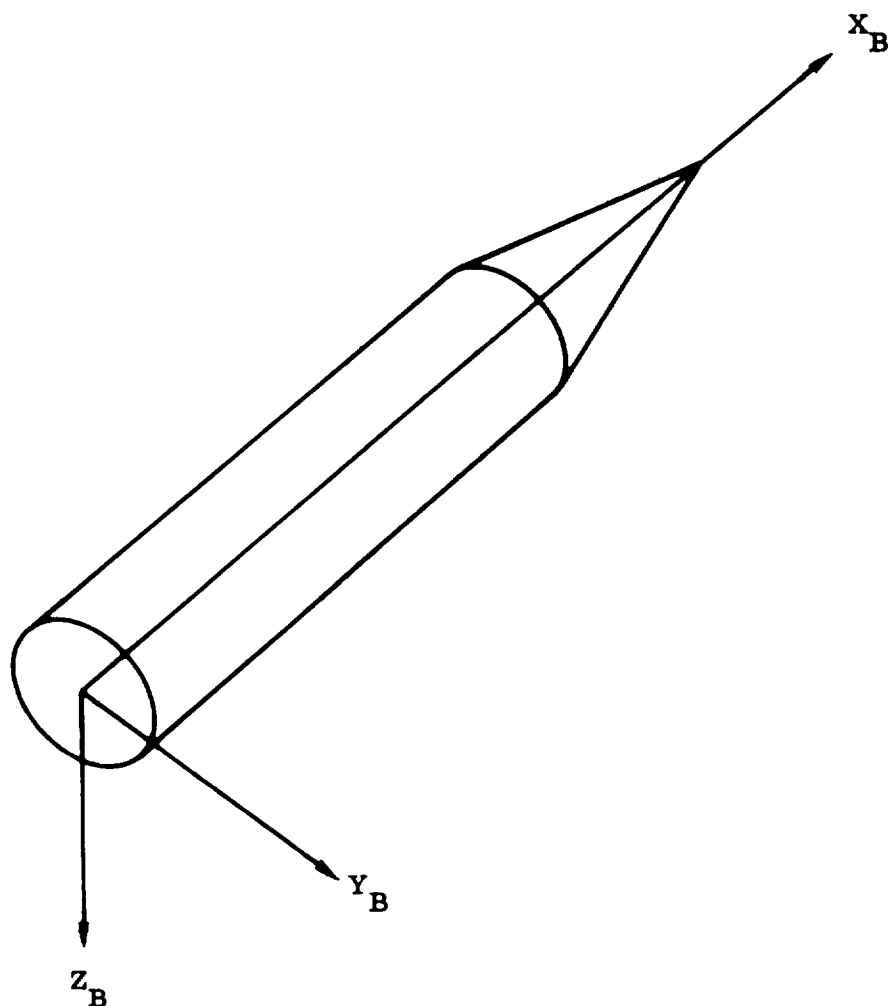
This system is translatable from the launch vehicle platform-accelerometer system at guidance reference release for the launch vehicle.

The  $X_N$  axis is parallel to the  $X_P$  axis of the launch vehicle platform-accelerometer system.

The  $Y_N$  axis is parallel to the  $Y_P$  axis of the launch vehicle platform-accelerometer system.

The  $Z_N$  axis completes a standard right-handed system.

Figure 5. Launch Vehicle Navigation Coordinate System



TYPE: Rotating, vehicle-referenced.

ORIGIN: A fixed point on the longitudinal axis.

ORIENTATION AND LABELING:

The  $X_B$  axis lies along the longitudinal axis of the vehicle, positive in the nominal direction of positive thrust acceleration.

The  $Y_B$  axis is directed along the "right wing."

The  $Z_B$  axis completes a standard right-handed system.

Figure 6. Body-Fixed Coordinate System





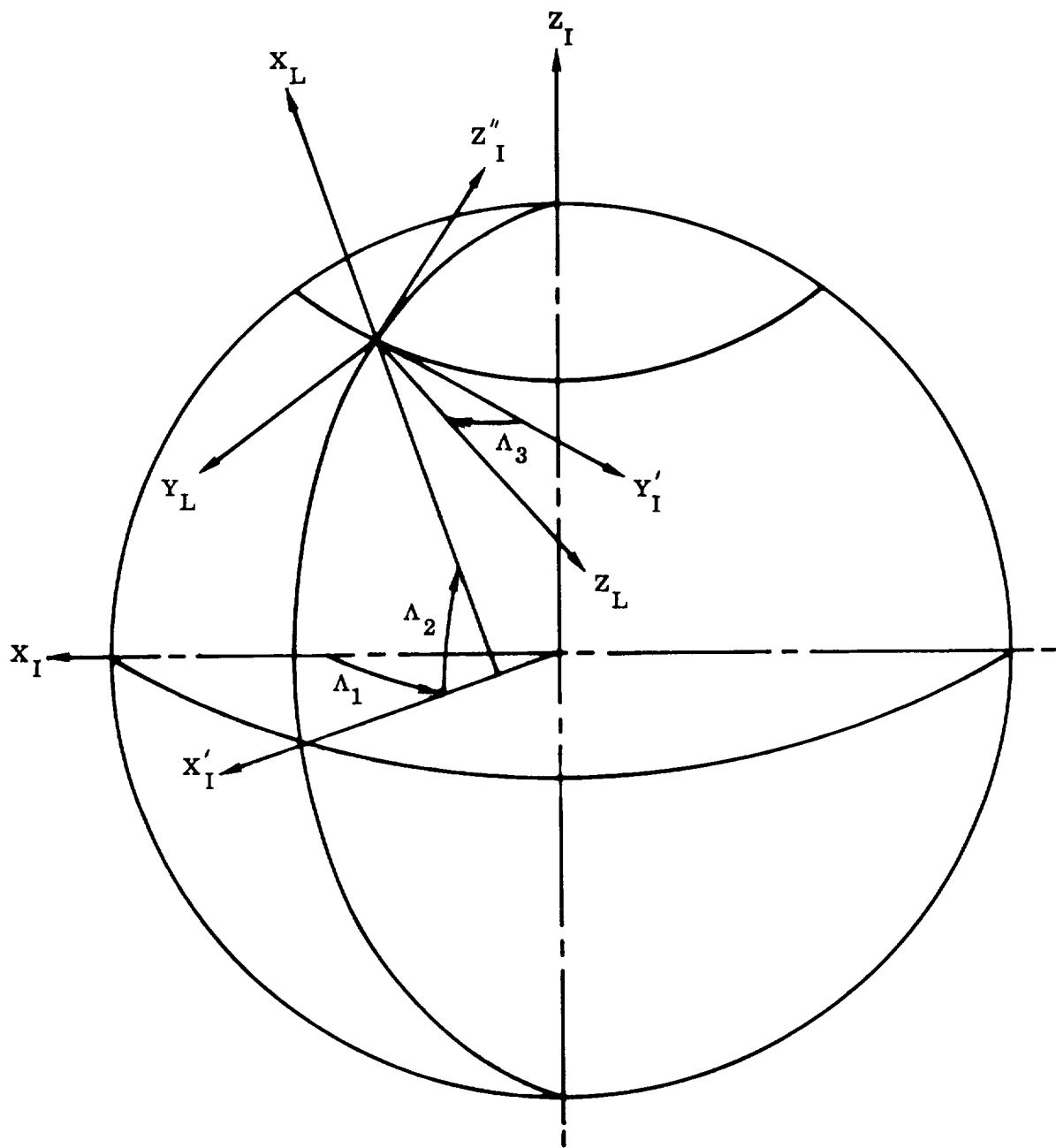


Figure 7. Geocentric Inertial to Earth-Fixed Launch Site  
Coordinate Transformation

amount  $\Lambda_2$ , resulting in the orientation  $(X_L, Y_I', Z_I'')$ . A further rotation about  $X_L$  in the negative direction by the amount  $(\Lambda_3 + 90^\circ)$  gives the final orientation of  $S_L$ . The reason for the rotation of  $(90^\circ + \Lambda_3)$  is that it is desirable to deal with angles which are nominally less than  $90^\circ$ . Since vehicles are generally launched in a southeasterly direction, it is necessary to specify the rotation shown in order for the  $Z_L$  axis to coincide with the downrange direction. Depending on the specific mission, however, any convenient rotation sequence may be specified.

The components of a vector in the  $S_L$  frame are related to the components in the  $S_I$  frame by

$$\bar{S}_L = A_{LI} \bar{S}_I \quad (1)$$

where the transformation matrix is\*

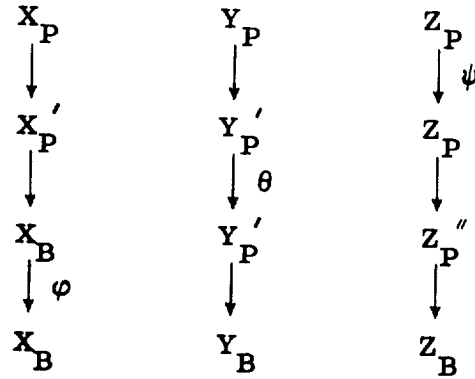
$$A_{LI} = \begin{bmatrix} c\Lambda_1 c\Lambda_2 & c\Lambda_2 s\Lambda_1 & s\Lambda_2 \\ c\Lambda_3 s\Lambda_2 c\Lambda_1 + s\Lambda_3 s\Lambda_1 & c\Lambda_3 s\Lambda_2 s\Lambda_1 - s\Lambda_3 c\Lambda_1 & -c\Lambda_3 c\Lambda_2 \\ s\Lambda_3 s\Lambda_2 c\Lambda_1 - c\Lambda_3 s\Lambda_1 & s\Lambda_3 s\Lambda_2 s\Lambda_1 + c\Lambda_3 c\Lambda_1 & -s\Lambda_3 c\Lambda_2 \end{bmatrix} \quad (2)$$

Note that  $\Lambda_1$  includes the effect of the earth's rotation, as follows.

$$\Lambda_1 = \Lambda_1^{(0)} + \Omega_E t$$

where  $\Lambda_1^{(0)}$  is the latitude of the launch site at time of launch and  $\Omega_E$  is the earth's angular velocity.

Launch Vehicle Platform-Accelerometer to Body-Fixed. For this case we have



\*For brevity, we write  $s\Lambda_1$ ,  $c\Lambda_1$  for  $\sin \Lambda_1 \cos \Lambda_1$ , etc.

Vector components are related by

$$\bar{S}_B = A_{BP} \bar{S}_P \quad (3)$$

where the transformation matrix is

$$A_{BP} = \begin{bmatrix} c\theta c\psi & c\theta s\psi & -s\theta \\ s\varphi s\theta c\psi - c\varphi s\psi & s\varphi s\theta s\psi + c\varphi c\psi & s\varphi c\theta \\ c\varphi s\theta c\psi + s\varphi s\psi & c\varphi s\theta s\psi - s\varphi c\psi & c\varphi c\theta \end{bmatrix} \quad (4)$$

Denoting the angular velocity of  $S_B$  by  $\bar{\omega}$ , we find by direct resolution of vectors

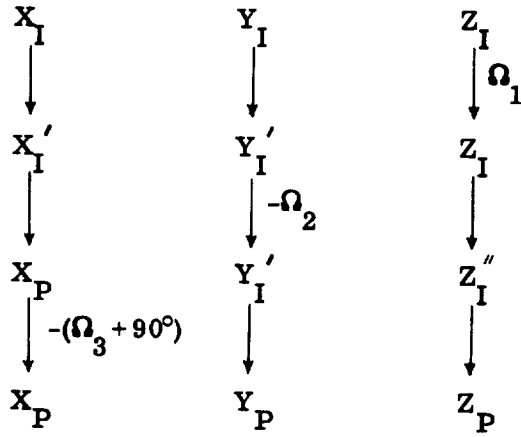
$$\begin{aligned} \omega_{X_B} &\equiv p = \dot{\phi} - \dot{\psi} \sin \theta \\ \omega_{Y_B} &\equiv q = \dot{\theta} \cos \varphi + \dot{\psi} \cos \theta \sin \varphi \\ \omega_{Z_B} &\equiv r = \dot{\psi} \cos \theta \cos \varphi - \dot{\theta} \sin \varphi \end{aligned} \quad (5)$$

Or, in inverse form

$$\begin{aligned} \dot{\psi} &= \sec \theta (r \cos \varphi + q \sin \varphi) \\ \dot{\theta} &= q \cos \varphi - r \sin \varphi \\ \dot{\phi} &= p + \tan \theta (r \cos \varphi + q \sin \varphi) \end{aligned} \quad (6)$$

When  $\theta \rightarrow \pm 90^\circ$ , the well known phenomenon of "gimbal lock" occurs. There are various ways of resolving this problem, <sup>(2,3)</sup> which, however, is beyond the scope of the present discussion.

Geocentric Inertial to Launch Vehicle Navigation. We will assume that at guidance reference release (which may be taken as the instant of launch), the system  $S_P$  is related to  $S_I$  by the rotation sequence



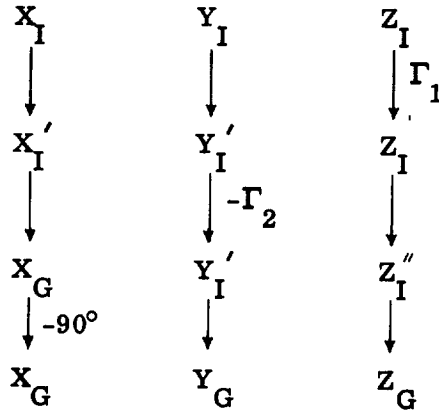
so that

$$\bar{S}_P = A_{PI} \bar{S}_I \quad (7)$$

The transformation matrix  $A_{PI}$  is identical to  $A_{LI}$  except that\*  $(\Omega_1, \Omega_2, \Omega_3)$  replace  $(\Lambda_1, \Lambda_2, \Lambda_3)$ . Furthermore, since by definition  $S_P$  is translatable from  $S_N$  at guidance reference release, we have

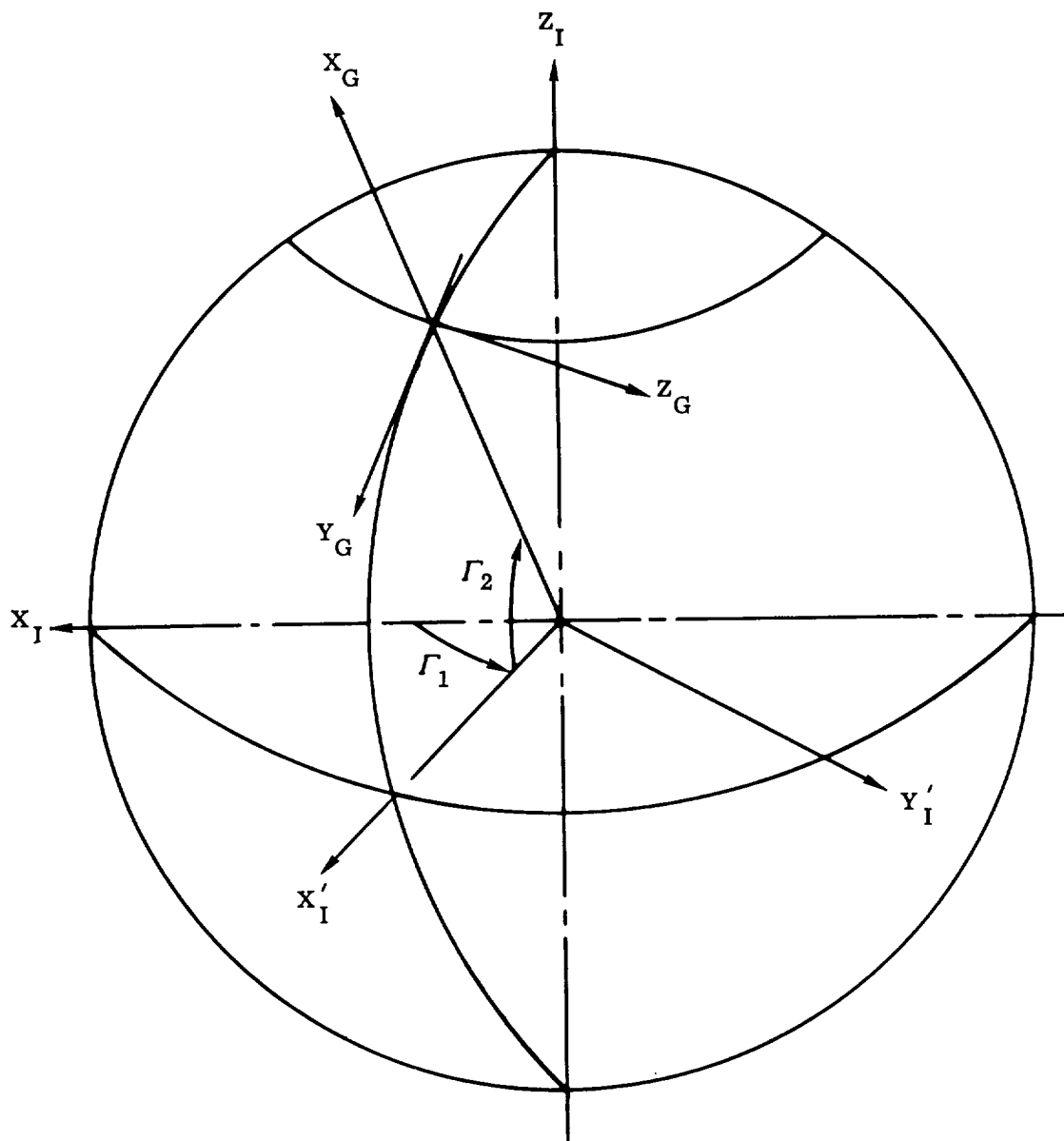
$$A_{PI} = A_{NI} \quad (8)$$

Local Geocentric Coordinate System. To describe the motion of the vehicle relative to the planet, it is convenient to define one more coordinate system,  $S_G$ , as shown in Fig. 8. The origin of  $S_G$  is on the surface of the planet and  $X_G$  is directed along a radial line which passes through the origin of  $S_B$ ; being positive in the upward direction, it is related to  $S_I$  via the sequence



\*Generally, at guidance reference release,  $S_P$  is translatable with  $S_L$ . In this case,

$$\Omega_1 = \Lambda_1^{(0)}, \Omega_2 = \Lambda_2, \Omega_3 = \Lambda_3.$$



TYPE: Rotating, earth-referenced.

ORIGIN: On the earth's surface.

ORIENTATION AND LABELING:

The  $X_G$  axis is along a radial line from the center of the earth to the origin of the body axis system.

The  $Z_G$  axis points in the direction of due east.

The  $Y_G$  axis completes a standard right-handed system.

Figure 8. Local Geocentric Coordinate System

Vector components are related by

$$\bar{S}_G = A_{GI} \bar{S}_I \quad (9)$$

where the transformation matrix is

$$A_{GI} = \begin{bmatrix} c\Gamma_1 & c\Gamma_2 & s\Gamma_1 & c\Gamma_2 & s\Gamma_2 \\ c\Gamma_1 & s\Gamma_2 & s\Gamma_1 & s\Gamma_2 & -c\Gamma_2 \\ -s\Gamma_1 & & c\Gamma_1 & & 0 \end{bmatrix} \quad (10)$$

### Properties of the Transformation Matrices

A generic transformation matrix,  $A_{MN}$ , satisfies the relation

$$A_{MN}^{-1} = A_{MN}^T \quad (11)$$

This follows from the orthogonality of the reference frame.\* Now

$$\bar{S}_M = A_{MN} \bar{S}_N$$

for any reference frames M and N. Therefore, using Eq. (11),

$$\bar{S}_N = A_{MN}^T \bar{S}_M$$

By defining

$$A_{NM} = A_{MN}^T \quad (12)$$

the various transformations of components of a vector may be expressed in a very systematic manner. Thus, for example,

$$\bar{S}_P = A_{PB} \bar{S}_B$$

$$\bar{S}_I = A_{IP} A_{PB} \bar{S}_B$$

$$\bar{S}_L = A_{LI} A_{IP} A_{PB} \bar{S}_B$$

---

\*A proof is available in any standard text on matrices.

etc. The following definitions are therefore meaningful and useful:

$$A_{IB} = A_{IP} A_{PB}$$

$$A_{LB} = A_{LI} A_{IB}$$

$$A_{LP} = A_{LI} A_{IP}$$

$$A_{BG} = A_{BP} A_{PI} A_{IG}$$

Many other transformation matrices may be similarly defined as needed.

### 3.2 EQUATIONS OF MOTION IN INERTIAL FRAME

This section is concerned with the derivation of the equations of motion that describe the powered-flight and coast-phase trajectory of a launch vehicle, leading either to surface impact or low earth orbit. The analysis is very general and takes account of such factors as jet damping, motion of the mass center relative to the vehicle, rotation of the earth, eccentric c.g., and nonspherical earth.

The equations of motion are most readily derived relative to an inertial frame. Using the results of the previous section, we will then relate the motion to earth-referenced and other coordinate systems as required.

The derivation of the equations of motion of a launch vehicle is complicated by the fact that the vehicle has variable mass and moment of inertia and also relative motion between various masses within the vehicle and the origin of the body axis system. In the latter category are included such factors as fuel sloshing, rocket engine rotation and vehicle flexibility. To take account of all these elements of the problem, we consider the very general configuration shown in Fig. 9. The inertial reference frame is  $(X_I, Y_I, Z_I)$ , and the body axis frame is denoted by  $(X_B, Y_B, Z_B)$ ; the origin of the latter is located at some fixed point on the body. It is assumed that the body under consideration is bounded by a fixed closed surface, and variation of mass occurs through particles leaving the system across this boundary. The angular velocity of the body frame with respect to the inertial reference is denoted by  $\bar{\omega}$ .

If now  $m_i$  is a generic mass particle, the total moment about the origin of the body frame is

$$\bar{M}_O = \sum_i \bar{\rho}_i \times \frac{d}{dt} (m_i \dot{\bar{R}}_i) \quad (13)$$

The time rate of change of the momentum,  $m_i \dot{\bar{R}}_i$ , is given by

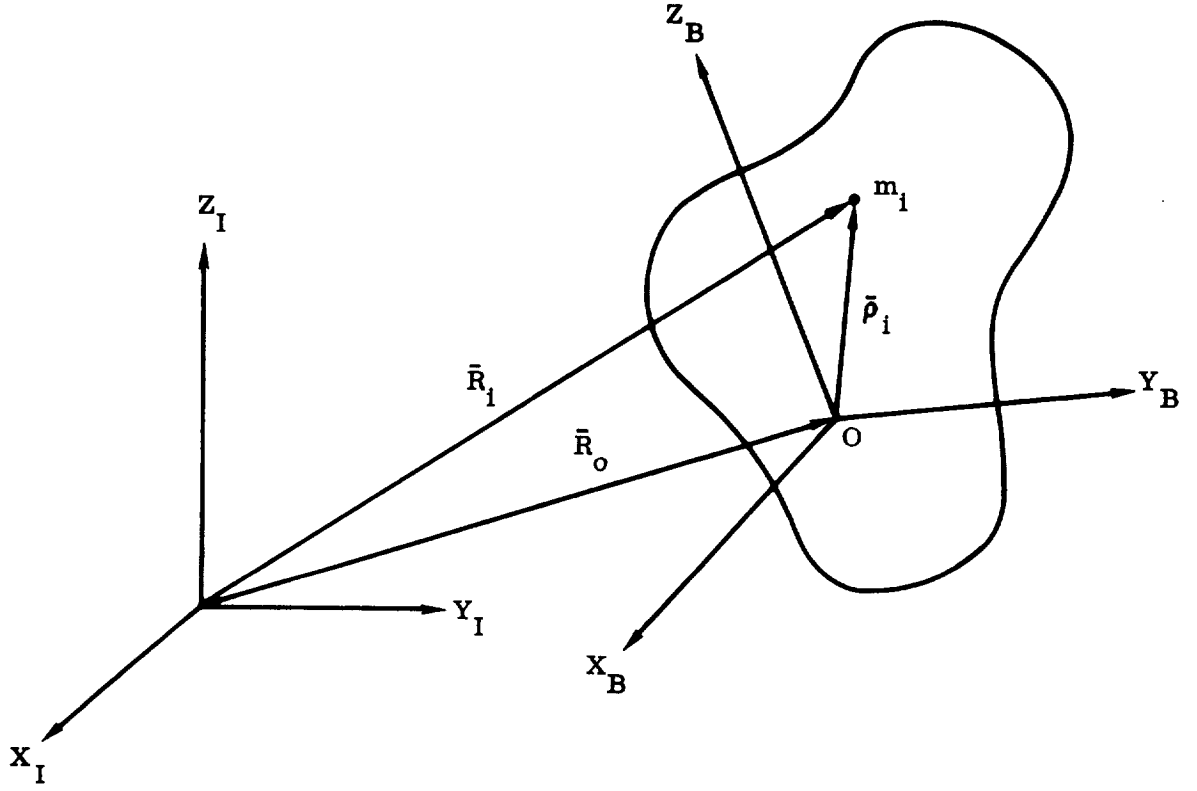


Figure 9. Configuration of Body of Variable Mass Relative to Inertial Reference

$$\frac{d}{dt}(m_i \dot{\bar{R}}_i) = m_i \ddot{\bar{R}}_i - \dot{m}_i \bar{c}_i \quad (14)$$

where the effect of variation in mass is accounted for (see Appendix A).

From Fig. 9

$$\bar{R}_i = \bar{R}_o + \bar{\rho}_i$$

Taking the derivative with respect to time,

$$\dot{\bar{R}}_i = \dot{\bar{R}}_o + \dot{\bar{\rho}}_i + \bar{\omega} \times \bar{\rho}_i \quad (15)$$

A further differentiation yields

$$\ddot{\bar{R}}_i = \ddot{\bar{R}}_o + \dot{\bar{\omega}} \times \bar{\rho}_i + \bar{\omega} \times (\bar{\omega} \times \bar{\rho}_i) + \ddot{\bar{\rho}}_i + 2\bar{\omega} \times \dot{\bar{\rho}}_i \quad (16)$$



Noting that  $\sum_i \bar{\rho}_i m_i = m \bar{\rho}_c$ , we find after substituting Eqs. (14) and (16) into Eq. (13)

$$\begin{aligned} \bar{\mathbf{M}}_o = m \bar{\rho}_c \times \ddot{\bar{\mathbf{R}}}_o + \sum_i \bar{\rho}_i \times (\dot{\bar{\omega}} \times m_i \bar{\rho}_i) + \sum_i \bar{\rho}_i \times [\bar{\omega} \times m_i (\bar{\omega} \times \bar{\rho}_i)] \\ + \sum_i \bar{\rho}_i \times m_i \ddot{\bar{\rho}}_i + 2 \sum_i \bar{\rho}_i \times (\bar{\omega} \times m_i \dot{\bar{\rho}}_i) - \sum_i \bar{\rho}_i \times \dot{m}_i \bar{c}_i \end{aligned} \quad (17)$$

By using the relations for the inertia dyadic developed in Appendix B, together with some standard formulas for vector products, Eq. (17) reduces to

$$\begin{aligned} \bar{\mathbf{M}}_o = m \bar{\rho}_c \times \ddot{\bar{\mathbf{R}}}_o + \frac{d}{dt} (\bar{\mathbf{I}} \cdot \bar{\omega}) - \sum_i \bar{\rho}_i \times \dot{m}_i (\bar{\omega} \times \bar{\rho}_i) - \sum_i \bar{\rho}_i \times \dot{m}_i \bar{c}_i \\ + \bar{\omega} \times \sum_i (\bar{\rho}_i \times m_i \dot{\bar{\rho}}_i) + \sum_i \bar{\rho}_i \times m_i \ddot{\bar{\rho}}_i \end{aligned} \quad (18)$$

The first term on the right-hand side of this equation represents the effect of the system center of mass being displaced from the origin of the body axis system. The second term corresponds to the usual rate of change of angular momentum. This takes account of mass variation as well as the effect of mass motion within the system. The third term represents the so-called "jet damping," while the fourth is due to thrust deflection. The last two terms represent relative motion of particles within the system due to fuel sloshing and bending.

The equation for linear acceleration follows directly from Newton's law, using Eq. (16); viz.,

$$\bar{\mathbf{F}} = m \left[ \ddot{\bar{\mathbf{R}}}_o + \bar{\omega} \times (\bar{\omega} \times \bar{\rho}_c) + \dot{\bar{\omega}} \times \bar{\rho}_c + 2 \bar{\omega} \times \dot{\bar{\rho}}_c + \ddot{\bar{\rho}}_c \right] - \sum_i \dot{m}_i \bar{c}_i \quad (19)$$

By writing this in the form

$$\begin{aligned} m \ddot{\bar{\rho}}_c = \bar{\mathbf{F}} - \left\{ m \ddot{\bar{\mathbf{R}}}_o + 2m (\bar{\omega} \times \dot{\bar{\rho}}_c) + m (\dot{\bar{\omega}} \times \bar{\rho}_c) \right. \\ \left. + m \bar{\omega} \times (\bar{\omega} \times \bar{\rho}_c) \right\} + \sum_i \dot{m}_i \bar{c}_i \end{aligned}$$

we may identify the terms as follows:

$$\bar{\mathbf{F}} \equiv \text{applied force}$$

$$m \ddot{\bar{\mathbf{R}}}_o \equiv \text{d'Alembert force}$$

$$2m (\bar{\omega} \times \dot{\bar{\rho}}_c) \equiv \text{Coriolis force}$$

$$m (\dot{\bar{\omega}} \times \bar{\rho}_c) \equiv \text{Euler force}$$

$$m \bar{\omega} \times (\bar{\omega} \times \bar{\rho}_c) \equiv \text{centrifugal force}$$

$$\sum_i \dot{\bar{m}}_i \bar{c}_i \equiv \text{thrust force due to variation in mass}$$

Equations (18) and (19) completely describe the motion of the system with respect to an inertial reference when the motion of the internal moving parts is prescribed. In the general case, the relative motion of internal parts may be due to propellers (in the case of aircraft), flywheel controllers (in orbiting satellites), or rocket engine deflection (in launch vehicles). In all of the aforementioned cases, this relative motion is a given function of time, and no further equations (other than kinematic constraints) are necessary to define the motion. However, sloshing pendulums or bending deflections constitute additional degrees of freedom and must be described by separate equations of motion. These effects, however, are of negligible importance in the trajectory problem and will therefore be neglected. They are nevertheless significant in describing the vehicle short-period dynamics and are considered in detail in Ref. 8.

Consider now the thrust term,  $\sum_i \dot{\bar{m}}_i \bar{c}_i$ . If this summation is performed over a typical launch vehicle, we would have

$$\sum_i \dot{\bar{m}}_i \bar{c}_i = \bar{F}_T = \begin{bmatrix} F_{TX_B} \\ F_{TY_B} \\ F_{TZ_B} \end{bmatrix} \equiv \begin{bmatrix} T_s + T_c \\ -T_c \delta_y \\ T_c \delta_p \end{bmatrix} \quad (20)$$

Here we take note of the fact that for some of the rocket engines,  $\bar{c}_i$  is always parallel to the  $X_B$  axis, while in pitch and yaw, this may be deflected by (small) angles,  $\delta_p$  and  $\delta_y$  respectively (see Fig. 10). Similarly, the thrust deflection term,  $\sum_i \bar{\rho}_i \times \dot{\bar{m}}_i \bar{c}_i$ , in Eq. (18) may be expressed as

$$\sum_i \bar{\rho}_i \times \dot{\bar{m}}_i \bar{c}_i = \bar{M}_T = \begin{bmatrix} M_{TX_B} \\ M_{TY_B} \\ M_{TZ_B} \end{bmatrix} \equiv \begin{bmatrix} T_r \ell_r \delta_r \\ T_c \ell_c \delta_p \\ T_c \ell_c \delta_y \end{bmatrix} \quad (21)$$

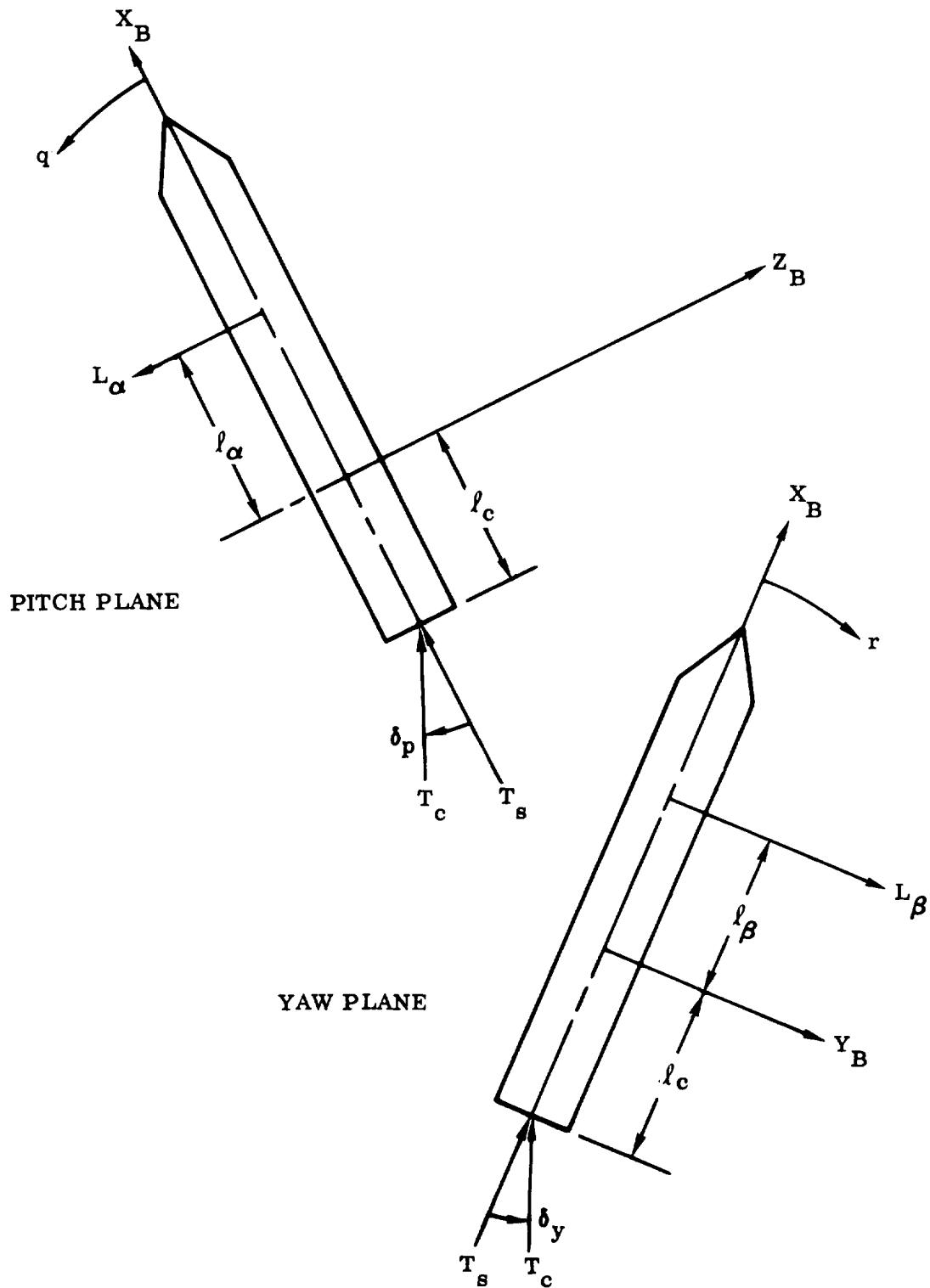


Figure 10. Thrust Configuration

For purposes of writing the trajectory equations, the terms in Eqs. (18) and (19) that are due to bending, sloshing, and jet damping are negligibly small and will be neglected. Since the location of the origin of the body axis system is arbitrary, vector  $\bar{\rho}_c$  is in general not a small quantity. However, for most large booster vehicles, the motion of the mass center relative to a fixed point on the body is small, and so is the rotation vector,  $\bar{\omega}$ . Consequently, terms involving products of  $\bar{\omega}$ ,  $\dot{\bar{\rho}}$ , and  $\ddot{\bar{\rho}}$  will be dropped. In this case, Eqs. (18) and (19) reduce to

$$\bar{F} + \bar{F}_T = m \ddot{\bar{R}}_o + m \dot{\bar{\omega}} \times \bar{\rho}_c \quad (22)$$

$$\bar{M}_o + \bar{M}_T = \frac{d}{dt} (\bar{I} \cdot \bar{\omega}) + m \bar{\rho}_c \times (\ddot{\bar{R}}_o + \ddot{\bar{\rho}}_c) \quad (23)$$

The external forces and moments in Eqs. (22) and (23) are due to aerodynamics and gravity; we express these as follows:

$$\bar{F} = \bar{F}_A + \bar{F}_g$$

$$\bar{M}_o = \bar{M}_A + \bar{M}_g$$

Now let  $\dot{\bar{R}}_o = \bar{U}$ . Then in expanded form Eqs. (22) and (23) may be written as

$$\bar{F}_A + \bar{F}_g + \bar{F}_T = m \left[ \bar{U} + \bar{\omega} \times \bar{U} + \dot{\bar{\omega}} \times \bar{\rho}_c \right] \quad (24)$$

$$\begin{aligned} \bar{M}_A + \bar{M}_g + \bar{M}_T = & \bar{I} \cdot \dot{\bar{\omega}} + \bar{I} \cdot \bar{\omega} + \bar{\omega} \times (\bar{I} \cdot \bar{\omega}) + m \bar{\rho}_c \\ & \times \left[ \bar{U} + \bar{\omega} \times \bar{U} + \ddot{\bar{\rho}}_c \right] \end{aligned} \quad (25)$$

These two equations describe the motion of the vehicle with respect to an inertial reference. The motion with respect to various frames of reference may be obtained by using the transformation matrices developed in Sec. 3.1. We now consider the explicit form of the external forces and moments applied to the vehicle.

### 3.3 FORCES AND MOMENTS

The forces and moments acting on the vehicle stem from three sources: thrust, gravity, and aerodynamics. We consider these in turn.

#### 3.3.1 Thrust

Expressions for the forces and moments due to thrust, in the case of swiveling rocket engines, have already been derived in Sec. 3.2. These are

$$\bar{F}_T = \begin{bmatrix} F_{TX_B} \\ F_{TY_B} \\ F_{TZ_B} \end{bmatrix} \equiv \begin{bmatrix} T_s + T_c \\ -T_c \delta_y \\ T_c \delta_p \end{bmatrix} \quad (26)$$

$$\bar{M}_T = \begin{bmatrix} M_{TX_B} \\ M_{TY_B} \\ M_{TZ_B} \end{bmatrix} \equiv \begin{bmatrix} T_r \ell_r \delta_r \\ T_c \ell_c \delta_p \\ T_c \ell_c \delta_y \end{bmatrix} \quad (27)$$

### 3.3.2 Gravity

For purposes of accurate guidance and navigation, it is necessary to account for the nonspherical shape of the earth. In computing the force of gravity on a body which is above the earth's surface, the latter is assumed to be an ellipsoid of revolution with an associated gravitational potential.<sup>(4)</sup> The components of the gravity vector in the local geocentric system are\* (see Fig. 11):

$$g_{X_G} = -\frac{\mu}{R_o^2} \left[ 1 + J_1 P_2 \left( \frac{R_e}{R_o} \right)^2 + \frac{4J_2 P_3}{5} \left( \frac{R_e}{R_o} \right)^3 + \frac{J_3 P_4}{6} \left( \frac{R_e}{R_o} \right)^4 \right] \quad (28)$$

$$g_{Y_G} = \frac{\mu}{R_o^2} \left[ 2J_1 P_5 \left( \frac{R_e}{R_o} \right)^2 - \frac{3J_2 P_6}{5} \left( \frac{R_e}{R_o} \right)^3 - \frac{2J_3 P_7}{3} \left( \frac{R_e}{R_o} \right)^4 \right] \quad (29)$$

$$g_{Z_G} = 0$$

where

$$\mu = 1.407698 \times 10^{16} \text{ ft}^3/\text{sec}^2$$

$$R_e = 20.925631 \times 10^6 \text{ ft}$$

$$J_1 = 1623.41 \times 10^{-6}$$

\*Cf. Ref. 15

26

$$J_2 = 6.04 \times 10^{-6}$$

$$J_3 = 6.37 \times 10^{-6}$$

$$P_2 = 1 - 3 \sin^2 \Gamma_2$$

$$P_3 = 3 \sin \Gamma_2 - 5 \sin^3 \Gamma_2$$

$$P_4 = 3 - 30 \sin^2 \Gamma_2 + 35 \sin^4 \Gamma_2$$

$$P_5 = \sin \Gamma_2 \cos \Gamma_2$$

$$P_6 = \cos \Gamma_2 (1 - 5 \sin^2 \Gamma_2)$$

$$P_7 = \sin \Gamma_2 \cos \Gamma_2 (7 \sin^2 \Gamma_2 - 3)$$

In the body axis system, the gravity components become

$$\begin{bmatrix} g_{X_B} \\ g_{Y_B} \\ g_{Z_B} \end{bmatrix} = A_{BG} \begin{bmatrix} g_{X_G} \\ g_{Y_G} \\ g_{Z_G} \end{bmatrix} \quad (30)$$

Using Fig. 12, the forces and moments due to gravity, expressed in body axis coordinates, are obtained as

$$\bar{F}_g = \begin{bmatrix} F_{g_{X_B}} \\ F_{g_{Y_B}} \\ F_{g_{Z_B}} \end{bmatrix} = m \begin{bmatrix} g_{X_B} \\ g_{Y_B} \\ g_{Z_B} \end{bmatrix} \quad (31)$$

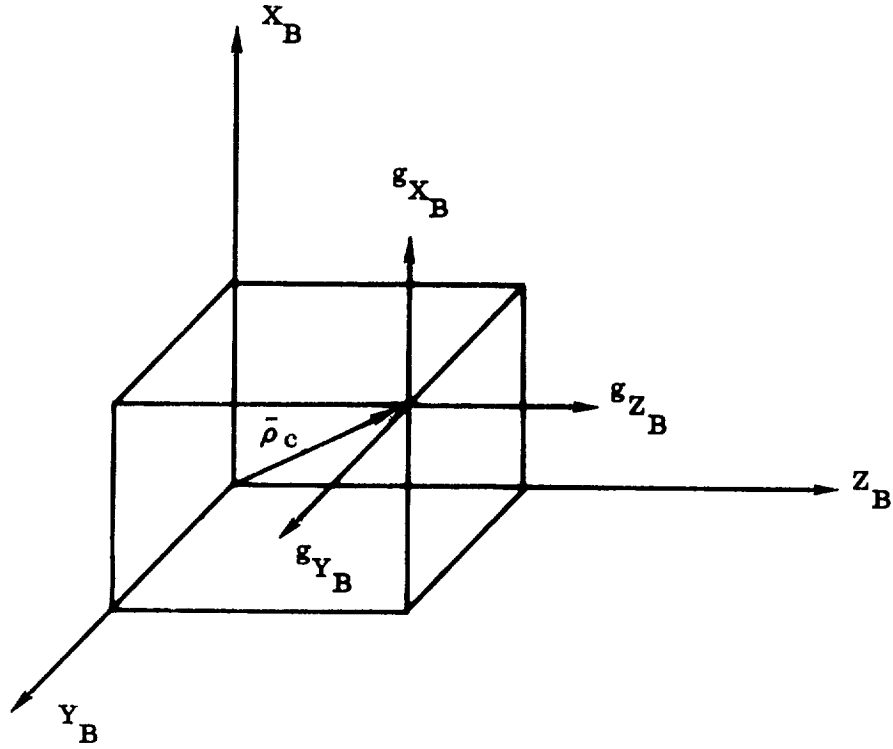


Figure 12. Gravity Components in Body Axis System

$$\bar{\mathbf{M}}_g = \begin{bmatrix} M_{gX_B} \\ M_{gY_B} \\ M_{gZ_B} \end{bmatrix} \equiv m \begin{bmatrix} g_{Z_B}^y{}_{cg} - g_{Y_B}^z{}_{cg} \\ g_{X_B}^z{}_{cg} - g_{Z_B}^x{}_{cg} \\ g_{Y_B}^x{}_{cg} - g_{X_B}^y{}_{cg} \end{bmatrix} \quad (32)$$

### 3.3.3 Aerodynamics

We write the components of the aerodynamic force and moment vectors relative to the body axis system as follows.

$$\bar{\mathbf{F}}_A = \begin{bmatrix} F_{AX_B} \\ F_{AY_B} \\ F_{AZ_B} \end{bmatrix} \quad (33)$$



$$\bar{\mathbf{M}}_A = \begin{bmatrix} M_{AX_B} \\ M_{AY_B} \\ M_{AZ_B} \end{bmatrix} \quad (34)$$

where, in the usual way,

$$F_{AX_B} = \frac{1}{2} \rho V^2 A_1 C_A \quad (35)$$

$$F_{AY_B} = \frac{1}{2} \rho V^2 A_2 C_Y \quad (36)$$

$$F_{AZ_B} = \frac{1}{2} \rho V^2 A_3 C_N \quad (37)$$

$$M_{AX_B} = \frac{1}{2} \rho V^2 A_4 \ell_1 C_\ell \quad (38)$$

$$M_{AY_B} = \frac{1}{2} \rho V^2 A_5 \ell_2 C_N \quad (39)$$

$$M_{AZ_B} = \frac{1}{2} \rho V^2 A_6 \ell_3 C_Y \quad (40)$$

V is the airspeed given by Eq. (52), and the  $\ell_i$  and  $A_i$  are reference lengths and areas respectively.

Each of the aerodynamic coefficients,  $C_\lambda$ , may be expressed in the form\*

$$\begin{aligned} C_\lambda = & C_{\lambda o} + C_{\lambda \alpha} \alpha + C_{\lambda \beta} \beta + \frac{\ell \nu}{2V} C_{\lambda \dot{\alpha}} \dot{\alpha} + \frac{\ell \nu}{2V} C_{\lambda \dot{\beta}} \dot{\beta} + \frac{\ell \nu}{2V} C_{\lambda p} p \\ & + \frac{\ell \nu}{2V} C_{\lambda q} q + \frac{\ell \nu}{2V} C_{\lambda r} r + \sum_i \left( C_{\lambda \delta_i} \delta_i + \frac{\ell \nu}{2V} C_{\lambda \dot{\delta}_i} \dot{\delta}_i \right) \end{aligned} \quad (41)$$

---

\*p, q, and r are defined by Eq. (5).

where  $\lambda$  stands for A, Y, N, or  $\ell$ , and  $C_{\lambda 0}$  represents the value of  $C_\lambda$  in the steady state, while

$$C_{\lambda \alpha} \equiv \frac{\partial C_\lambda}{\partial \alpha}, \text{ etc.}$$

Also, the subscript,  $\nu$ , on  $\ell_\nu$  equals 1, 2, or 3, corresponding to  $\lambda$  equals  $\ell$ , N, or Y. The quantities of  $\delta_i$  account for control surface deflections. In the quasilinear theory, coefficients  $C_{\lambda \alpha}$ ,  $C_{\lambda \beta}$ , etc. are assumed independent of  $\alpha$ ,  $\beta$ ,  $\dot{\alpha}$ ,  $\dot{\beta}$ ,  $p$ ,  $q$ ,  $r$ ,  $\delta_i$ , and  $\dot{\delta}_i$ . The truncation of the Taylor expansion (41) implies that the variables shown are small quantities.

Using the general form of the aerodynamic forces and moments given by Eqs. (35) - (40), any degree of refinement (including nonlinear and cross-coupling terms) may be incorporated, depending on the specific vehicle and mission. We consider only the simplest case of a large booster vehicle having a high degree of axial symmetry and no appreciable aerodynamic lift surfaces. In this case, the only significant stability derivatives are  $C_{N\alpha}$  and  $C_{Y\beta}$ , while the only aerodynamic force in the  $X_B$  direction is the drag, which is assumed independent of angle of attack. Consequently, Eqs. (35) - (40) reduce to

$$F_{AX_B} = -\frac{1}{2} \rho V^2 A_1 C_D \quad (42)$$

$$F_{AY_B} = L_\beta \beta \quad (43)$$

$$F_{AZ_B} = -L_\alpha \alpha \quad (44)$$

$$M_{AX_B} \approx 0 \quad (45)$$

$$M_{AY_B} = L_\alpha \ell_\alpha \alpha \quad (46)$$

$$M_{AZ_B} = L_\beta \ell_\beta \beta \quad (47)$$

In accordance with common practice, we have assumed that the drag force acts in the negative  $X_B$  direction and have written the drag coefficient  $C_D$  to highlight this convention. It is also common practice to assume that the normal force in the pitch plane acts in the negative  $Z_B$  direction, which accounts for the negative sign in

Eq. (44). Also,  $\ell_\alpha$  and  $\ell_\beta$  represent the distances (measured from the origin of  $S_B$ ) to the centers of pressure in the pitch and yaw planes. Finally, we note that\*

$$L_\alpha = \frac{1}{2} \rho V^2 A_5 \int_0^L \frac{\partial C_N(\ell)}{\partial \alpha} d\ell \quad (48)$$

$$L_\beta = \frac{1}{2} \rho V^2 A_6 \int_0^L \frac{\partial C_Y(\ell)}{\partial \beta} d\ell \quad (49)$$

Evaluation of Eqs. (43) - (47) requires the determination of the angles of attack in pitch and yaw. This is done as follows. Expressing the components of the wind velocity vector in the local geocentric system, we have\*\*

$$\bar{W} = \begin{bmatrix} W_{X_G} \\ W_{Y_G} \\ W_{Z_G} \end{bmatrix} = \begin{bmatrix} 0 \\ -W_N \\ W_E + R_O \Omega_E \cos \Gamma_2 \end{bmatrix} \quad (50)$$

The velocity of the origin of the body axis system is (in body axis coordinates)

$$\dot{\bar{R}}_O = \bar{U} = \begin{bmatrix} U_{X_B} \\ U_{Y_B} \\ U_{Z_B} \end{bmatrix} \equiv \begin{bmatrix} u \\ v \\ w \end{bmatrix} \quad (51)$$

Consequently, the airspeed is given by

---

\*See Sec. 3.3.5 of Ref. 8.

\*\*Note that  $R_O \Omega_E \cos \Gamma_2$  is the component parallel to the  $Z_G$  axis of the vector product  $\bar{\Omega}_E \times \bar{R}_O$ .

$$\bar{V} = \bar{U} - \bar{W} = \begin{bmatrix} u \\ v \\ w \end{bmatrix} - A_{BG} \begin{bmatrix} 0 \\ -W_N \\ W_E + R_o \Omega_E \cos \Gamma_2 \end{bmatrix} \equiv \begin{bmatrix} u' \\ v' \\ w' \end{bmatrix} \quad (52)$$

The required angles of attack are

$$\alpha = \tan^{-1} \left( \frac{w'}{v} \right) \quad (53)$$

$$\beta = \tan^{-1} \left( \frac{v'}{v} \right) \quad (54)$$

where

$$V = \left[ (u')^2 + (v')^2 + (w')^2 \right]^{1/2} \quad (55)$$

### 3.4 COMPLETE EQUATIONS OF MOTION

A complete description of the motion of the vehicle is contained in Eqs. (24) and (25), which are repeated here for convenience.

$$\bar{F}_A + \bar{F}_g + \bar{F}_T = m \left[ \bar{\ddot{U}} + \bar{\omega} \times \bar{U} + \dot{\bar{\omega}} \times \bar{\rho}_c \right] \quad (56)$$

$$\begin{aligned} \bar{M}_A + \bar{M}_g + \bar{M}_T &= \bar{I} \cdot \dot{\bar{\omega}} + \bar{I} \cdot \bar{\omega} + \bar{\omega} \times (\bar{I} \cdot \bar{\omega}) + m \bar{\rho}_c \\ &\times \left[ \bar{\ddot{U}} + \bar{\omega} \times \bar{U} + \dot{\bar{\omega}} \times \bar{\rho}_c \right] \end{aligned} \quad (57)$$

The components of the forces and moments relative to body axes have been developed in the preceding section. Thus the motion of the vehicle relative to an inertial reference is completely determined.

In order to emphasize fundamental principles, we have thus far resisted the temptation to expand the vector matrix quantities. Also, the precise manner in which the equations are expanded depends on a stipulation of the parameters of interest and the degree of accuracy required. One may, for example, be concerned chiefly with determining an accurate trajectory relative to the earth's surface. On the other hand, one may be primarily interested in calculating loads on the vehicle as it passes through

the atmosphere. Or, for purposes of ascertaining orbital parameters, one may be interested mainly in values at burnout.

Of course, by working with the complete system, any or all of these quantities are obtainable by applying the coordinate transformation matrices where required. For specialized cases, certain formulations are more efficient, and various simplifications may be introduced.

However, in order to exhibit the computational sequence required for computer simulation, we will now reduce the equations of motion to scalar form, indicating the means whereby various quantities of interest are determined.

From Eqs. (56), (51), (44), (43), (42), (31), (30), (26), and (5), we have

$$\begin{aligned}
 m \begin{bmatrix} \dot{u} + qw - rv + z_{cg} \dot{q} - y_{cg} \dot{r} \\ \dot{v} + ru - pw + x_{cg} \dot{r} - z_{cg} \dot{p} \\ \dot{w} + pv - qu + y_{cg} \dot{p} - x_{cg} \dot{q} \end{bmatrix} &= \begin{bmatrix} -\frac{1}{2} \rho V^2 A_1 C_D \\ L_\beta \beta \\ -L_\alpha \alpha \end{bmatrix} \\
 + m A_{BG} \begin{bmatrix} g_{X_G} \\ g_{Y_G} \\ 0 \end{bmatrix} + \begin{bmatrix} T_s + T_c \\ -T_c \delta_y \\ T_c \delta_p \end{bmatrix} & \quad (58)
 \end{aligned}$$

Also, from Eqs. (57), (47), (46), (45), (32), and (27),

$$\begin{bmatrix}
I_{xx} \dot{p} + \dot{I}_{xx} p + (I_{zz} - I_{yy}) qr + y_{cg} (\dot{w} + pv - qu + \ddot{z}_{cg}) - z_{cg} (\dot{v} + ru - pw + \ddot{y}_{cg}) \\
I_{yy} \dot{q} + \dot{I}_{yy} q + (I_{xx} - I_{zz}) pr + z_{cg} (\dot{u} + qw - rv + \ddot{x}_{cg}) - x_{cg} (\dot{w} + pv - qu + \ddot{z}_{cg}) \\
I_{zz} \dot{r} + \dot{I}_{zz} r + (I_{yy} - I_{xx}) pq + x_{cg} (\dot{v} + ru - pw + \ddot{y}_{cg}) - y_{cg} (\dot{u} + qw - rv + \ddot{x}_{cg})
\end{bmatrix}$$

$$= \begin{bmatrix} 0 \\ L_{\alpha} \ell_{\alpha} \alpha \\ L_{\beta} \ell_{\beta} \beta \end{bmatrix} + m \begin{bmatrix} g_{Z_B} y_{cg} - g_{Y_B} z_{cg} \\ g_{X_B} z_{cg} - g_{Z_B} x_{cg} \\ g_{Y_B} x_{cg} - g_{X_B} y_{cg} \end{bmatrix} + \begin{bmatrix} T_r \ell_r \delta_r \\ T_c \ell_c \delta_p \\ T_c \ell_c \delta_y \end{bmatrix} \quad (59)$$

Here we have assumed that products of inertia are negligibly small and may be discarded.

We have also (see Sec. 3.3.3)

$$V = \left[ (u')^2 + (v')^2 + (w')^2 \right]^{1/2} \quad (60)$$

$$\begin{bmatrix} u' \\ v' \\ w' \end{bmatrix} = \begin{bmatrix} u \\ v \\ w \end{bmatrix} - A_{BG} \begin{bmatrix} 0 \\ -W_N \\ W_E + R_o \Omega_E \cos \Gamma_2 \end{bmatrix} \quad (61)$$

$$\alpha = \tan^{-1} \left( \frac{w'}{V} \right) \quad (62)$$

$$\beta = \tan^{-1} \left( \frac{v'}{V} \right) \quad (63)$$

The velocity vector has components in the geocentric inertial system, which are obtainable by

$$\begin{bmatrix} u_I \\ v_I \\ w_I \end{bmatrix} = A_{IP} A_{PB} \begin{bmatrix} u \\ v \\ w \end{bmatrix} \quad (64)$$

Integrating this, we obtain the components of the vehicle position vector expressed in geocentric inertial coordinates; viz.,

$$\begin{cases} \int u_I dt = R_{oX_I} + C_1 \\ \int v_I dt = R_{oY_I} + C_2 \\ \int w_I dt = R_{oZ_I} + C_3 \end{cases} \quad (65)$$

where the constants,  $C_i$ , depend on the initial conditions. With the help of Fig. 8, we find

$$\Gamma_1 = \cos^{-1} \left[ \frac{R_{oX_I}}{\left( R_{oX_I}^2 + R_{oY_I}^2 \right)^{1/2}} \right] \quad (66)$$

$$\Gamma_2 = \tan^{-1} \left[ \frac{R_{oZ_I}}{\left( R_{oX_I}^2 + R_{oY_I}^2 \right)^{1/2}} \right] \quad (67)$$

Finally, we note that

$$\dot{\Lambda}_1 = \Omega_E \quad (68)$$

while  $\Lambda_2$ ,  $\Lambda_3$ ,  $\Omega_1$ ,  $\Omega_2$ , and  $\Omega_3$  are known constants.

The foregoing equations are sufficient to describe the motion relative to an inertial reference. To relate the trajectory to the earth's surface, some further

transformations are required. We introduce a coordinate system  $(X_G', Y_G', Z_G')$ , which we shall call  $S_G'$ , whose origin coincides with the origin of  $S_B$  and which is translatable with  $S_G$ . The angular velocity of  $S_G'$  is

$$\bar{\Omega} = \begin{bmatrix} \Omega_{X_G} \\ \Omega_{Y_G} \\ \Omega_{Z_G} \end{bmatrix} = \begin{bmatrix} \Omega_E \sin \Gamma_2 \\ -\Omega_E \cos \Gamma_2 \\ 0 \end{bmatrix} \quad (69)$$

Now

$$\bar{U} = \bar{R}_o + \bar{\Omega} \times \bar{R}_o \quad (70)$$

The components of  $\bar{R}_o$  in the  $S_G'$  frame are denoted by

$$\bar{R}_o = \begin{bmatrix} u_G \\ v_G \\ w_G \end{bmatrix}$$

Since

$$\bar{R}_o = \begin{bmatrix} R_o \\ 0 \\ 0 \end{bmatrix}$$

in the  $S_G'$  frame, Eq. (70) reduces to

$$\begin{bmatrix} u_G \\ v_G \\ w_G \end{bmatrix} = A_{GB} \begin{bmatrix} u \\ v \\ w \end{bmatrix} - \begin{bmatrix} 0 \\ 0 \\ R_o \Omega_E \cos \Gamma_2 \end{bmatrix} \quad (71)$$

A flight path angle,  $\gamma$ , and an azimuth angle,  $\sigma$ , are defined in Fig. 13. It follows immediately that



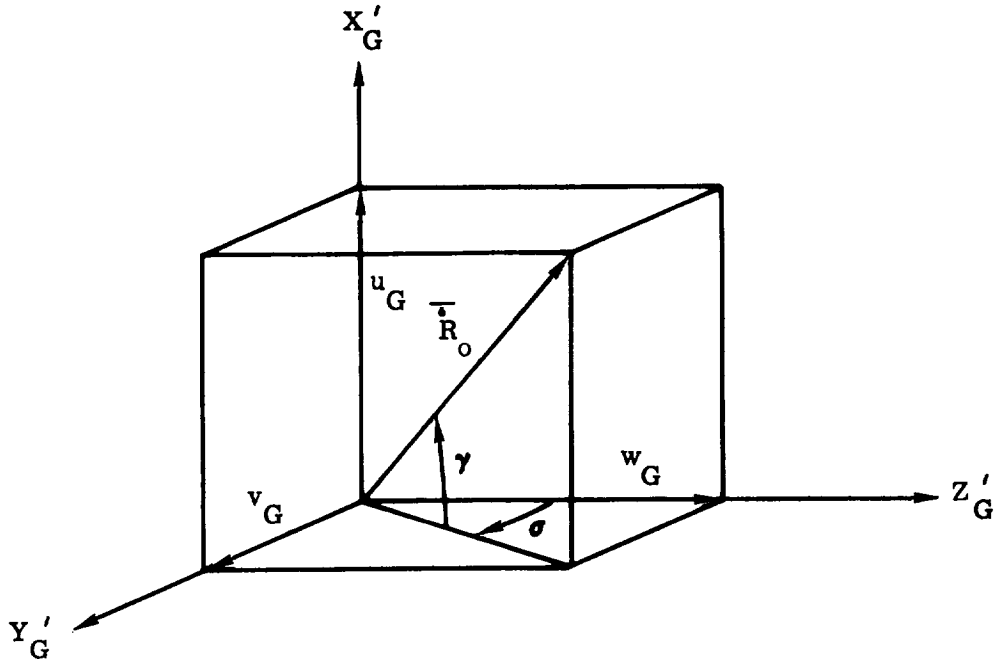


Figure 13. Definition of Flight Path and Azimuth Angles

$$\gamma = \sin^{-1} \left[ \frac{u_G}{\left( u_G^2 + v_G^2 + w_G^2 \right)^{1/2}} \right] \quad (72)$$

$$\sigma = \sin^{-1} \left[ \frac{v_G}{\left( v_G^2 + w_G^2 \right)^{1/2}} \right] \quad (73)$$

For high-precision trajectories, it is necessary to relate the motion to a surface in the shape of an oblate spheroid. The situation is depicted in Fig. 14, where the line OP represents the position vector,  $\bar{R}_O$ . We seek to determine the geodetic altitude, AP, the geodetic latitude,  $\Gamma_G$ , and the flight path and azimuth angles expressed in geodetic coordinates. The available quantities are the position vector,  $\bar{R}_O$ , and the geocentric latitude,  $\Gamma_2$ .

The equation for the surface in the meridian plane is given by

$$\frac{X^2}{R_{EA}^2} + \frac{Z^2}{R_{EB}^2} = 1 \quad (74)$$

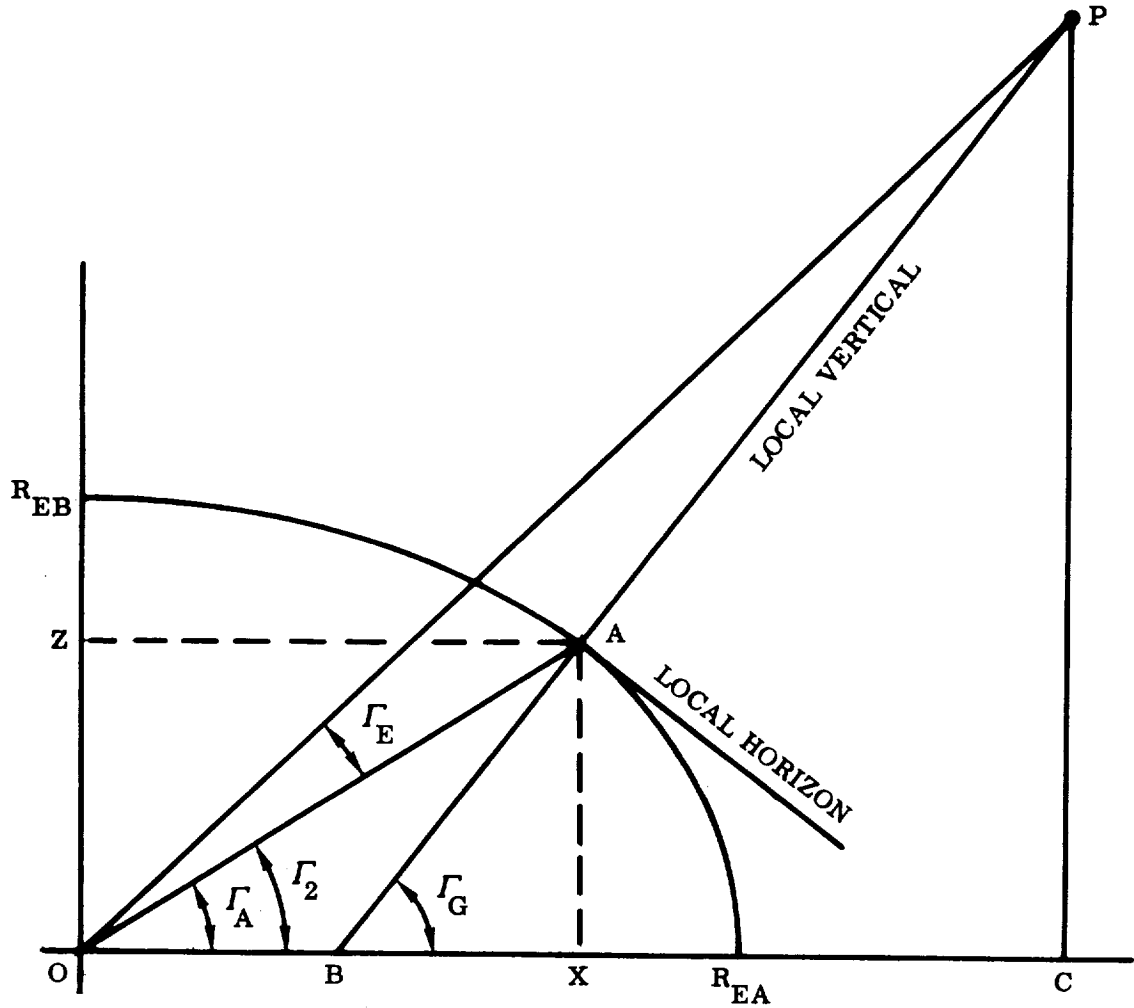


Figure 14. Meridian Plane Through an Oblate Spheroid Earth

From the geometry of the ellipse, we have

$$\Gamma_G = \cos^{-1} \left\{ \frac{R_{EB} X}{R_{EA} \left[ R_{EA}^2 - \left( 1 - \frac{R_{EB}^2}{R_{EA}^2} \right) X^2 \right]^{1/2}} \right\} \quad (75)$$

Also

$$\widehat{OA} \equiv R_G = \left[ R_{EB}^2 + \left( 1 - \frac{R_{EB}^2}{R_{EA}^2} \right) X^2 \right]^{1/2} \quad (76)$$

$$\widehat{OB} \equiv R_A = \left( 1 - \frac{R_{EB}^2}{R_{EA}^2} \right) X \quad (77)$$

$$\Gamma_E = \Gamma_2 - \Gamma_A \quad (78)$$

$$\widehat{AB} \equiv R_H = \left[ R_{EB}^2 + \frac{R_{EB}^2}{R_{EA}^2} \left( \frac{R_{EB}^2}{R_{EA}^2} - 1 \right) X^2 \right]^{1/2} \quad (79)$$

$$\widehat{AP} \equiv H_G = \left[ R_o^2 + R_G^2 - 2R_o R_G \cos \Gamma_E \right]^{1/2} \quad (80)$$

There is the additional relation

$$H_G = \frac{R_o \cos \Gamma_2 - R_A}{\cos \Gamma_G} - R_H \quad (81)$$

By substituting Eqs. (79) and (81) into Eq. (80), we obtain an equation for  $X$  in terms of  $R_o$  and  $\Gamma_2$ . This equation is transcendental and must be solved by iterative methods. Having  $X$ , the values for  $H_G$  and  $\Gamma_G$  follow directly from Eqs. (75) and (81).

To express the flight path and azimuth angles in geodetic coordinates, we define the local geodetic coordinate system,  $S_C$ , in the manner shown in Fig. 15. The coordinate transformation from  $S_G$  to  $S_C$  is given by

$$\bar{S}_C = A_{CG} \bar{S}_G \quad (82)$$

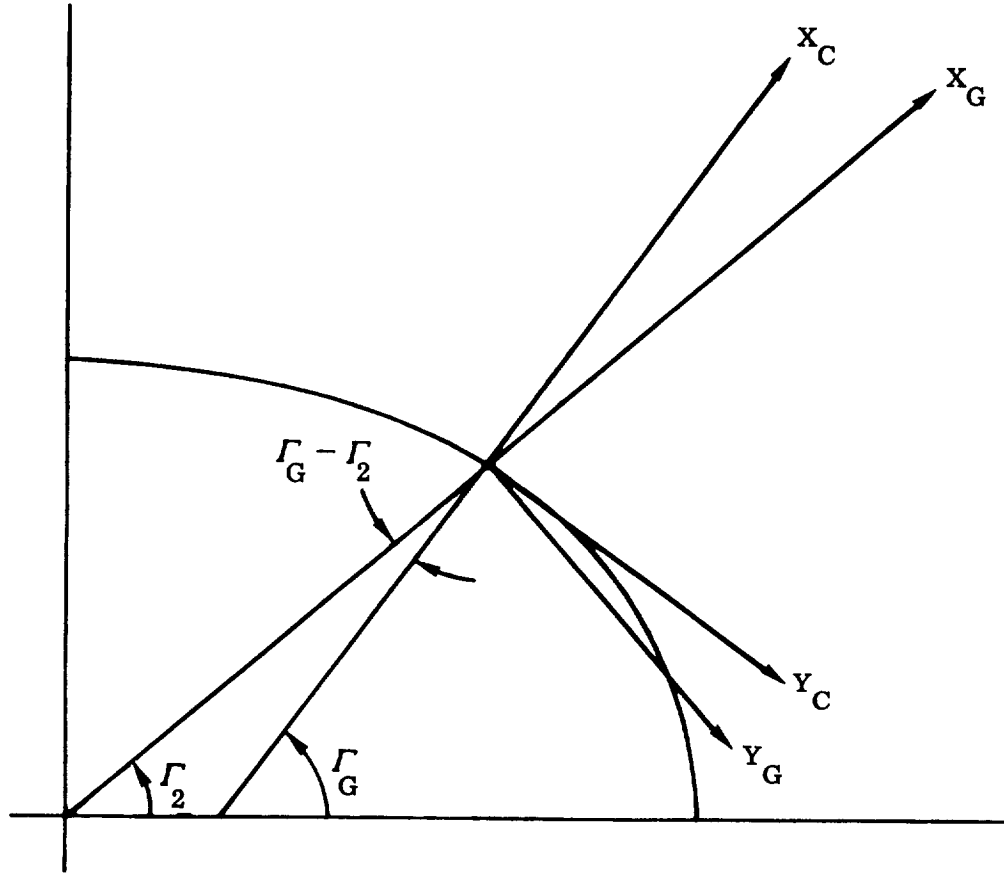


Figure 15. Orientation of Local Geodetic Coordinate System

where

$$A_{CG} = \begin{bmatrix} \cos (\Gamma_G - \Gamma_2) & -\sin (\Gamma_G - \Gamma_2) & 0 \\ \sin (\Gamma_G - \Gamma_2) & \cos (\Gamma_G - \Gamma_2) & 0 \\ 0 & 0 & 1 \end{bmatrix}$$

Because  $(\Gamma_G - \Gamma_2)$  is a very small angle,\* it is permissible to write

$$A_{CG} = \begin{bmatrix} 1 & -(\Gamma_G - \Gamma_2) & 0 \\ (\Gamma_G - \Gamma_2) & 1 & 0 \\ 0 & 0 & 1 \end{bmatrix} \quad (83)$$

\*The maximum value of  $(\Gamma_G - \Gamma_2)$  on earth is approximately 10 minutes of arc.

Consequently, the components of velocity in the local geodetic system are given by

$$\begin{bmatrix} u_C \\ v_C \\ w_C \end{bmatrix} = A_{CG} \begin{bmatrix} u_G \\ v_G \\ w_G \end{bmatrix} \quad (84)$$

The flight path and azimuth angles are then expressed in the local geodetic system by

$$\gamma_C = \sin^{-1} \left[ \frac{u_C}{\left( u_C^2 + v_C^2 + w_C^2 \right)^{1/2}} \right] \quad (85)$$

and

$$\sigma_C = \sin^{-1} \left[ \frac{v_C}{\left( v_C^2 + w_C^2 \right)^{1/2}} \right] \quad (86)$$

The set of equations (58) through 86) affords a complete description of the motion with respect to both inertial and planet-referenced coordinate systems. The forcing or control functions are the rocket angle deflections,  $\delta_p$  and  $\delta_y$ , in pitch and yaw, while  $\delta_r$  represents the driving signal for roll moment. The manner of specifying the control functions is dependent on the mission and the type of guidance used. An extensive treatment of this subject is beyond the scope of the present monograph. However, to exhibit the essential features of a complete guidance/control simulation, we will consider one special case in detail in the next section.

### 3.5 TRAJECTORY EQUATIONS DURING LAUNCH

One important aspect of the design of launch vehicle control systems is the assurance that bending loads imposed on the vehicle by atmospheric disturbances do not exceed permissible values. Since we are concerned with dynamic rather than static effects, it is necessary to determine relevant parameters by solving the equations of motion. The results of the last section are directly applicable with, however, some crucial simplifications. For present purposes, the assumption of a spherical, nonrotating earth is eminently satisfactory. Also, since the altitudes will be relatively small, the gravity acceleration may be assumed constant with negligible error. Furthermore, it is convenient to adopt the Launch Vehicle Navigation system,  $S_N$ , as

the inertial reference. If guidance reference release is assumed to be the instant of launch,\*

$$S_N = S_P = S_L = S_E$$

The results of the previous sections may then be used directly with  $\Lambda_1 = \Lambda_2 = \Lambda_3 = 0$ . Within the region in which the equations are valid, the range will be assumed small such that  $\Gamma_1$  and  $\Gamma_2$  may be treated as small angles. Note that since the inertial reference is assumed to be parallel with the launch site,  $\Gamma_1$  and  $\Gamma_2$  measure displacements relative to the launch site.

The following additional assumptions characterize the present analysis:

- a.  $\psi$  and  $\varphi$  are small.  $\theta$  is not necessarily small.
- b.  $p$ ,  $q$ ,  $r$ , and their time derivatives are small.
- c.  $v$ ,  $w$ , and their time derivatives are small.  $u$  is not necessarily small. However,  $\dot{u}$  is assumed small.
- d. Finally, because the c.g. eccentricity is generally not appreciable,  $y_{cg}$  and  $z_{cg}$  may be assumed to be small, while  $x_{cg}$  is not in general a small quantity since no stipulation has been made concerning the location of the origin of the body axes relative to the c.g. along the longitudinal axis. However, the time derivatives of all these quantities are assumed small.

As a result of these assumptions, the transformation matrices given by Eqs. (2), (10), and (4) reduce to

$$A_{LI} = \begin{bmatrix} 1 & 0 & 0 \\ 0 & 0 & -1 \\ 0 & 1 & 0 \end{bmatrix} = A_{PI} \quad (87)$$

$$A_{GI} = \begin{bmatrix} 1 & \Gamma_1 & \Gamma_2 \\ \Gamma_2 & 0 & -\Gamma_2 \\ -\Gamma_1 & 1 & 0 \end{bmatrix} \quad (88)$$

$$A_{BP} = \begin{bmatrix} c\theta & \psi c\theta & -s\theta \\ (\varphi s\theta - \psi) & 1 & \varphi c\theta \\ s\theta & (\psi s\theta - \varphi) & c\theta \end{bmatrix} \quad (89)$$

---

\*The equal sign for the coordinate reference frames implies that they are translatable.

Now

$$\begin{aligned}
A_{BG} &= A_{BP} A_{PI} A_{IG} \\
&= \begin{bmatrix} c\theta & \psi c\theta & -s\theta \\ (\varphi s\theta - \psi) & 1 & \varphi c\theta \\ s\theta & (\psi s\theta - \varphi) & c\theta \end{bmatrix} \begin{bmatrix} 1 & 0 & 0 \\ 0 & 0 & -1 \\ 0 & 1 & 0 \end{bmatrix} \begin{bmatrix} 1 & \Gamma_2 & -\Gamma_1 \\ \Gamma_1 & 0 & 1 \\ \Gamma_2 & -\Gamma_2 & 0 \end{bmatrix} \\
A_{BG} &= \begin{bmatrix} (c\theta - \Gamma_1 s\theta) & \Gamma_2 c\theta & -(s\theta + \Gamma_1 c\theta) \\ (\varphi s\theta - \psi - \Gamma_2) & \Gamma_2 & \varphi c\theta \\ (s\theta - \Gamma_1 c\theta) & \Gamma_2 s\theta & (c\theta - \Gamma_1 s\theta) \end{bmatrix} \quad (90)
\end{aligned}$$

And

$$\begin{aligned}
A_{IB} &= A_{IP} A_{PB} \\
&= \begin{bmatrix} 1 & 0 & 0 \\ 0 & 0 & 1 \\ 0 & -1 & 0 \end{bmatrix} \begin{bmatrix} c\theta & (\varphi s\theta - \psi) & s\theta \\ \psi c\theta & 1 & (\psi s\theta - \varphi) \\ -s\theta & \varphi c\theta & c\theta \end{bmatrix} \\
A_{IB} &= \begin{bmatrix} c\theta & (\varphi s\theta - \psi) & s\theta \\ -s\theta & \varphi c\theta & c\theta \\ -\psi c\theta & -1 & -(\psi s\theta - \varphi) \end{bmatrix} \quad (91)
\end{aligned}$$

Therefore, from Eq. (30)

$$g_{X_B} = -g (\cos\theta - \Gamma_1 \sin\theta) \quad (92)$$

$$g_{Y_B} = -g (\varphi \sin\theta - \psi - \Gamma_2) \quad (93)$$

$$g_{Z_B} = -g (\sin\theta + \Gamma_1 \cos\theta) \quad (94)$$

Substituting in Eqs. (58) and (59) and expanding, we obtain, after dropping higher-order terms,

$$m \dot{u} = T_s + T_c - \frac{1}{2} \rho V^2 A_1 C_D - mg (\cos \theta - \Gamma_1 \sin \theta) \quad (95)$$

$$m (\dot{v} + ru + x_{cg} \dot{r}) = -T_c \delta_y + L_\beta \beta - mg (\varphi \sin \theta - \psi - \Gamma_2) \quad (96)$$

$$m (\dot{w} - qu - x_{cg} \dot{q}) = T_c \delta_p - L_\alpha \alpha - mg (\sin \theta + \Gamma_1 \cos \theta) \quad (97)$$

$$I_{xx} \dot{p} + \dot{I}_{xx} p = T_r \ell_r \delta_r - mg y_{cg} \sin \theta \quad (98)$$

$$I_{yy} \dot{q} + \dot{I}_{yy} q - x_{cg} (\dot{w} - qu + \ddot{z}_{xg}) = T_c \ell_c \delta_p + L_\alpha \ell_\alpha \alpha - mg [(z_{cg} - \Gamma_1 x_{cg}) \cos \theta - x_{cg} \sin \theta] \quad (99)$$

$$I_{zz} \dot{r} + \dot{I}_{zz} r + x_{cg} (\dot{v} + ru + \ddot{y}_{cg}) = T_c \ell_c \delta_y + L_\beta \ell_\beta \beta - mg [x_{cg} \varphi \sin \theta - y_{cg} \cos \theta - x_{cg} (\psi + \Gamma_2)] \quad (100)$$

where

$$L_\alpha = \frac{1}{2} \rho V^2 B \int_0^L \frac{\partial C_N^{(\ell)}}{\partial \alpha} d\ell$$

$$L_\beta = \frac{1}{2} \rho V^2 B \int_0^L \frac{\partial C_N^{(\ell)}}{\partial \beta} d\ell$$

From Eq. 6 we have

$$\dot{\psi} = r \sec \theta \quad (101)$$

$$\dot{\theta} = q \quad (102)$$

$$\dot{\varphi} = p + r \tan \theta \quad (103)$$



Also, from Eq. 52,

$$u' = u + \Gamma_2 W_N \cos \theta + (W_E + R_O \Omega_E) (\sin \theta + \Gamma_1 \cos \theta) \quad (104)$$

$$v' = v + \Gamma_2 W_N - (W_E + R_O \Omega_E) \varphi \cos \theta \quad (105)$$

$$w' = w + \Gamma_2 W_N \sin \theta - (W_E + R_O \Omega_E) (\cos \theta - \Gamma_1 \sin \theta) \quad (106)$$

and

$$\alpha = \tan^{-1} \left( \frac{w'}{v} \right) \quad (107)$$

$$\beta = \tan^{-1} \left( \frac{v'}{v} \right) \quad (108)$$

$$V = \left[ (u')^2 + (v')^2 + (w')^2 \right]^{1/2} \quad (109)$$

From Eqs. (64) through (67)

$$u_I = u \cos \theta + v (\varphi \sin \theta - \psi) + w \sin \theta \quad (110)$$

$$v_I = -u \sin \theta + v \varphi \cos \theta + w \cos \theta \quad (111)$$

$$w_I = -u \psi \cos \theta - v - w (\psi \sin \theta - \varphi) \quad (112)$$

$$\int u_I dt = R_{oX_I} + C_1 \quad (113)$$

$$\int v_I dt = R_{oY_I} + C_2 \quad (114)$$

$$\int w_I dt = R_{oZ_I} + C_3 \quad (115)$$

$$\Gamma_1 = \cos^{-1} \left[ \frac{R_{oX_I}}{\left( R_{oX_I}^2 + R_{oY_I}^2 \right)^{1/2}} \right] \quad (116)$$

$$\Gamma_2 = \tan^{-1} \left[ \frac{R_{oZ_I}}{\left( R_{oX_I}^2 + R_{oY_I}^2 \right)^{1/2}} \right] \quad (117)$$

The altitude above the earth's surface is given by

$$H_G = \left[ R_{oX_I}^2 + R_{oY_I}^2 + R_{oZ_I}^2 \right]^{1/2} - R_e \quad (118)$$

Finally, from Eqs. (71) through (73), we obtain the flight path and azimuth angles as

$$\gamma = \sin^{-1} \left[ \frac{u_G}{\left( u_G^2 + v_G^2 + w_G^2 \right)^{1/2}} \right] \quad (119)$$

$$\sigma = \sin^{-1} \left[ \frac{v_G}{\left( v_G^2 + w_G^2 \right)^{1/2}} \right] \quad (120)$$

where

$$u_G = u (\cos \theta - \Gamma_1 \sin \theta) + w \sin \theta \quad (121)$$

$$v_G = u \Gamma_2 \cos \theta \quad (122)$$

$$w_G = -u (\sin \theta + \Gamma_1 \cos \theta) + w \cos \theta - R_o \Omega_E \quad (123)$$

The set of equations (95) through (123) describes the motion of the vehicle once the functions  $\delta_p$ ,  $\delta_y$ ,  $\delta_r$ , and the wind profile are specified. More precisely,  $\delta_p$ ,  $\delta_y$ , and  $\delta_r$  are derived from attitude rate control signals  $\dot{\psi}_c$ ,  $\dot{\theta}_c$ , and  $\dot{\phi}_c$  applied to the vehicle autopilot, a typical schematic of which is shown in Fig. 16. It is the

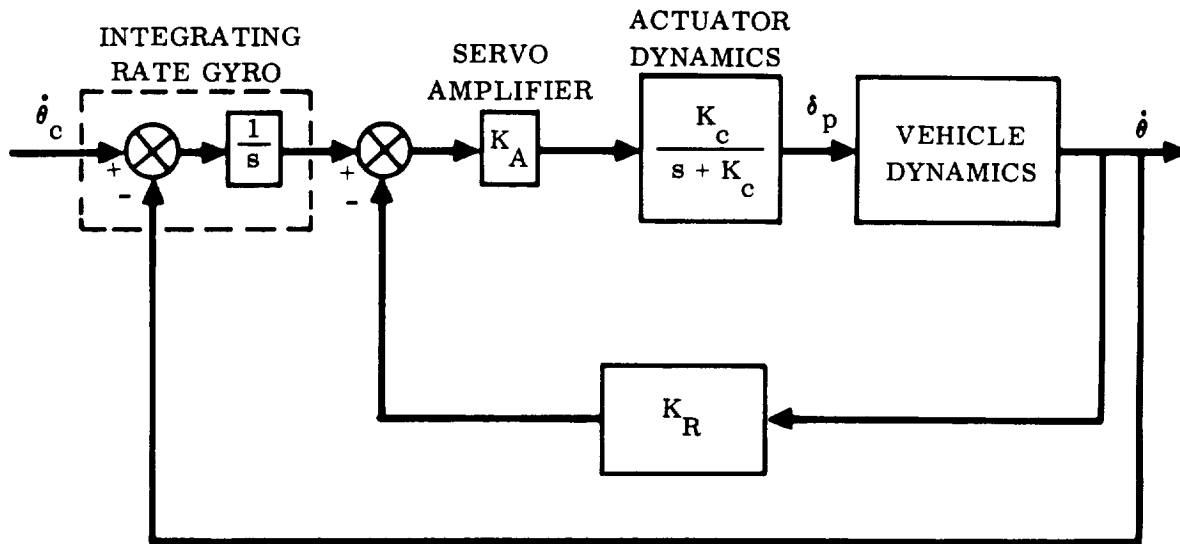


Figure 16. Pitch Attitude Control Channel

function of the guidance system to supply the input commands,  $\dot{\psi}_c$ ,  $\dot{\theta}_c$ , and  $\dot{\phi}_c$ , in order that the particular mission objective be achieved. Some general aspects of the guidance problem are discussed in Sec. 3.6.

It is perhaps pertinent to note that for purposes of analysis, the autopilot of Fig. 16 may be viewed as either a rate or displacement type of feedback system. For example, an equivalent schematic of Fig. 16 is shown in Fig. 16a, which highlights attitude rather than attitude rate as the primary feedback. Whichever viewpoint is taken is immaterial as far as the analytical aspects are concerned. The schematic of Fig. 16 corresponds more closely to the actual hardware implementation.

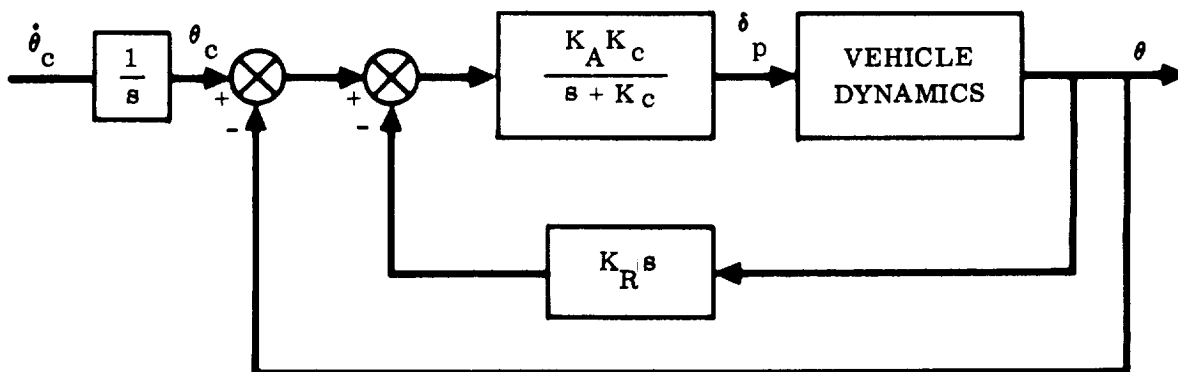


Figure 16a. Alternate Schematic of Autopilot of Figure 16

Furthermore, for purposes of guidance, the attitude or attitude rate is not the primary quantity of interest. In the guidance problem, the attitude rate input to the autopilot is applied in order to control the vector displacement and velocity of the vehicle. The factors influencing this problem are considered in Sec. 3.6.

The specification of the input commands and the wind velocities,  $W_E$  and  $W_N$ , expressed as a function of attitude (i.e., the wind profile), provides a complete input format for purposes of solving the equations of motion. When this is done, various quantities of interest may be calculated during the course of the solution.

For example, a parameter of fundamental importance is the bending moment induced in the vehicle by atmospheric disturbances. This quantity may be simply determined as follows. If  $\ell_j$  denotes the distance from the nose of the vehicle to station  $j$ , the moment at station  $j$  in the pitch plane is

$$M_j^{(p)} = -\frac{1}{2} \rho V^2 A_5 \sum_i (\ell_j - \ell_i) \left\{ \frac{\partial C_N(\ell_i)}{\partial \alpha} \alpha - m_i \left[ \dot{w} - q u \right. \right. \\ \left. \left. + mg (\sin \theta + \Gamma_1 \cos \theta) - \ell_i \ddot{\theta} \right] \right\} \quad (124)$$

and in the yaw plane

$$M_j^{(y)} = \frac{1}{2} \rho V^2 A_6 \sum_i (\ell_j - \ell_i) \left\{ \frac{\partial C_N(\ell_i)}{\partial \beta} \beta - m_i \left[ \dot{v} + r u \right. \right. \\ \left. \left. + mg (\varphi \sin \theta - \psi - \Gamma_2) + \ell_i \dot{r} \right] \right\} \quad (125)$$

The summation is taken for all terms forward of station  $j$ ; i.e., only those terms for which  $(\ell_j - \ell_i) > 0$ .

Time histories of various significant parameters are available in the process of solving the equations, e.g.,  $\alpha(t)$ ,  $\beta(t)$ ,  $\delta_p(t)$ , etc. Additional quantities of interest may be calculated as desired. For example, in Fig. 17, the range distances  $\widehat{CD}$  and  $\widehat{AB}$  may be calculated from

$$\widehat{CD} = \int_{t_1}^{t_2} V_G dt \quad (126)$$

$$\widehat{AB} = R_e \int_{t_1}^{t_2} \frac{V_G}{R_o} \cos \gamma dt \quad (127)$$

where

$$V_G = (u_G^2 + v_G^2 + w_G^2)^{1/2}$$

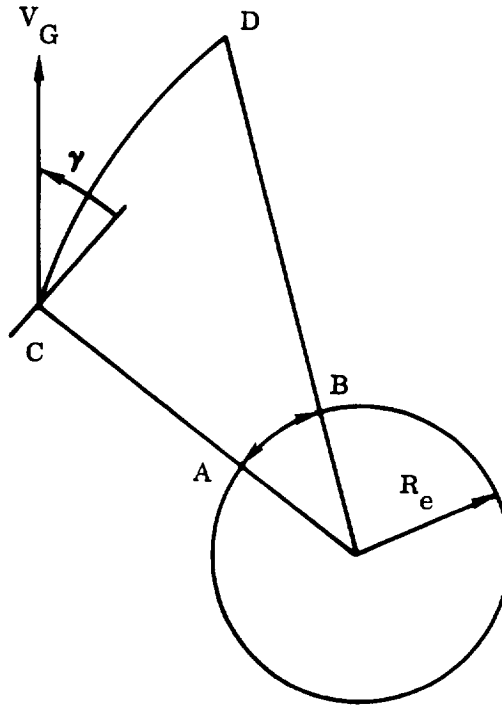


Figure 17. Determination of Range

### 3.6 GUIDANCE CONSIDERATIONS

It was pointed out in the previous section that the input format is complete when the wind profile and attitude rate commands are specified. In order to discuss the philosophy and motivation for the latter, we are led to consider the operation of a guidance system, the essential elements of which are depicted in Fig. 18. The pitch plane channel of the vehicle dynamics block in this figure is of the form shown in Fig. 16. However, for purposes of trajectory computation, all higher-order lags in the autopilot are neglected. Thus, for example, in Fig. 16, the  $\theta(s)/\delta_p(s)$  transfer function is taken as  $\mu_c/s^2$ , and the effects of actuator dynamics are neglected. This is permissible, since the trajectory (long-period) dynamics and the autopilot (short-period) dynamics are separated by about a factor of five in the fundamental time constant.

**The guidance system must:**

- a. Measure the position and velocity of the vehicle.

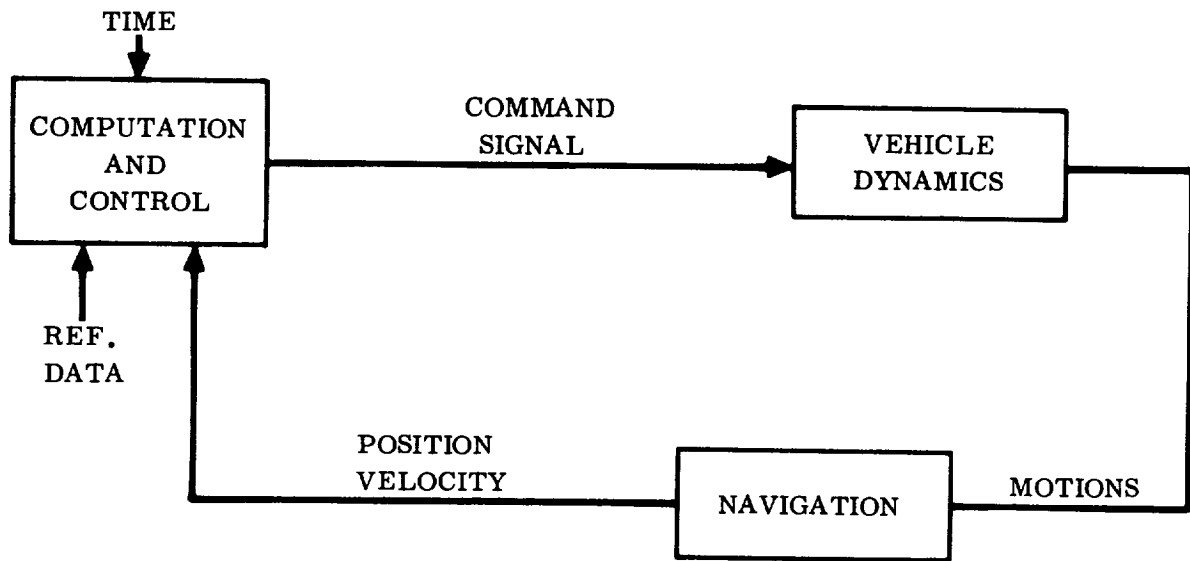


Figure 18. Elements of a Guidance System

- b. Evaluate this information in the sense of determining whether the vehicle is "on course" (e.g., by comparing with a reference trajectory).
- c. Generate command or steering signals to correct for deviations.

These functions are performed by the Navigation, Computation, and Control elements of the guidance system.

Essentially, the role of the Navigation facility is to determine the vehicle's position and velocity in some specific frame of reference. Depending on the type of guidance employed (radio or inertial), this may involve the use of inertial or radar devices or a combination of the two.

The purpose of the Computation facility is to utilize the navigation data and generate an error or status signal that is a measure of the vehicle's present ability to accomplish the desired mission. This is done by means of the "guidance equations."

The purpose of the Control function is to direct the flight path of the vehicle in such a way that the error signal is driven to zero. This also includes the task of generating the engine shutoff signal when a prescribed set of constraints is satisfied.

As previously noted, the guidance system is either radio or inertial, depending on the physical hardware employed. Figs. 19 and 20 show typical configurations for each. The radio guidance system was the earliest used on ballistic missiles and space vehicles. It employs radar tracking stations that sense the slant range and

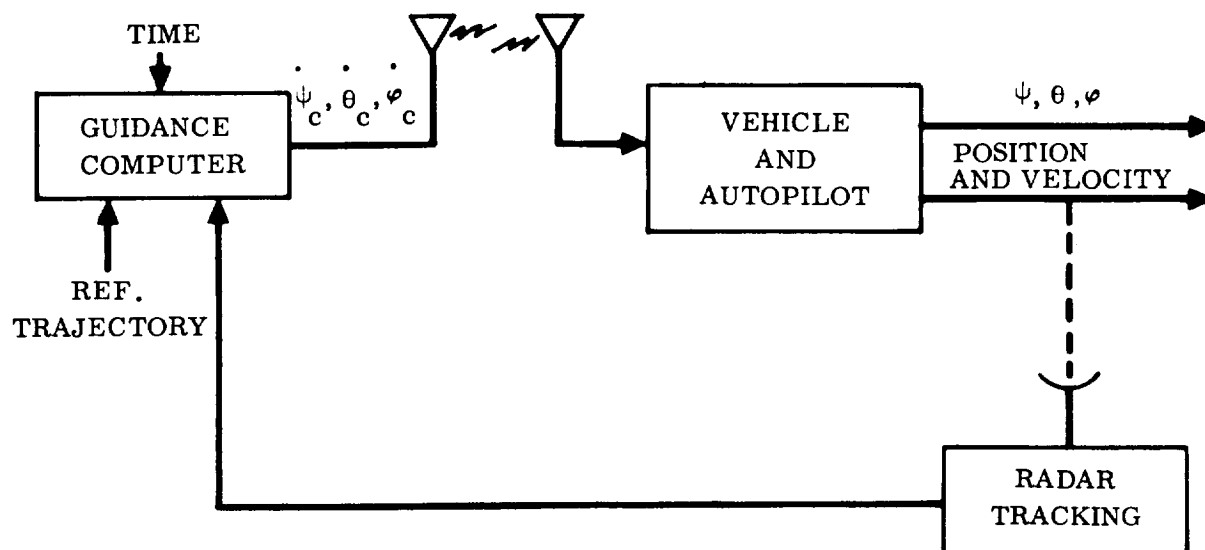


Figure 19. Elements of a Radio Guidance System

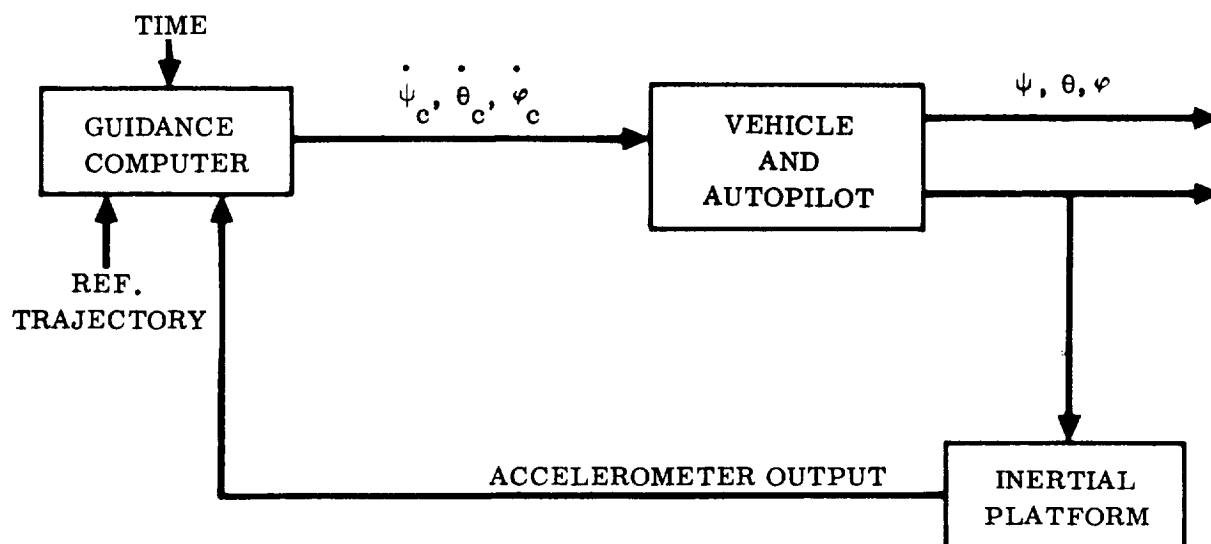


Figure 20. Schematic of an Inertial Guidance System

the azimuth and elevation displacements and rates of the vehicle with respect to a spherical coordinate system centered at the radar site. This data is then transmitted to the guidance computer, which performs the various matrix transformations to make the vehicle position and velocity information compatible with the guidance equations. The form of the guidance equations is generally derived from the concept of a "required velocity vector." The basic premise involved is that at each point in the powered flight region, a required velocity vector

$$\bar{V}_R = \bar{V}_R(\bar{R}, t)$$

may be defined and computed such that the resulting free-flight trajectory will satisfy the general guidance constraints. In most launch vehicles, there are three degrees of control; i.e., pitch steering, yaw steering, and thrust termination. This means that it is possible to satisfy four guidance constraints by causing three of the constraints to occur simultaneously with the natural occurrence of the fourth. More guidance constraints can be satisfied if additional degrees of control are available; i.e., variable magnitude thrust.

Typical guidance constraints are:

- a. Burnout velocity magnitude.
- b. Burnout velocity angle.
- c. Altitude at burnout.
- d. Burnout momentum.
- e. Time of free flight.

The guidance equations are such that based on the required velocity, steering signals are generated in the form of attitude rate commands in pitch and yaw.\* However, because booster vehicles are comparatively fragile structures, violent maneuvering in regions of appreciable dynamic pressure are to be avoided. Consequently, the steering of the vehicle is generally divided into two phases: atmospheric and vacuum.

During the atmospheric phase, either of two approaches may be adopted. The vehicle may be steered by means of some moderately well-behaved function that essentially commands a given velocity profile. This may be accomplished, for example, by nulling deviations in lateral velocity via yaw control and commanding a prescribed functional relation between forward and normal velocity, using pitch control.

---

\*The roll rate commands do not affect the trajectory.



The second alternative involves flying the vehicle "open-loop" during the atmospheric phase by programming the pitch and yaw attitude as a function of time. This approach has been used extensively and will be described in some detail.

It is natural to seek to optimize some fundamental mission parameters, such as payload weight, orbit altitude, or burnout velocity. However, the primary constraint during the atmospheric phase is the structural limitation of the vehicle, and this consideration governs the final form of the pitch program.

If it is assumed that such parameters as thrust level, stage mass ratios, and propellant specific impulse are fixed for a particular vehicle design, then attitude control is the fundamental means of trajectory-shaping. Determining an optimum attitude vs. time program is, in principle, a simple application of variational calculus. However, the complexity of the equations of motion during the atmospheric phase and the problem constraints such as heating, aerodynamic loading, and thrust deflection limits make a purely analytical approach unfeasible.

Since the primary constraint in the atmospheric portion of the trajectory is the structural integrity of the vehicle, first attention is given to the maximum bending loads. Without considering dynamic effects, the bending loads are a function of the applied aerodynamic moment, which is balanced by an equivalent moment produced by the thrust angle deflection. Since the applied aerodynamic moment is proportional to angle of attack, the obvious solution is to employ a zero lift trajectory within the atmospheric portion of the trajectory. A zero lift (also called gravity turn) trajectory is defined as that trajectory which results from keeping the thrust vector always parallel to the velocity, starting from some nonzero, nonvertical initial velocity. Physically, the vehicle is made to rise vertically off the launch pad; after a few seconds, the vehicle's attitude and velocity vector are both rotated downward to begin the gravity turn. Since the velocity vector of a real vehicle cannot be rotated instantaneously, the transition from vertical rise to gravity turn takes place over a finite length of time. An angle of attack must necessarily exist during this time, but generally this can be made to occur before the dynamic pressure is appreciable.

However, because of the presence of atmospheric winds, this approach must be modified, since rapid changes in angle of attack can cause prohibitive inertial loads. The approach generally adopted is that of generating a "pitch program" or pitch rate vs. time\* that will minimize the maximum aerodynamic moment encountered during the atmospheric phase when all possible wind distributions are considered.

The first step in determining the pitch program is to obtain the pitch rate vs. time history for a no-wind, zero-lift turn. This is generally accomplished by flight simulation runs on a computer, with pitch control used to constrain the vehicle longitudinal axis to be coincident with the velocity vector. Before this constraint is applied,

---

\*The discussion applies also to the "yaw program."

a short vertical rise period (about 15 seconds) is simulated, followed by a short period of constant pitch down rate to produce initial rotation of the velocity vector from its vertical orientation. As indicated in Fig. 21, it is necessary to accept a negative angle of attack in pitch during this time. Pitch rate and duration are adjusted to effect a smooth transition to the zero lift turn, with further adjustments made to attain the desired end condition before transition to the closed-loop guidance phase. Fig. 21 illustrates a typical convergence procedure.

Generally, a smooth pitch rate vs. time curve cannot be physically realized by the autopilot, which, as a rule, is capable only of providing a limited number of discrete time intervals during each of which a constant pitch rate signal is applied. Thus, as indicated in Fig. 22, it is necessary to approximate the desired pitch rate curve with a step pitch program having the required number of steps.

This first approximation to the pitch program must now be modified to take account of atmospheric winds. Since applied aerodynamic moments are very nearly proportional to both aerodynamic pressure,  $q$ , and angle of attack,  $\alpha$ , it is sufficient to determine the maximum product of these variables,  $\alpha q$ , in order to check maximum bending loads. Trajectory simulations are run with assumed winds aloft profiles, and the resulting  $\alpha q$  histories are examined to determine peak values, as shown in Fig. 23. Various winds aloft conditions are assumed, which are normally chosen from statistical analyses of weather data at the launch site. The  $\alpha q$  peaks are adjusted by varying the pitch rate history. The peak that results in the highest confidence level for not exceeding prescribed bending moments is then finalized. A more complete account of this procedure is contained in "Response Studies," which is part 10 of Vol. III in the present series.

A pitch program for a typical large booster vehicle is shown in Fig. 24. The time histories of various parameters of interest are depicted in Figs. 25 through 41. The precise definitions of the trajectory parameters are listed in Table 1.

The guidance elements for the exo atmospheric phase are shown in Fig. 19 for radio guidance and Fig. 20 for inertial guidance. As noted earlier, essentially the same functions are performed by both; the differences arise mainly in the instrumentation employed and in how the information is processed.

Also, the basic guidance concept may be the same; the most commonly used is the "required velocity" type. However, the specific implementation generally differs, due to the computation equipment available. In radio guidance systems where the computing facilities are ground based, the guidance equations are of the so-called "explicit" type, which requires essentially that the equations of motion be solved in real time once or twice a second. Since this generally requires rather formidable computing equipment, it is feasible only when the computation is performed on the ground, as is normally the case for radio guidance systems. If the computer equipment is to be airborne, as is generally true for all inertial-type guidance systems,

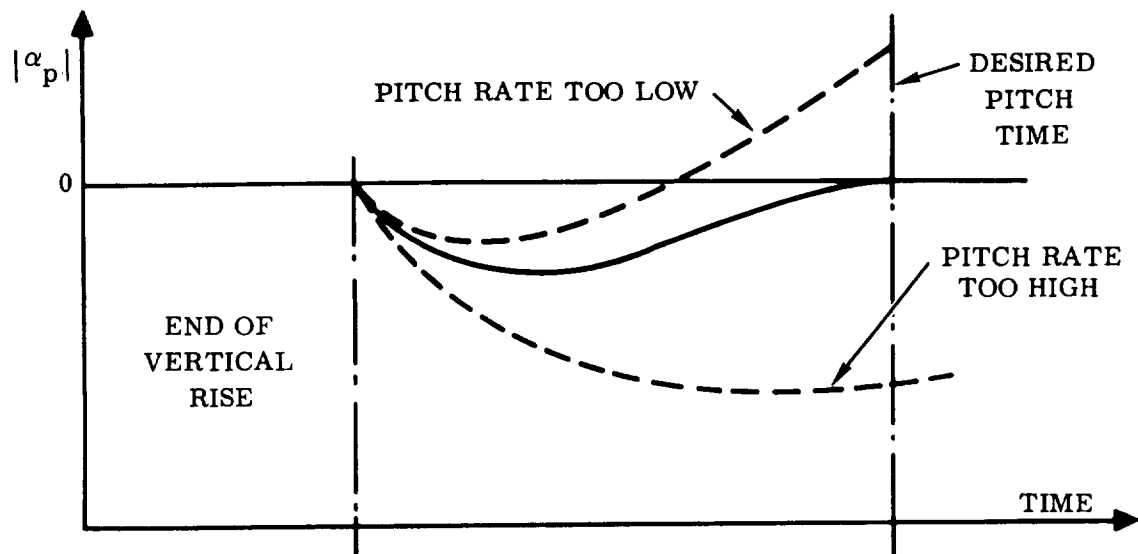


Figure 21. Transition from Vertical Rise to Zero Lift Turn

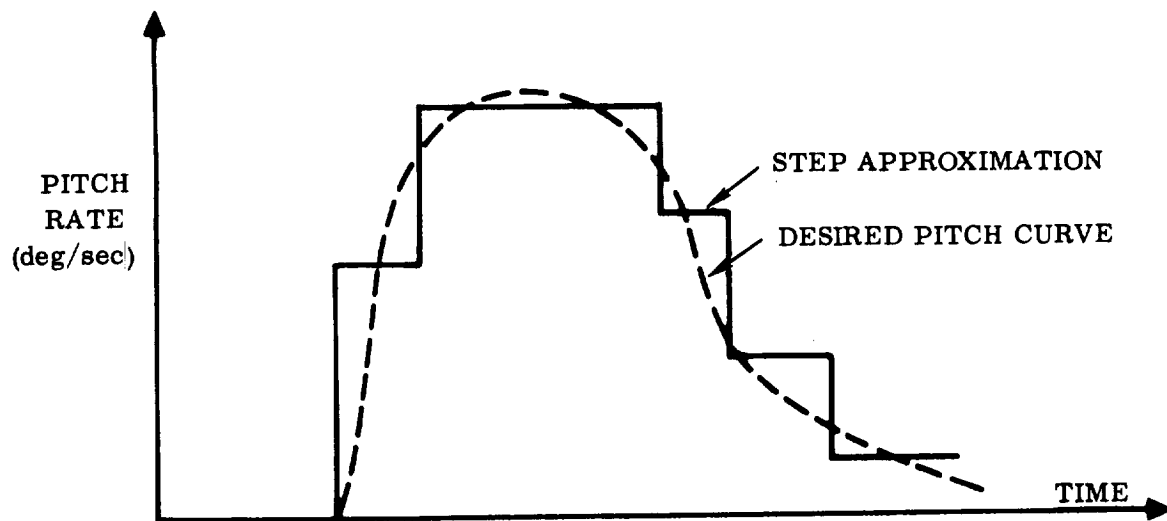


Figure 22. Step Approximation to Pitch Rate Program

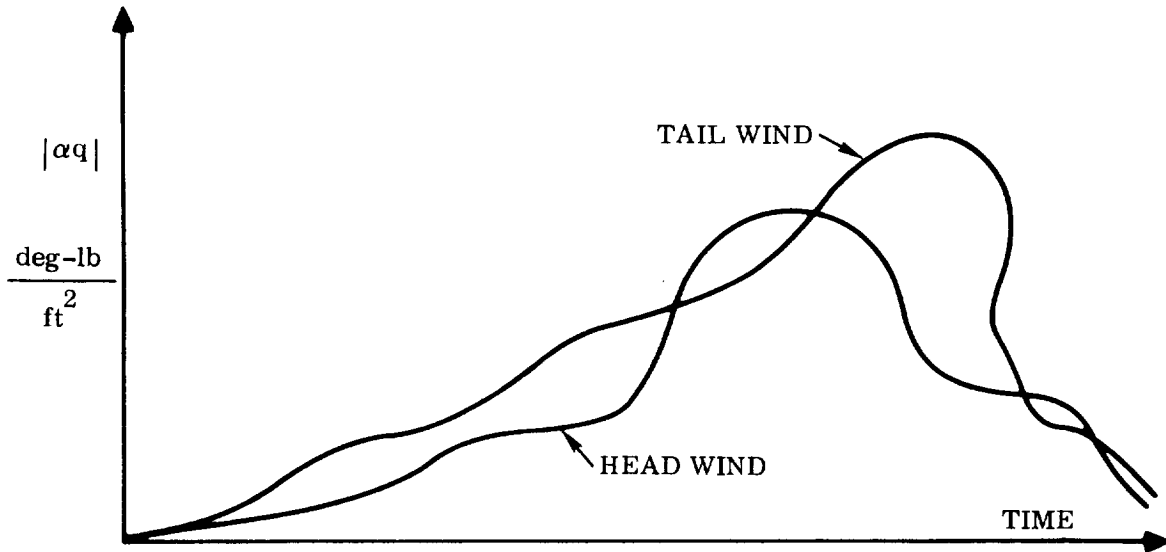


Figure 23. Typical  $\alpha q$  Time Histories for Winds Aloft

the guidance equations must be in a form that minimizes the storage and computation time burden on the computer. In this case, the guidance equations are based on perturbations about a nominal trajectory that employs delta quantities (deviations from nominal); hence the name "delta" equations. For a detailed discussion of these guidance philosophies, the reader is referred to the literature.<sup>(13)</sup>

The other obvious difference between radio and inertial systems is in the sensing of vehicle position and velocity. It has already been noted that a radio system normally measures slant range and the azimuth and elevation displacements and rates in a spherical coordinate system centered at the radar site. The all-inertial system uses a stable platform whose primary output is vehicle acceleration relative to inertial space. More specifically, the accelerometers measure only nongravitational forces; therefore a precise navigational facility must include provisions for taking account of gravitational acceleration. Total velocity and position in an inertial reference is then determined by successive integrations, and in conjunction with suitable matrix transformations, provides the basic information on the trajectory of the vehicle, which forms the basis for generating the steering commands.

Since a detailed discussion of the analysis and implementation of guidance is beyond the scope of the present monograph, the reader is referred to the literature for a more complete treatment.<sup>(2, 13)</sup>

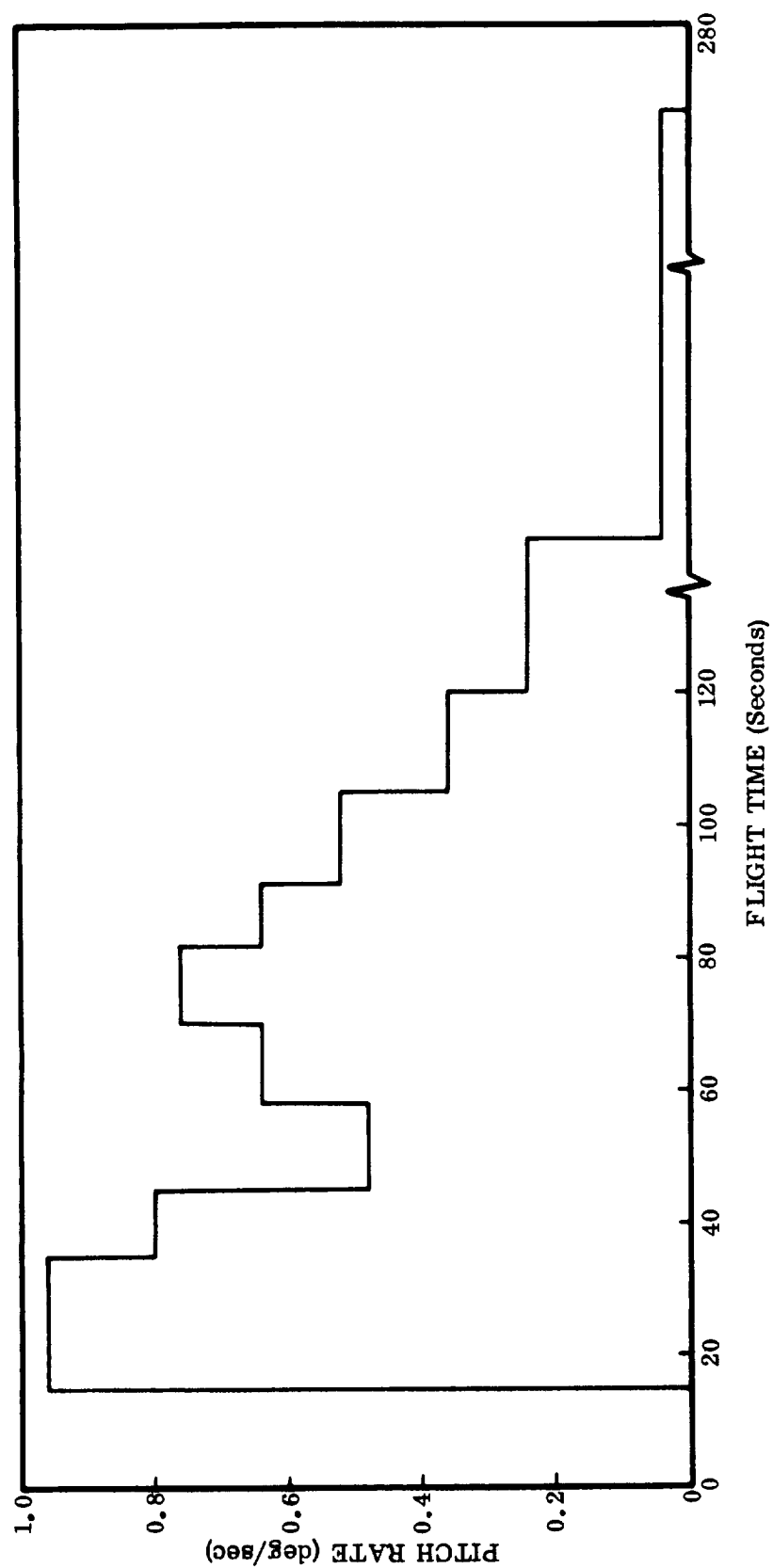


Figure 24. Typical Pitch Rate vs. Time Program

Table 1. Trajectory Parameter Definitions

Altitude	- Distance above the earth (reference ellipsoid).
Range	- Surface distance from launch pad to sub-vehicle point.
Relative Velocity	- Velocity referenced to a coordinate system rotating with the earth.
Inertial Velocity	- Velocity relative to inertial coordinate system.
Relative Flight Path Angle	- Angle between relative velocity vector and local horizontal plane.
Mach Number	- Ratio of vehicle relative velocity to the local speed of sound.
Axial Acceleration	- The longitudinal component of the quantity thrust minus drag, divided by weight.
Dynamic Pressure	- Aerodynamic loading term equal to one-half the product of ambient density and the relative velocity squared.
Pitch Angle of Attack	- The angle (alpha) between the projection of the relative velocity vector onto the pitch plane and the vehicle longitudinal axis.
Yaw Angle of Attack	- The angle (beta) between the projection of the relative velocity vector onto the yaw plane and the vehicle longitudinal axis.
Pitch Attitude	- Angle between the vehicle longitudinal axis and the space fixed launch plane.
Axial Force	- Aerodynamic force along the vehicle longitudinal axis.
Normal Force	- Aerodynamic force in the pitch plane acting normal to the vehicle longitudinal axis and applied at the normal force center of pressure.
Side Force	- Aerodynamic force in the yaw plane acting normal to the vehicle longitudinal axis and applied at the yaw force center of pressure.
Weight	- Total or gross weight of the vehicle.
Longitude	- Angular position measured from Greenwich meridian, positive west.
Geocentric Latitude	- Angular position measured from the equator, positive north.

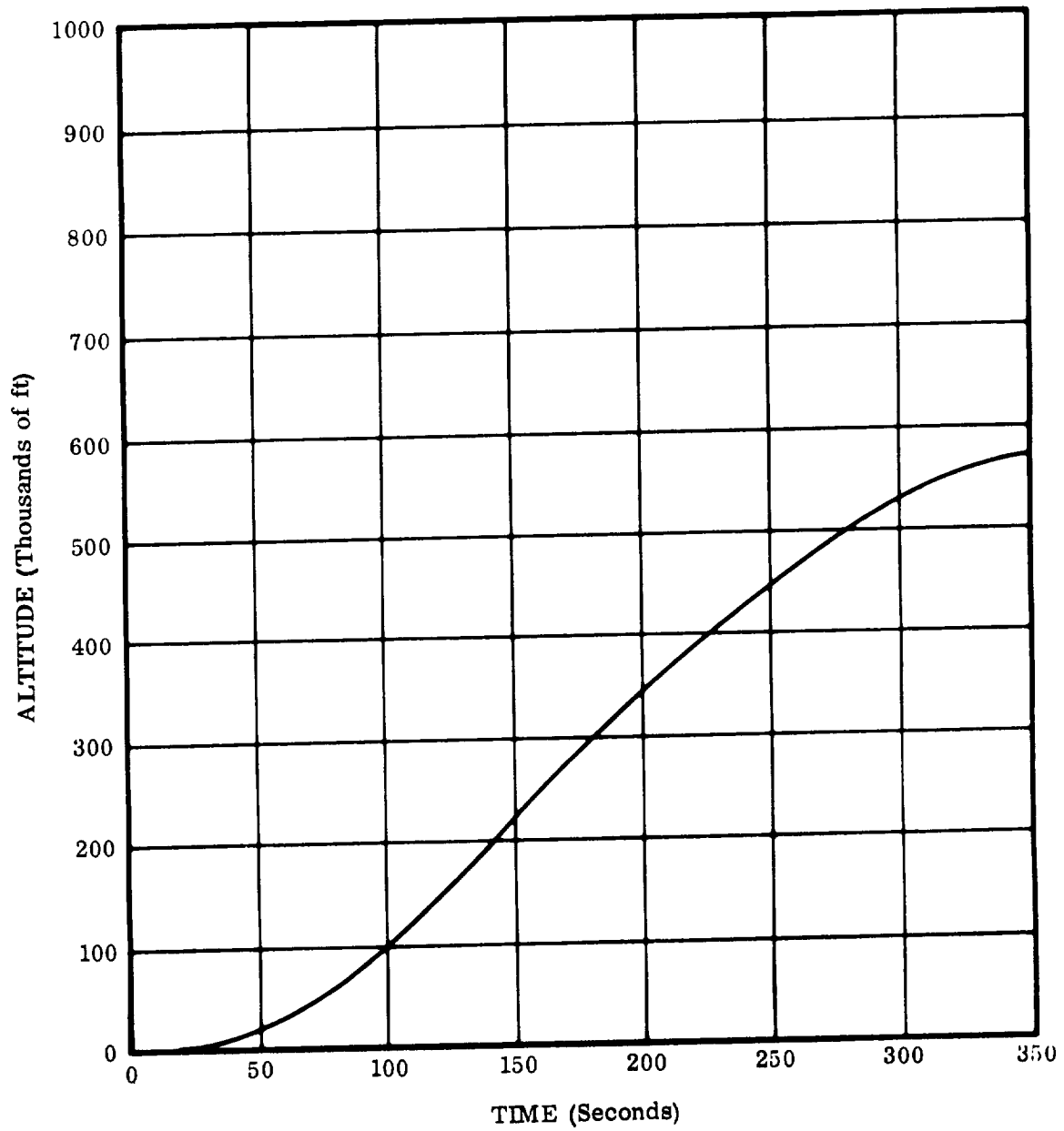


Figure 25. Altitude Time History

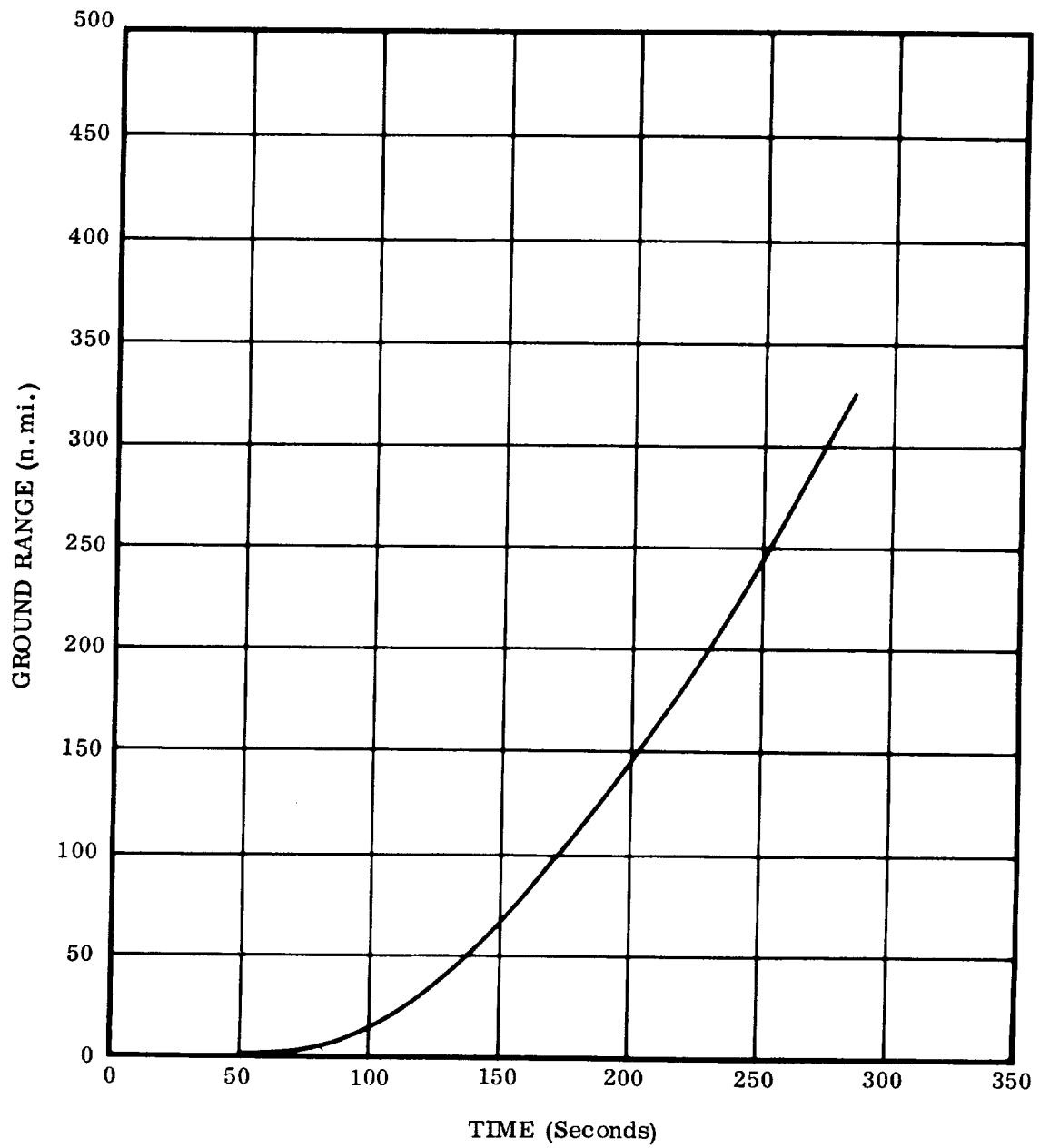


Figure 26. Ground Range Time History



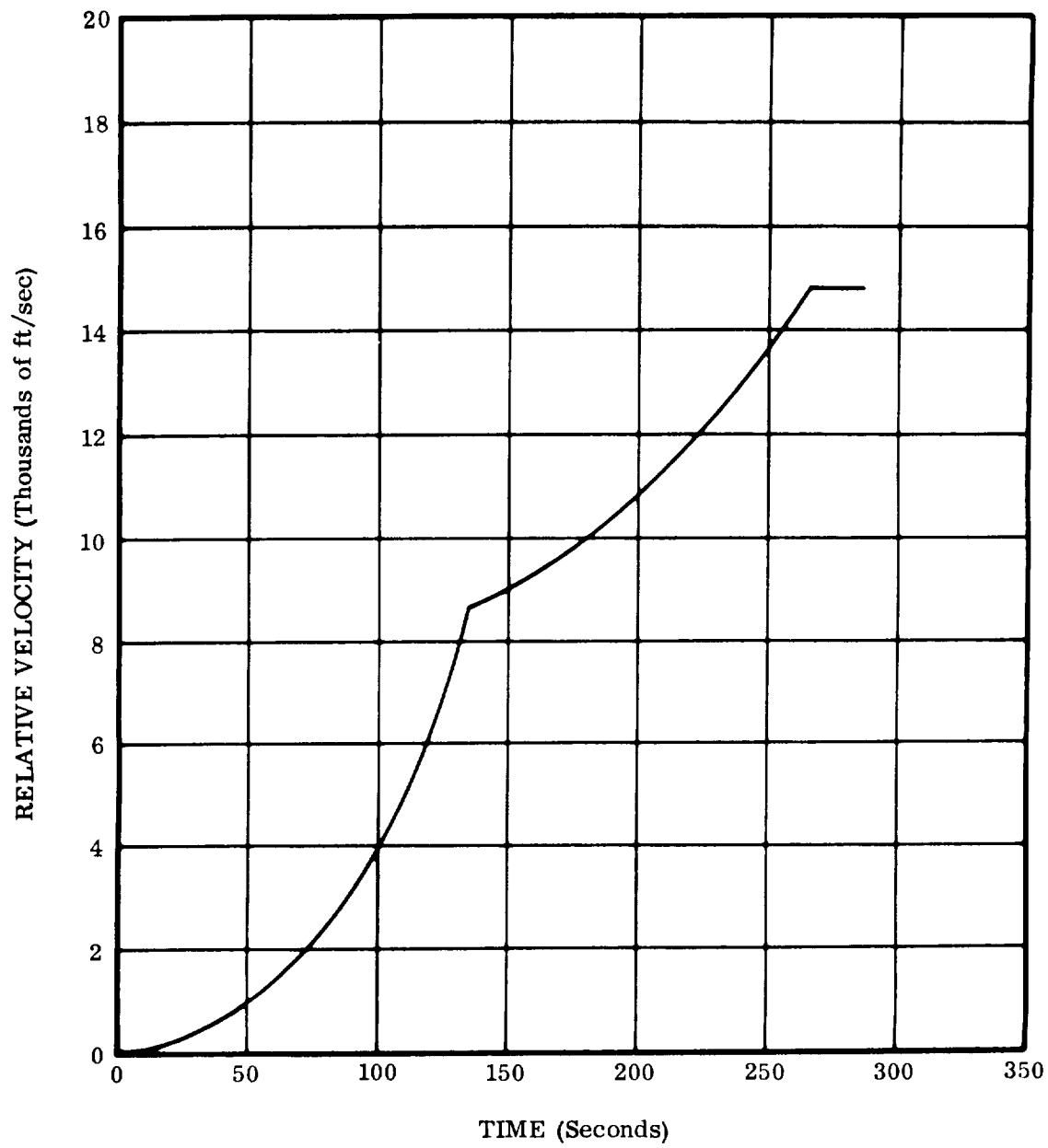


Figure 27. Relative Velocity Time History

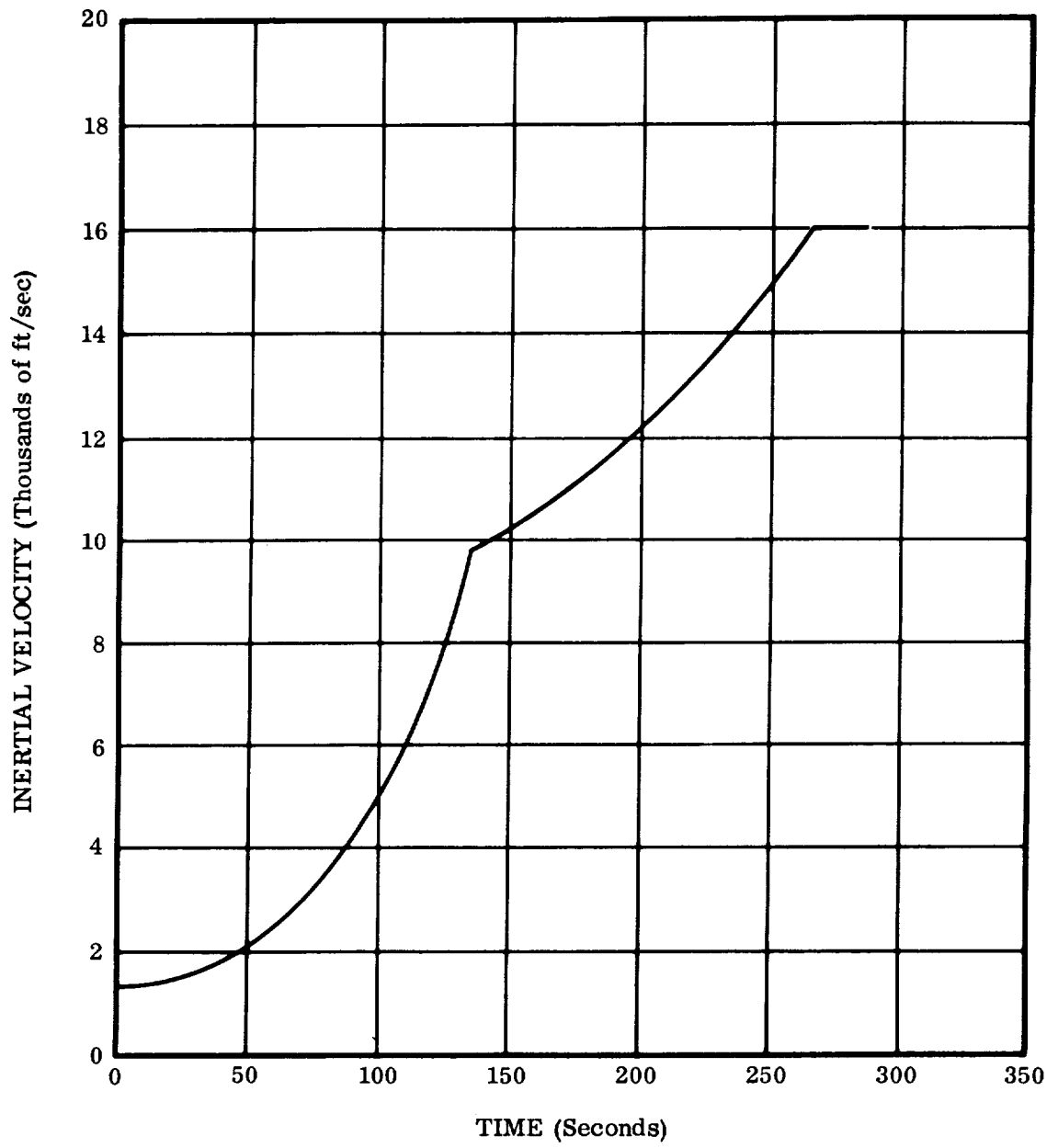


Figure 28. Inertial Velocity Time History

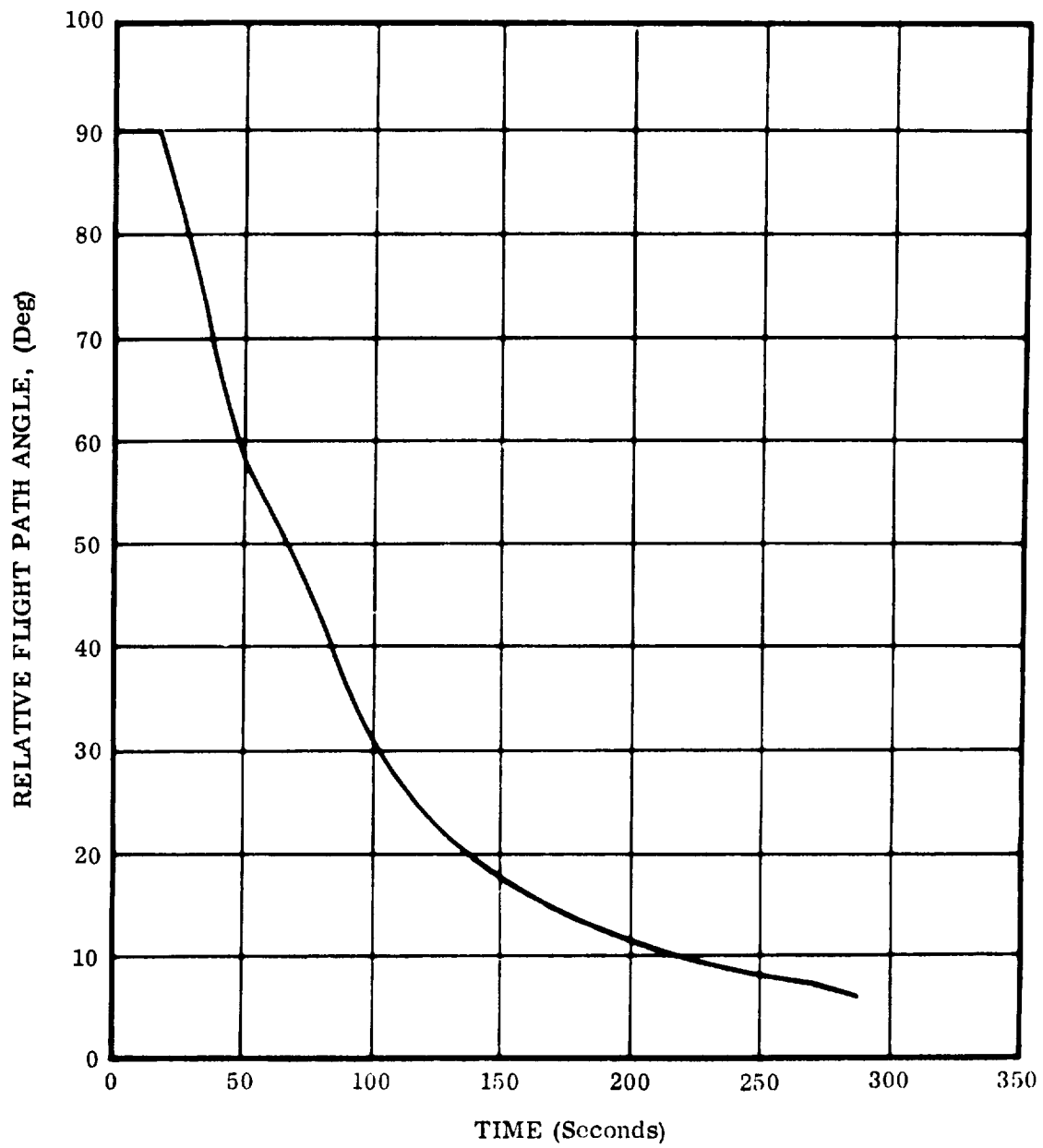


Figure 29. Relative Flight Path Angle Time History

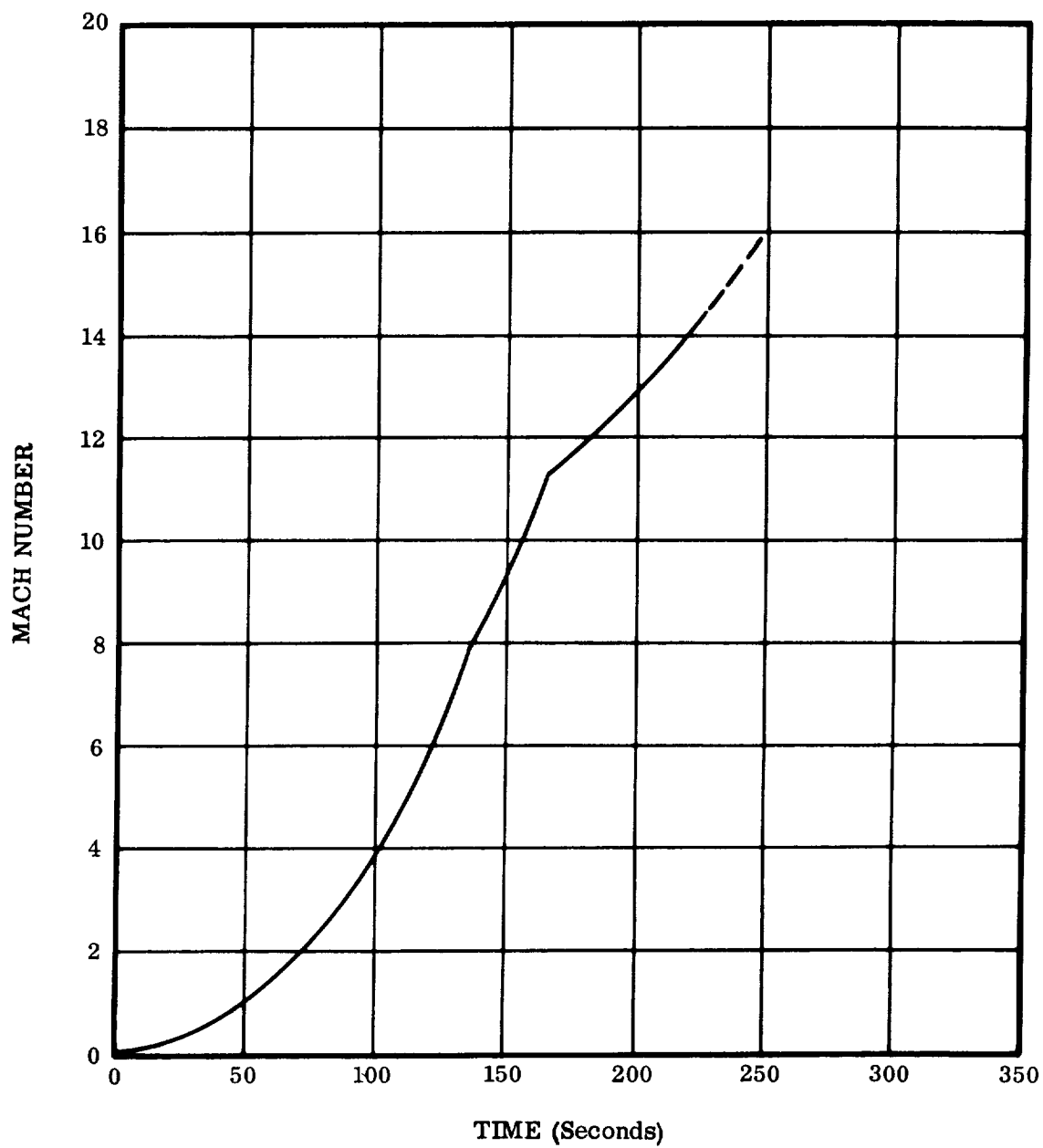


Figure 30. Mach Number Time History

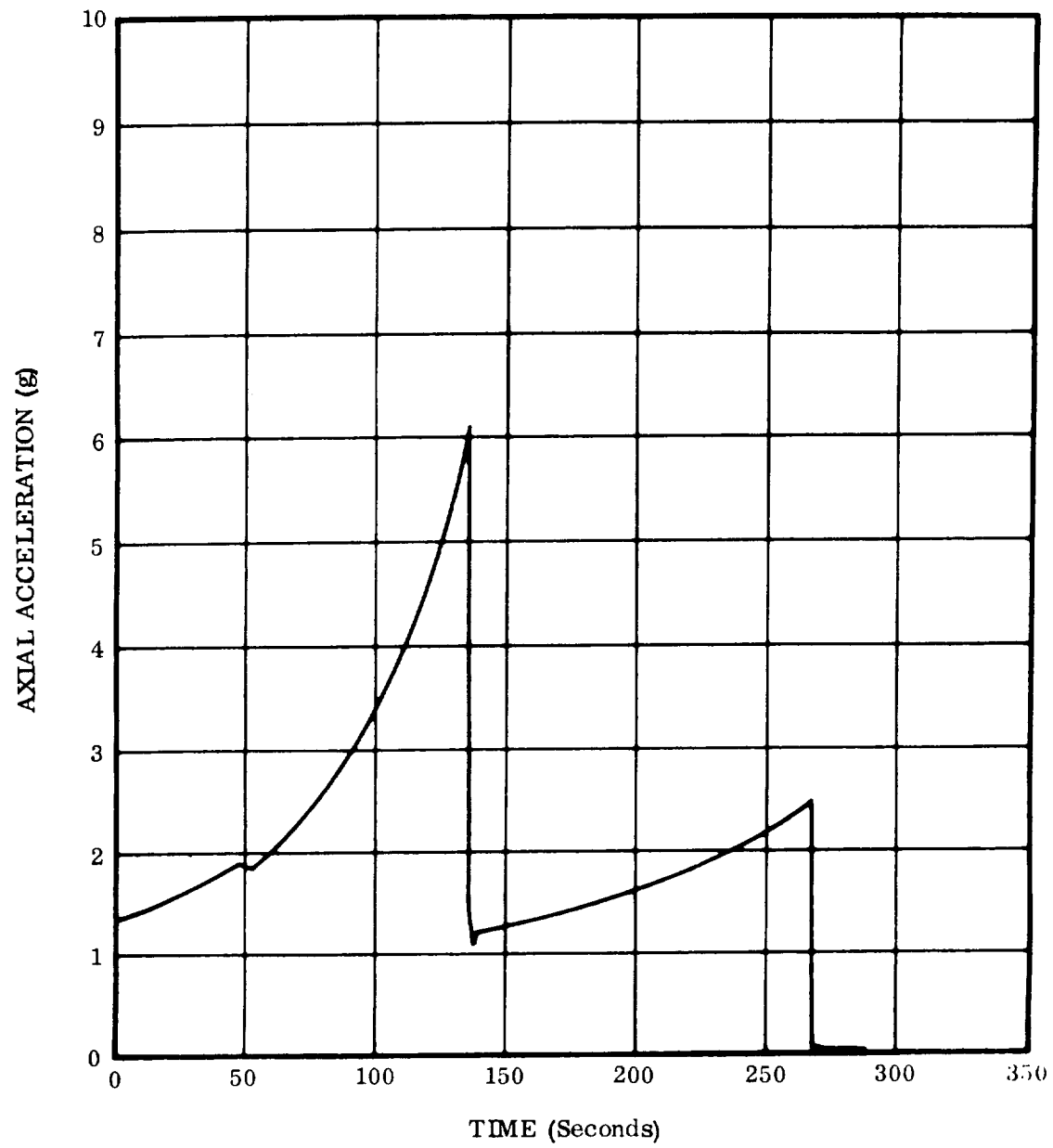


Figure 31. Axial Acceleration Time History

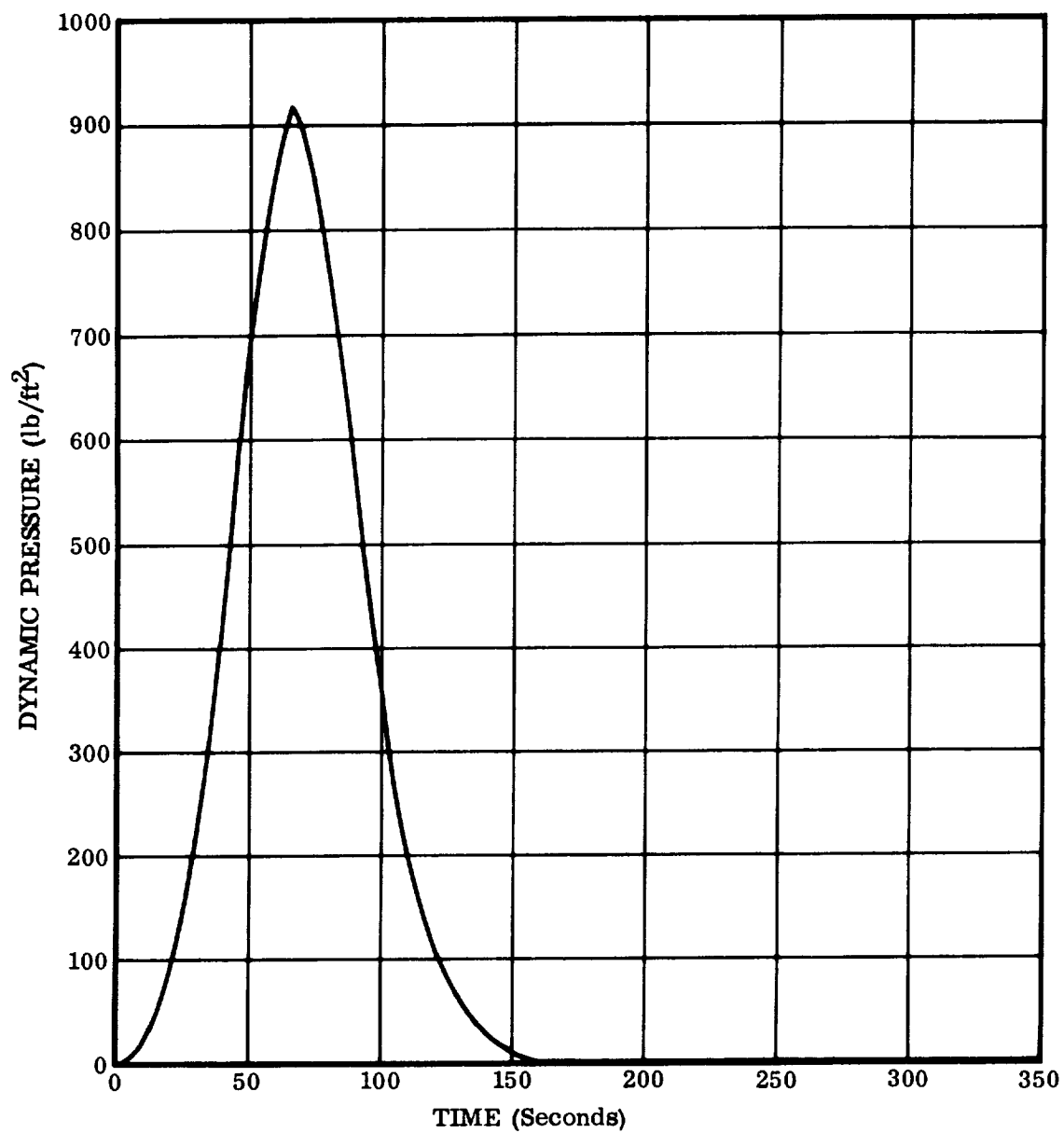


Figure 32. Dynamic Pressure Time History

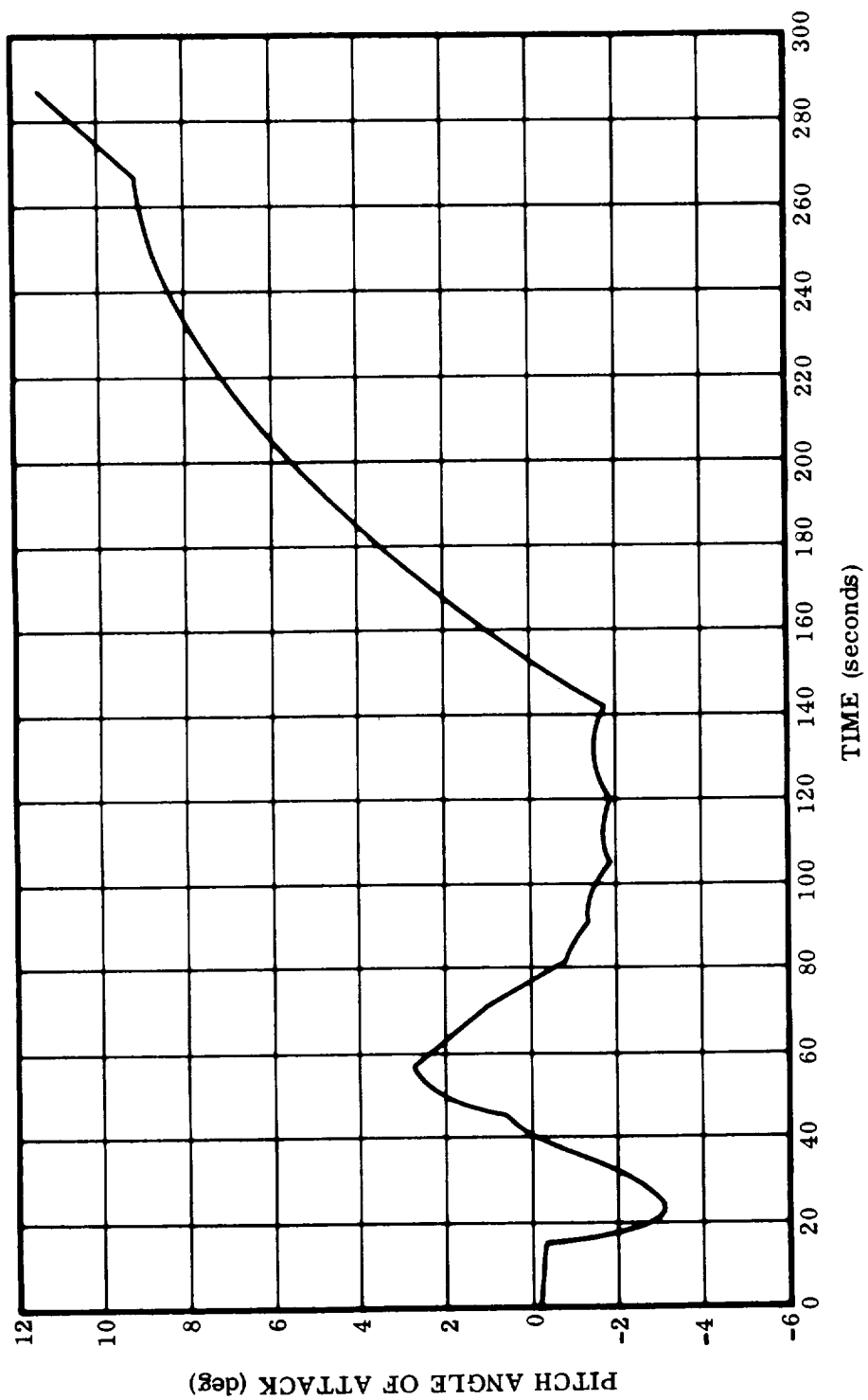


Figure 33. Pitch Angle of Attack Time History

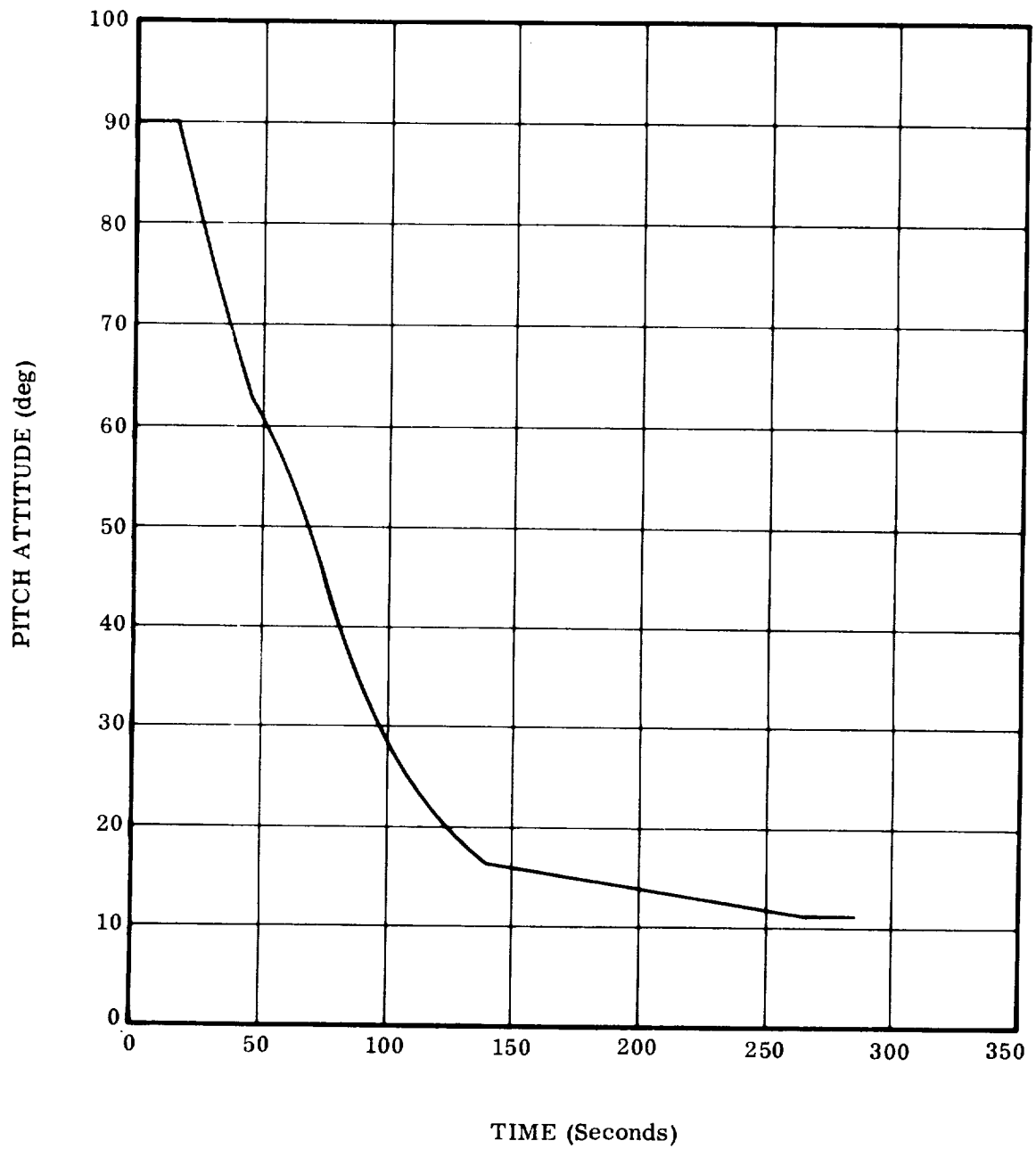


Figure 34. Pitch Attitude Time History



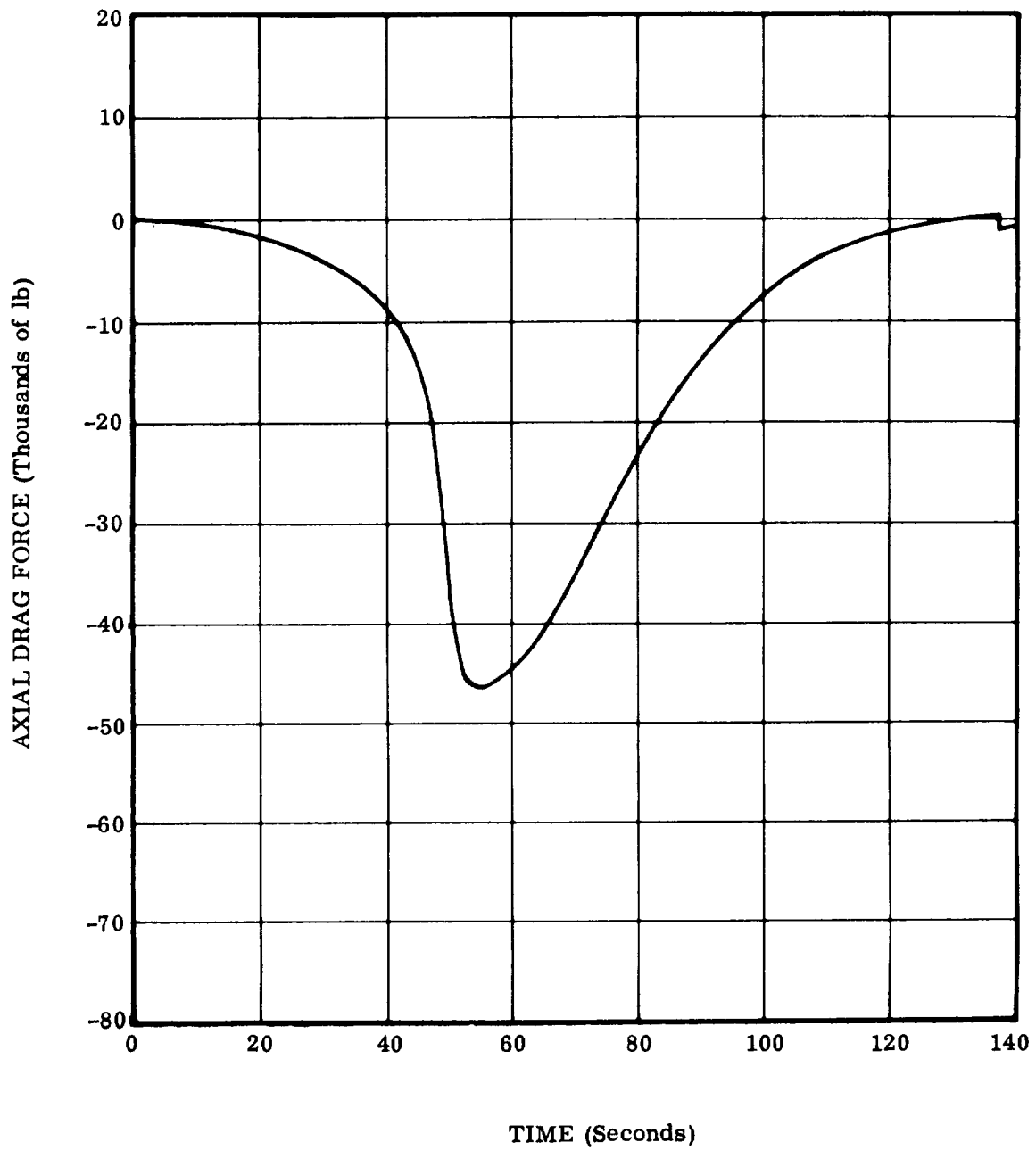


Figure 35. Axial Drag Force Time History

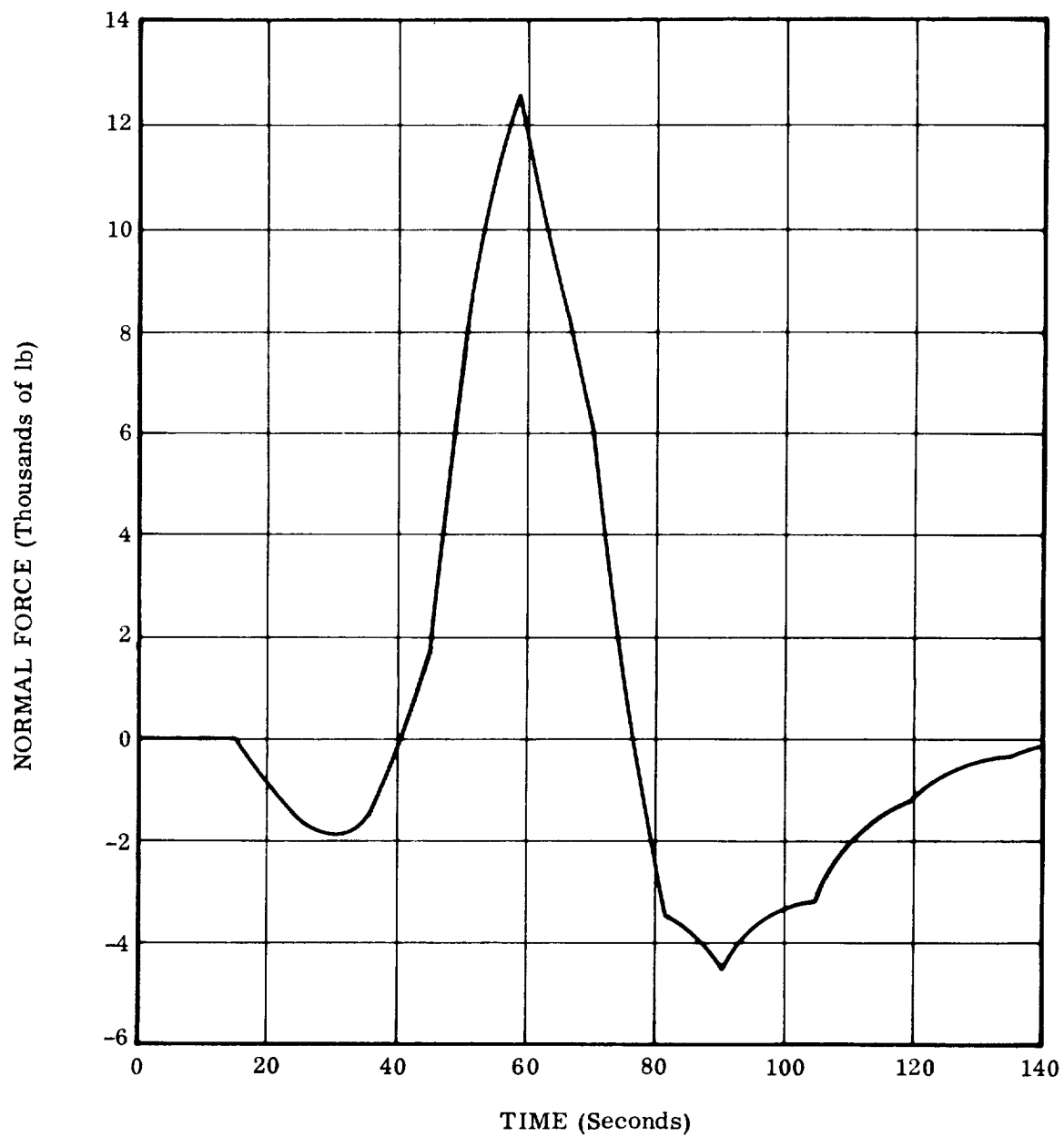


Figure 36. Normal Force Time History

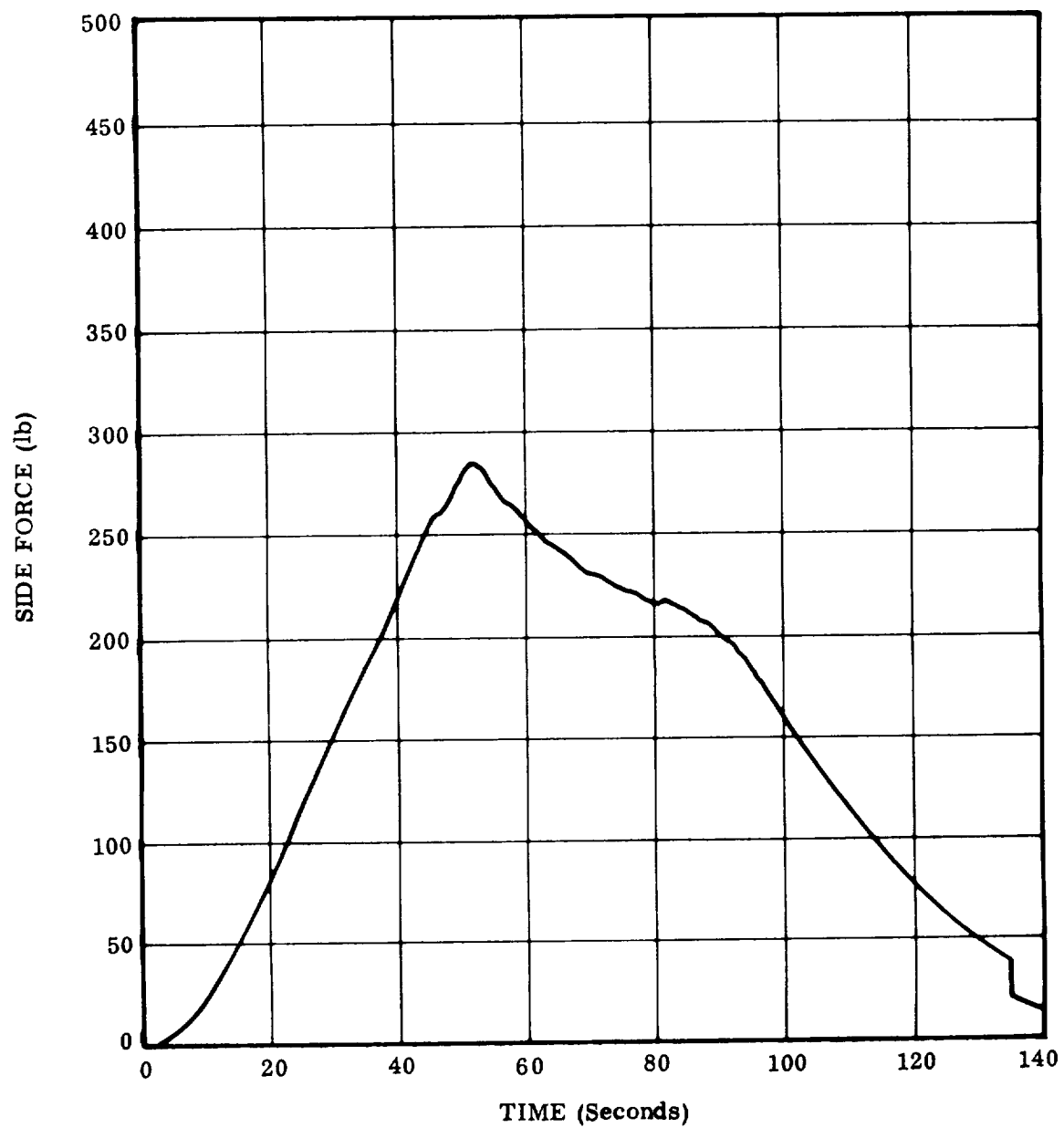


Figure 37. Side Force Time History

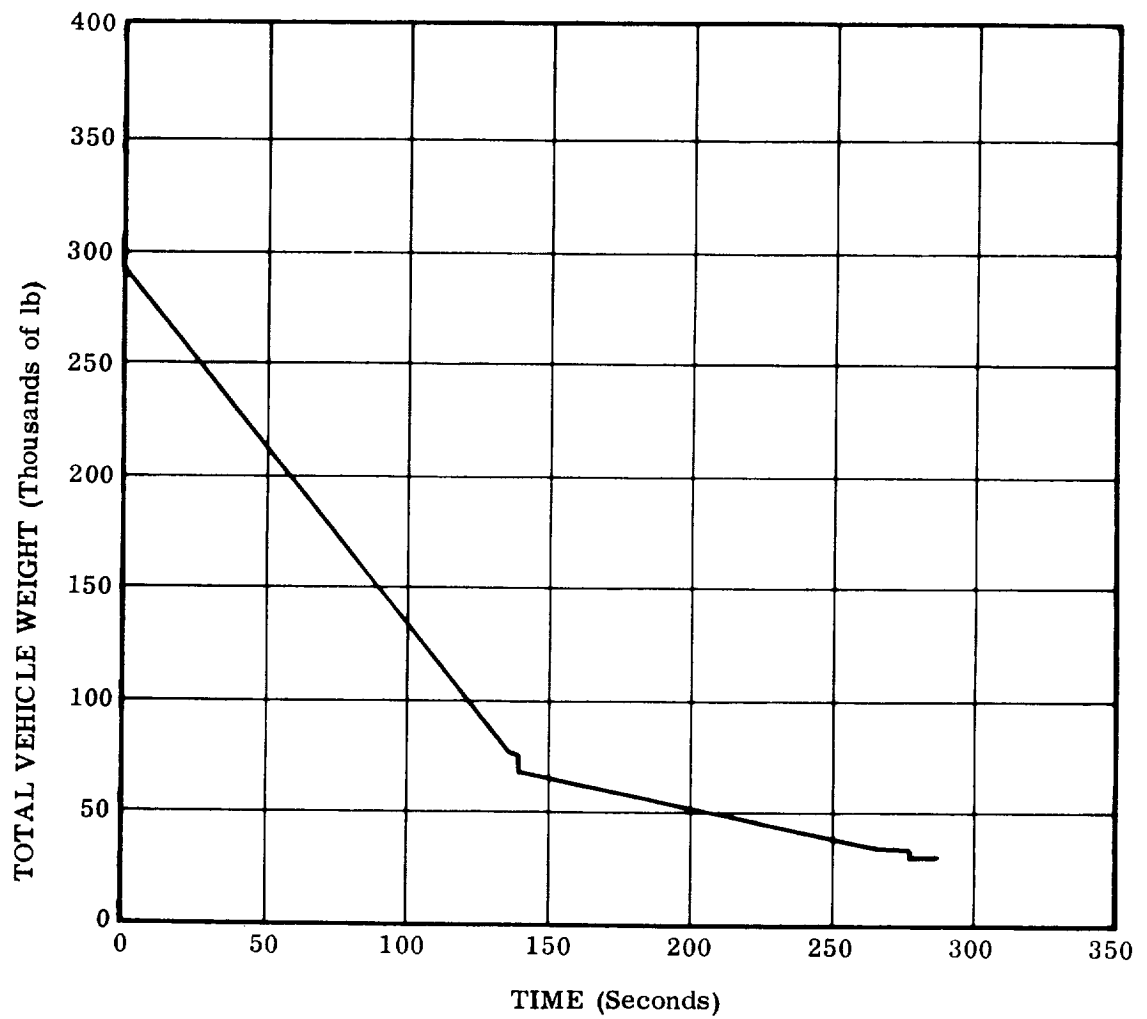


Figure 38. Total Vehicle Weight Time History

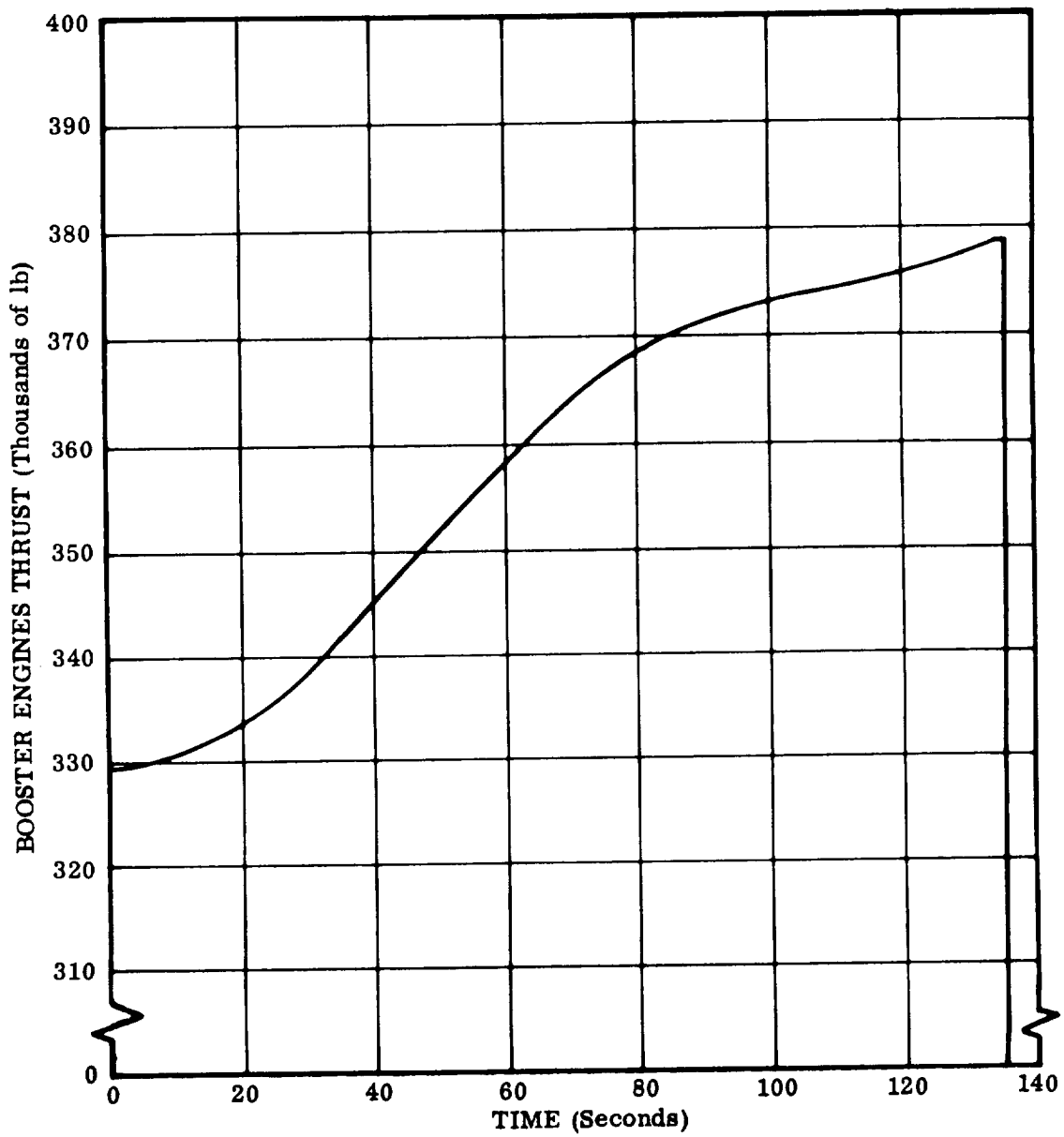


Figure 39. Booster Engine Thrust Time History

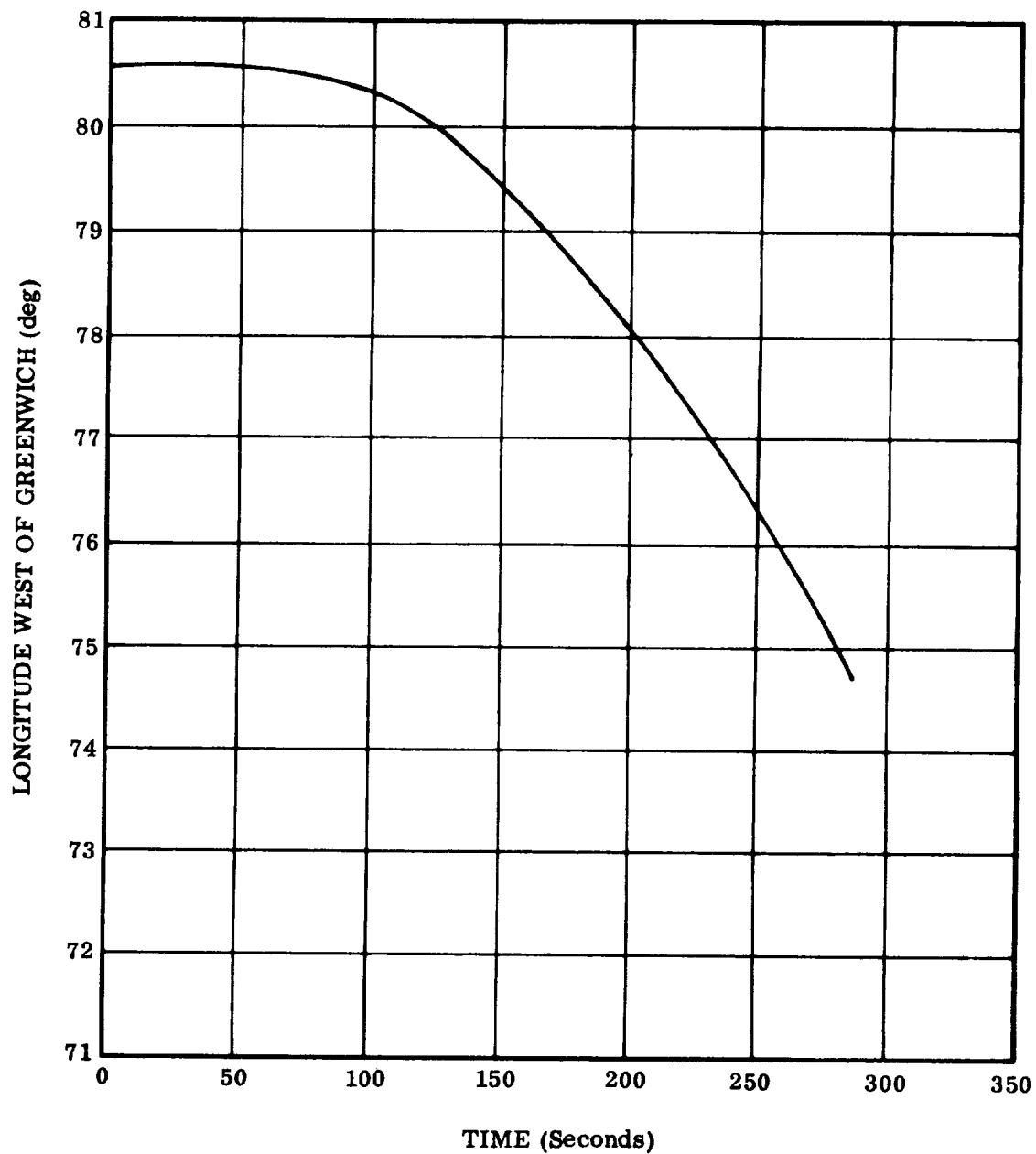


Figure 40. Longitude Time History

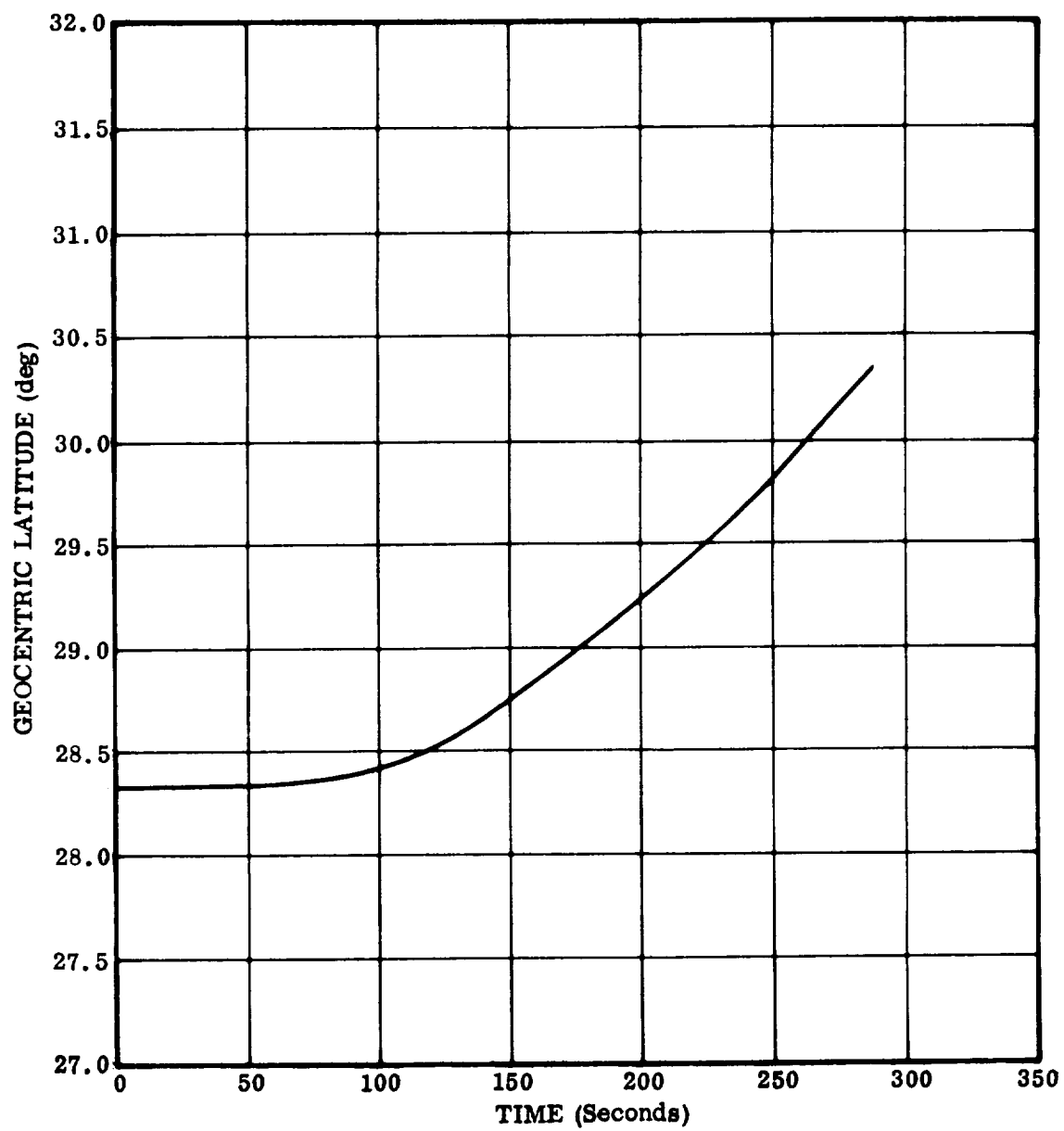


Figure 41. Geocentric Latitude Time History





# APPENDIX A TIME RATE OF CHANGE OF LINEAR AND ANGULAR MOMENTUM FOR VARIABLE MASS SYSTEMS

A formal differentiation of the momentum quantity,  $m v$ , for a variable mass system gives

$$\frac{d}{dt}(m v) = m \dot{v} + \dot{m} v$$

This result is incorrect since the residual momentum of the expelled mass has not been accounted for. The correct derivation is available in many standard texts on dynamics and is given here for completeness.

Referring to Fig. A-1, we have for the momentum of the system at time  $t$ ,

$$\bar{\mu} = \sum_i m_i \dot{\bar{R}}_i \quad (A1)$$

At time  $t + \Delta t$ , the momentum is

$$\bar{\mu} + \Delta \bar{\mu} = \sum_i \left[ (m_i + \dot{m}_i \Delta t) (\dot{\bar{R}}_i + \Delta \dot{\bar{R}}_i) - \dot{m}_i \Delta t (\dot{\bar{R}}_i + \bar{c}_i) \right] \quad (A2)$$

When the system is losing mass,  $\dot{m}_i$  is a negative quantity. In the above equation,  $\bar{c}_i$  is the velocity of the ejected mass relative to the system. It is negative if directed in a sense opposite to  $\dot{\bar{R}}_i$ .

Subtracting Eq. (A1) from Eq. (A2), dividing through by  $\Delta t$ , and letting  $\Delta t$  approach zero, we find

$$\bar{F} = \dot{\bar{\mu}} = \sum_i m_i \ddot{\bar{R}}_i - \sum_i \dot{m}_i \bar{c}_i \quad (A3)$$

where  $\bar{F}$  is the external force on the system.

It is also a straightforward procedure to determine the rate of change of angular momentum of the variable mass system. Let  $O$  be some arbitrary point. Then, by definition, the angular momentum about  $O$  at any time  $t$  is

$$\bar{h}_O = \sum_i \bar{\rho}_i \times m_i \dot{\bar{R}}_i \quad (A4)$$

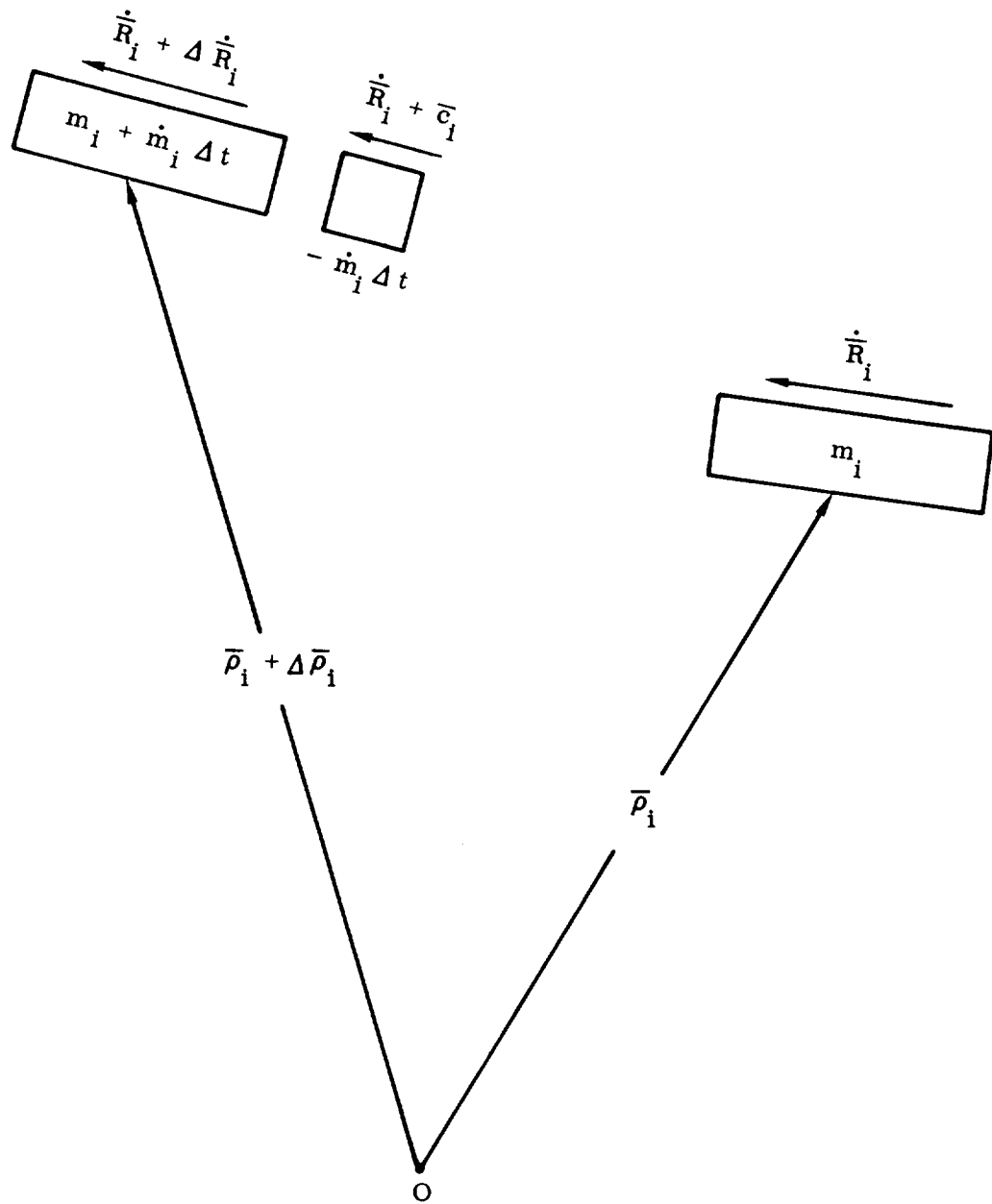


Figure A-1. Momentum Change for Variable Mass Systems

At time  $t + \Delta t$ , the angular momentum is

$$\begin{aligned} \bar{h}_o + \Delta \bar{h}_o = \sum_i \left[ (\bar{\rho}_i + \Delta \bar{\rho}_i) \times (m_i + \dot{m}_i \Delta t) (\dot{\bar{R}}_i + \Delta \dot{\bar{R}}_i) \right. \\ \left. + (\bar{\rho}_i + \Delta \bar{\rho}_i) \times (-\dot{m}_i \Delta t) (\dot{\bar{R}}_i + \dot{\bar{c}}_i) \right] \end{aligned} \quad (A5)$$

Subtracting Eq. (A4) from Eq. (A5), dividing through by  $\Delta t$ , and letting  $\Delta t$  approach zero yields

$$\dot{h}_o = \sum_i \left[ \bar{\rho}_i \times (m_i \ddot{\bar{R}}_i - \dot{m}_i \dot{\bar{c}}_i) + \dot{\bar{\rho}}_i \times m_i \dot{\bar{R}}_i \right]$$

However

$$\sum_i \dot{\bar{\rho}}_i \times m_i \dot{\bar{R}}_i = \sum_i \dot{\bar{\rho}}_i \times m_i (\dot{\bar{R}}_o + \dot{\bar{\rho}}_i) = m \dot{\bar{\rho}}_c \times \dot{\bar{R}}_o \quad (A6)$$

Therefore

$$\dot{h}_o = \sum_i \left[ \bar{\rho}_i \times (m_i \ddot{\bar{R}}_i - \dot{m}_i \dot{\bar{c}}_i) \right] + m \dot{\bar{\rho}}_c \times \dot{\bar{R}}_o \quad (A7)$$

The use of Eq. (A7) in writing the expression for the moment about an arbitrary point O requires some caution. The latter is obtained as follows. For any system (variable mass or not), we have from Eq. (A4)

$$\dot{h}_o = \sum_i \left[ \bar{\rho}_i \times \frac{d}{dt} (m_i \dot{\bar{R}}_i) + \dot{\bar{\rho}}_i \times m_i \dot{\bar{R}}_i \right]$$

which, by virtue of Eq. (A6) becomes

$$\dot{h}_o = \sum_i \bar{\rho}_i \times \frac{d}{dt} (m_i \dot{\bar{R}}_i) + m \dot{\bar{\rho}}_c \times \dot{\bar{R}}_o$$

The first term on the right-hand side is in fact the definition of the moment about O. We have therefore

$$\bar{M}_o = \dot{h}_o - \dot{\bar{\rho}}_c \times m \dot{\bar{R}}_o \quad (A8)$$

The equation for the moment about an arbitrary point differs from the usual Euler equation by the additional term,  $\dot{\bar{\rho}}_c \times m_i \bar{\mathbf{R}}_o$ . The latter is zero if

- a. The point, O, is stationary,
- b. The velocity of the mass center relative to the origin is zero, or
- c. The velocities,  $\dot{\bar{\rho}}_c$  and  $\dot{\bar{\mathbf{R}}}_o$  are parallel.

For a fixed mass system, we find by direct expansion of Eq. (A4) and the relations of Appendix B,

$$\bar{\mathbf{h}}_o = \dot{\bar{\rho}}_c \times m \dot{\bar{\mathbf{R}}}_o + \bar{\mathbf{I}} \cdot \bar{\boldsymbol{\omega}} + \sum_i \bar{\rho}_i \times m_i \dot{\bar{\rho}}_i \quad (\text{A9})$$

When the system mass is invariant, this expression may be used in Eq. (A8). In the variable mass case, the  $\dot{\bar{\mathbf{h}}}_o$  of Eq. (A7) must be used in Eq. (A8) with the result that  $\bar{\mathbf{M}}_o$  becomes

$$\bar{\mathbf{M}}_o = \sum_i \left[ \bar{\rho}_i \times (m_i \ddot{\bar{\mathbf{R}}}_i - \dot{m}_i \bar{\mathbf{c}}_i) \right] \quad (\text{A10})$$

APPENDIX B  
RELATIONS FOR THE INERTIA DYADIC

Consider a rigid body of arbitrary shape to which is attached a body coordinate frame ( $X_B, Y_B, Z_B$ ) whose origin is at some arbitrary point,  $O$ .

The velocity of any mass particle,  $m_i$ , is then

$$\dot{\bar{\mathbf{R}}}_O + \bar{\boldsymbol{\omega}} \times \bar{\boldsymbol{\rho}}_i$$

where  $\dot{\bar{\mathbf{R}}}_O$  is the velocity of  $O$ ,  $\bar{\boldsymbol{\rho}}_i$  is a radius vector from  $O$  to  $m_i$ , and  $\bar{\boldsymbol{\omega}}$  is the angular velocity of the body. By definition, the moment of momentum (angular momentum) about  $O$  is

$$\bar{\mathbf{h}}_O = \sum_i \bar{\boldsymbol{\rho}}_i \times m_i (\dot{\bar{\mathbf{R}}}_O + \bar{\boldsymbol{\omega}} \times \bar{\boldsymbol{\rho}}_i) = \sum_i \bar{\boldsymbol{\rho}}_i \times m_i (\bar{\boldsymbol{\omega}} \times \bar{\boldsymbol{\rho}}_i) + m \bar{\boldsymbol{\rho}}_c \times \dot{\bar{\mathbf{R}}}_O$$

If the point  $O$  is fixed or else is the center of mass, then this reduces to

$$\bar{\mathbf{h}}_O = \sum_i \bar{\boldsymbol{\rho}}_i \times m_i (\bar{\boldsymbol{\omega}} \times \bar{\boldsymbol{\rho}}_i) \tag{B1}$$

Now denote the components of  $\bar{\boldsymbol{\rho}}_i$  in the body frame by

$$\bar{\boldsymbol{\rho}}_i = \begin{bmatrix} x_i \\ y_i \\ z_i \end{bmatrix}$$

Define the moments of inertia of the body by

$$I_{xx} = \sum_i m_i (y_i^2 + z_i^2)$$

$$I_{yy} = \sum_i m_i (x_i^2 + z_i^2)$$

$$I_{zz} = \sum_i m_i (x_i^2 + y_i^2)$$

and the products of inertia as

$$I_{xy} = \sum_i m_i x_i y_i$$

$$I_{xz} = \sum_i m_i x_i z_i$$

$$I_{yz} = \sum_i m_i y_i z_i$$

If we now define an inertia dyadic by

$$\bar{I} = \begin{bmatrix} \bar{i} \bar{i} I_{xx} & -\bar{i} \bar{j} I_{xy} & -\bar{i} \bar{k} I_{xz} \\ -\bar{j} \bar{i} I_{xy} & \bar{j} \bar{j} I_{yy} & -\bar{j} \bar{k} I_{yz} \\ -\bar{k} \bar{i} I_{xz} & -\bar{k} \bar{j} I_{yz} & \bar{k} \bar{k} I_{zz} \end{bmatrix} \quad (B2)$$

then Eq. (B1) may be expressed in concise form as follows

$$\bar{h}_O = \bar{I} \cdot \bar{\omega} \quad (B3)$$

The time rate of change of this quantity is equal to the external moment about O; viz.,

$$\bar{M}_O = \frac{d}{dt} (\bar{I} \cdot \bar{\omega}) = \bar{I} \cdot \dot{\bar{\omega}} + \dot{\bar{I}} \cdot \bar{\omega} = \bar{I} \cdot \dot{\bar{\omega}} + \dot{\bar{I}} \cdot \bar{\omega} + \bar{\omega} \times \bar{h}_O \quad (B4)$$

The following additional relations may be derived via straightforward expansions and the rules of vector analysis.

$$\bar{I} \cdot \dot{\bar{\omega}} = \sum_i \bar{\rho}_i \times (\dot{\bar{\omega}} \times m_i \bar{\rho}_i) \quad (B5)$$

$$\bar{\omega} \times \bar{I} \cdot \bar{\omega} = \sum_i \bar{\rho}_i \times \left[ \bar{\omega} \times m_i (\bar{\omega} \times \bar{\rho}_i) \right] \quad (B6)$$

$$\dot{\bar{I}} \cdot \bar{\omega} = \sum_i \left[ \dot{\bar{\rho}}_i \times m_i (\bar{\omega} \times \bar{\rho}_i) + \bar{\rho}_i \times (\dot{\bar{\omega}} \times m_i \bar{\rho}_i) + \bar{\rho}_i \times \dot{m}_i (\bar{\omega} \times \bar{\rho}_i) \right] \quad (B7)$$

This last equation represents the time derivative of  $(\bar{I} \cdot \bar{\omega})$  with respect to body coordinates. Note that it contains a term due to mass variation. An alternate form

of Eq. (B7), which is useful in certain instances, may be obtained by noting that  $\bar{\mathbf{I}}$  may be expressed as

$$\bar{\mathbf{I}} = \sum_i m_i (\bar{\rho}_i \cdot \bar{\rho}_i \bar{\mathbf{E}} - \bar{\rho}_i \bar{\rho}_i) \quad (\text{B8})$$

where

$$\bar{\mathbf{E}} = \bar{\mathbf{i}} \bar{\mathbf{i}} + \bar{\mathbf{j}} \bar{\mathbf{j}} + \bar{\mathbf{k}} \bar{\mathbf{k}}$$

is the unit dyad.

Then it follows that

$$\begin{aligned} \bar{\mathbf{I}} = \sum_i m_i (\dot{\bar{\rho}}_i \cdot \bar{\rho}_i \mathbf{E} + \bar{\rho}_i \cdot \dot{\bar{\rho}}_i \mathbf{E} - \dot{\bar{\rho}}_i \bar{\rho}_i - \bar{\rho}_i \dot{\bar{\rho}}_i) \\ + \sum_i m_i (\bar{\rho}_i \cdot \bar{\rho}_i \mathbf{E} - \bar{\rho}_i \bar{\rho}_i) \end{aligned} \quad (\text{B9})$$





APPENDIX C  
THRUST OF A ROCKET ENGINE

Nomenclature

$A_e$	area of exit surface
$F$	body force per unit mass
$M$	mass flow rate
$\bar{n}$	outward unit vector normal to surface
$p$	pressure in fluid
$p_e$	pressure at exit surface
$p_o$	ambient pressure
$q$	velocity of fluid
$S$	surface area
$t$	time
$T$	thrust
$V$	volume
$\rho$	density of fluid
$\nabla( ) \equiv$	gradient of ( )
$(\bar{\quad}) \equiv$	vector quantity

The derivation of the rocket thrust equation presented in Appendix A is based on elementary considerations and neglects several factors of significance. A more accurate analysis should take account of the properties of compressible gas flow and the pressure forces produced, as well as those due to momentum of particles. The development that follows will be based on fundamental concepts in the theory of hydrodynamics.

Consider any closed surface,  $S$ , bounding a volume,  $V$ . Let  $p$  be the pressure, which is the same in all directions. Then the inward force on any element  $dS$  is  $(-p \bar{n} dS)$  where  $\bar{n}$  is the outward unit vector normal to  $dS$ . The resultant force on  $S$  is

$$-\int_S p \bar{n} dS \quad \text{or} \quad -\int_V \nabla p dV$$

by the Divergence Theorem.

Denoting by  $\bar{F}$  the body force per unit mass and letting  $\rho$  be the density at any point of the fluid, the equation of motion is given by

$$\int_V \rho \frac{d\bar{q}}{dt} dV = \int_V \bar{F} \rho dV - \int_V \nabla p dV \quad (C1)$$

where  $\bar{q}$  is the velocity of the fluid.

Since  $V$  is arbitrary, Eq. (C1) reduces to

$$\rho \frac{d\bar{q}}{dt} = \bar{F} \rho - \nabla p \quad (C2)$$

Eq. (C2) is the vector equation of motion of the fluid. Now

$$\frac{d\bar{q}}{dt} = \bar{q} \cdot \nabla \bar{q} + \frac{\partial \bar{q}}{\partial t} \quad (C3)$$

Hence

$$\int_V \left[ \rho \bar{q} \cdot \nabla \bar{q} + \rho \frac{\partial \bar{q}}{\partial t} - \bar{F} \rho + \nabla p \right] dV = 0 \quad (C4)$$

But

$$\nabla \cdot (\rho \bar{q} \bar{q}) = \bar{q} (\nabla \cdot \rho \bar{q}) + \rho \bar{q} \cdot \nabla \bar{q} \quad (C5)$$

Therefore

$$\int_V \left[ \nabla \cdot (\rho \bar{q} \bar{q}) - \bar{q} (\nabla \cdot \rho \bar{q}) + \rho \frac{\partial \bar{q}}{\partial t} - \bar{F} \rho + \nabla p \right] dV = 0 \quad (C6)$$

or

$$\int_V \left[ \nabla \cdot (\rho \bar{q} \bar{q}) - \bar{q} (\nabla \cdot \rho \bar{q}) + \frac{\partial}{\partial t} (\rho \bar{q}) - \bar{q} \frac{\partial \rho}{\partial t} - \bar{F} \rho + \nabla p \right] dV = 0 \quad (C7)$$

By virtue of the equation of continuity

$$\nabla \cdot \rho \bar{q} + \frac{\partial \rho}{\partial t} = 0 \quad (C8)$$

Eq. (C7) reduces to

$$\int_V \left[ \nabla \cdot (\rho \bar{q} \bar{q}) + \frac{\partial}{\partial t} (\rho \bar{q}) - \bar{F} \rho + \nabla p \right] dV = 0 \quad (C9)$$

By the Divergence Theorem

$$\int_V \nabla \cdot (\rho \bar{q} \bar{q}) dV = \int_S \bar{n} \cdot (\rho \bar{q} \bar{q}) dS \quad (C10)$$

and

$$\int_V \nabla p dV = \int_S \bar{n} p dS \quad (C11)$$

There Eq. (C9) becomes

$$\frac{\partial}{\partial t} \int_V \rho \bar{q} dV - \int_V \bar{F} \rho dV + \int_S \bar{n} \cdot (\rho \bar{q} \bar{q}) dS + \int_S \bar{n} p dS = 0 \quad (C12)$$

This is the momentum equation of hydrodynamics.

For steady-state conditions in the absence of body forces, Eq. (C12) reduces to

$$\int_S \bar{n} \cdot (\rho \bar{q} \bar{q}) dS + \int_S \bar{n} p dS = 0 \quad (C13)$$

Consider now a closed surface in which there is one orifice of area  $A_e$  through which fluid flows outward with velocity  $\bar{q}$ . For this case, Eq. (C13) becomes

$$\int_{S_1} \bar{n} \cdot (\rho \bar{q} \bar{q}) dS_1 + \int_{S_2} \bar{n} p_c dS_2 + \int_{S_1} \bar{n} p dS_1 = 0 \quad (C14)$$

where the first and third integrals are evaluated across the exit surface area  $A_e$ , the second integral is evaluated over the surface bounding the enclosed fluid (i.e., walls of nozzle and combustion chamber), and  $p_c$  represents the pressure within the closed surface. If we now let  $p_e$  be the pressure at the exit surface of area  $A_e$ , and denoting the ambient pressure by  $p_o$ , we have

$$\bar{n} \cdot (\bar{q} \bar{q}) \rho A_e + \bar{T} + \bar{n} (p_e - p_o) A_e = 0 \quad (C15)$$

where

$$\bar{T} = \int_{S_2} \bar{n} p_c dS_2 = \text{thrust of rocket}$$

Referring to the configuration of Fig. C-1 and dropping the vector notation after taking due account of signs, we have

$$T = Mq + (p_e - p_o) A_e \quad (C16)$$

where  $M$  is the flow rate given by

$$M = \rho q A_e$$

We have the result that for a compressible fluid, the thrust equation contains the additional term,  $(p_e - p_o) A_e$ . This thrust is a maximum when  $p_o = 0$ , i.e., in vacuo.

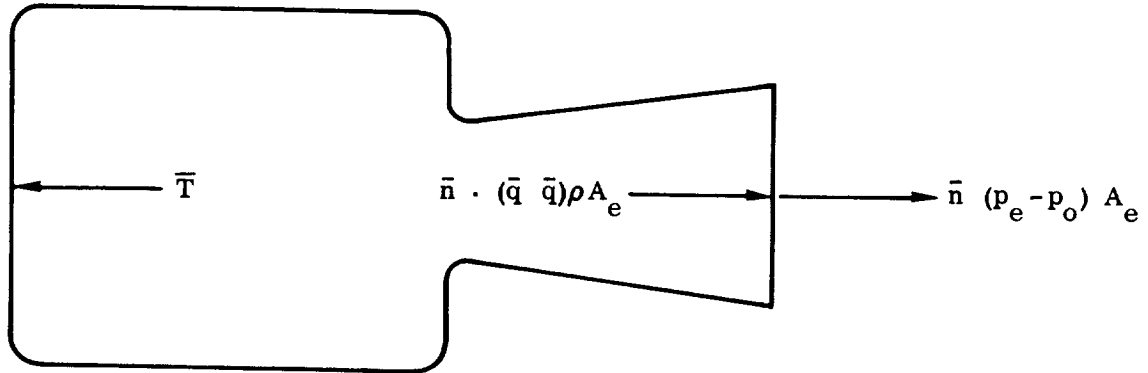


Figure C-1. Rocket Engine Thrust Configuration

APPENDIX D  
GEOPHYSICAL CONSTANTS\*

Mean Radius (spherical earth)

$$R_e = 20,925,631 \text{ ft}$$

Polar Radius (oblate spheroid earth)

$$R_{EB} = 20,855,965 \text{ ft}$$

Equatorial Radius (oblate spheroid earth)

$$R_{EA} = 20,926,428 \text{ ft}$$

Rotation Angular Velocity of Earth

$$\Omega_E = 7.29211508 \times 10^{-5} \text{ rad/sec}$$

Reference Gravity Acceleration

$$g_{\text{ref}} = 32.174 \text{ ft/sec}^2$$

Gravitational Constant

$$\mu = 1.407698 \times 10^{16} \text{ ft}^3/\text{sec}^2$$

One International Nautical Mile = 6076.1 ft

One Statute Mile = 5280.0 ft

One Astronomical Unit =  $9.289742538 \times 10^7$  statute miles

---

\*These values are abstracted from Ref. 15



# REFERENCES

1. Anonymous Project Apollo Coordinate System Standards,  
NASA Report SE 008-001-1, June 1965.
2. Seifert, H. Space Technology, John Wiley & Sons, Inc.,  
New York, 1959.
3. Mitchell, E. L. and Rogers, A. E. "Quaternion Parameters in the Simulation of a  
Spinning Rigid Body," Simulation, Vol. 4, No. 6,  
June 1965, p. 390.
4. Heiskanen, W. and Maines, V. The Earth and Its Gravitational Field, McGraw  
Hill Book Co., Inc., New York, 1958.
5. Schmitt, A. F., et. al. Approximate Transfer Functions for Flexible  
Booster and Autopilot Analysis, Report WADD-  
TR-61-93, April 1961.
6. Hilton, H. B. The Combo Flight Program, General Dynamics  
Convair Report GDA63-0967, 14 Nov. 1963.
7. Brown, R. C., et. al. Six Degree of Freedom Flight Path Study--Gen-  
eralized Computer Program, Report RTD-TDR-  
64-1, Air Force Flight Dynamics Laboratory,  
Wright Patterson Air Force Base, Oct. 1964.
8. Greensite, A. Design Criteria for Control of Space Vehicles;  
Vol. I, part 1, Short Period Dynamics, Convair  
Report GDC-DDE65-055, 1 Oct. 1965.
9. Miner, W. E. Methods for Trajectory Computation, Marshall  
Space Flight Center Report MTP-AERO-63-9,  
30 Jan. 1963.
10. DeGrafft, W. E. An IBM 7090 Six Degree of Freedom Trajectory  
Program, Naval Ordnance Laboratory Report  
NOLTR64-225, 9 Feb. 1965.
11. Baker, R. M. and Makemson, M. W. An Introduction to Astrodynamics, Academic  
Press Inc., New York, N.Y., 1960.

12. Goldstein, H. Classical Mechanics, Addison Wesley Publishing Co., Reading, Mass., 1950.
13. Leondes, C. T. Guidance and Control of Aerospace Vehicles, McGraw Hill Book Co., Inc., New York, 1963.
14. Thomson, W. T. Introduction to Space Dynamics, John Wiley & Sons, Inc., New York, 1961.
15. Brown, R. C. et.al. Six Degree of Freedom Flight Path Study Generalized Computer Program, WADD Tech. Report TDR-64-1, Oct. 1964.